Cellular Pathways for Productive HIV-1 Entry and Molecular Mechanisms of its Inhibition

by

Hanna Song

A dissertation submitted in partial fulfillment
of the requirements for the degree of
Doctor of Philosophy
(Pharmaceutical Sciences)
in the University of Michigan
2015

Doctoral Committee:

Associate Professor Wei Cheng, Chair
Professor Kathleen L. Collins
Professor Kyung-Dall Lee
Associate Professor Gustavo R. Rosania

To my God, family, and friends
: with my love and respects

Acknowledgements

I am greatly indebted to many people who have helped me complete my graduate studies. I would not be where I am without them. First and foremost, I would like to thank my advisor, Dr. Wei Cheng. He was a great mentor throughout many years. I am grateful for his constant support, encouragement, advice, and ideas throughout my Ph.D. study. His expertise, insight and guidance improved my knowledge, scientific thinking process and provided me with invaluable preparation for future challenges. I would like to thank my doctoral committee members, Dr. Kathleen L. Collins, Dr. Kyung-Dall Lee, and Dr. Gustavo R. Rosania for their patient guidance with kind and pertinent discussions.

My sincere thanks also go to the Cheng group members, past and present, Dr. Jin H. Kim, Dr. Yuanjie Pang, Dr. Michael C. DeSantis, Dr. Byumseok Koh, Dr. Ximiao Hou, Jamie L. Austin, Kristin Schimert, Ziah Dean, Chunjuan Tian, Zhilin Chen for always providing feedback and enjoying discussions. I especially thank to Dr. Jin H. Kim for his generous help regarding all basic molecular experiments and willingly discussing many stupid questions from me.

I would like to thank my friends I've met in Ann Arbor. They have helped me get through tough times and made my life at Ann Arbor enriched and enjoyable. I cannot forget memorable times spent with them. Finally, I would like to dedicate my work to my family: my parents Jae Kee Song and Eun Kyeung Kim, my sister Jimin, and my twin brothers

Wonho and Junho, my brother-in-law SeungSuk Choi, and my lovely nephew Martin. I am always grateful for their presence, constant love and support throughout my whole life.

Table of Contents

List of Figures

List of Abbreviations

AIDS	Acquired immunodeficiency syndrome
BlaM	beta-lactamase
CA	Capsid
CHR	C terminal heptad repeat
Ci.p.	Concentration of infectious particles
Cp.p.	Concentration of physical particles
DEAE-dextran	Diethylaminoethyl dextran
DMEM	Dulbecco’s modified eagle medium
Dyn I	Dynamin I
EEA1	Early endosome antigen 1
ESCRT	Endosomal sorting complex required for transport
EGFP	Enhanced green fluorescent protein
EM	Electron Microscopy
Env/E	HIV-1 envelope glycoproteins (subunits: gp120/gp41)
FBS	Fetal bovine serum
FOV	Field of view
Gag	HIV-1 polyprotein (MA-CA-NC)
HAART	Highly active antiretroviral therapy

HIV-1	Human immunodeficiency virus type 1
HR	Heptad repeat domain
MA	Matrix
mAb	Monoclonal antibody
MOI	Multiplicity of infection
MOP	Multiplicity of particle
NAb	Neutralizing antibody
NC	Nucleocapsid
NHR	N terminal heptad repeat
ORF	Open reading frame
PBS	Phosphate buffered saline
PIC	Pre-integration complex
PCR	Polymerase chain reaction
PLL	Poly-L-lysine
R	Vpr
REC	Rev/Envelope expression cassette
RPMI	Roswell park memorial institute medium
RT	Reverse transcriptase
TBS	Tris buffered saline
VSV-G	Vesicular stomatitis Indiana virus G protein

Abstract

Understanding of human immunodeficiency virus (HIV), productive viral entry, and its inhibition is important to elucidate viral pathogenesis and further develop therapeutics that is aimed to block HIV entry to $CD4^+$ T cells. Although direct fusion with the plasma membrane has been long thought to be the pathway for HIV-1 entry, this notion has been challenged recently by various studies. In this thesis, we focus on the cellular pathways that lead to productive infection and mechanisms of its inhibition by membrane-impermeable fusion inhibitors, using fluorescently-labeled HIV as an important tool. Although there have been many studies using fluorescently-labeled virions, understanding of their features in terms of infectivity, labeling efficiency, or intensity profiles has been limited. The results from our study characterizing single-cycle replicative, fluorescently-labeled HIV-1 give us better understanding of HIV-1 and interpretation of data when using virions for further mechanistic studies. Using the characterized HIV-1, we determine to investigate entry pathways that lead to productive HIV-1 infection by seeking the potential correlation between the inhibition of cell endocytosis and the inhibition of HIV-1 infection. Possible scenarios for productive viral entry are direct fusion at cellular plasma membrane, fusion with endosomes, or both. The results from three different cell lines with various inhibitors that are known to block various steps of endocytosis suggest that endocytosis

can indeed lead to productive infection, as revealed by the specific inhibition of HIV-1 infection by dynamin I K44A mutant. However, endocytosis may not be the only productive pathway for HIV-1 infection because all these inhibition data that we have observed appear to be partial, which is in sharp contrast to the inhibition by T20. As a matter of fact, for both antibodies and T20, HIV-1 infection can be blocked close to 100%, indicating that these drugs are efficacious enough *in vitro* even though HIV can establish productive infection through endocytosis. These results also demonstrate that endocytosed virions need to fuse with endosomal membrane for productive infection. In comparison to direct fusion at the plasma membrane, endocytosis may allow virus to escape from membrane impermeable drugs. The conclusion that endocytosis can initiate productive infection of HIV-1 virions led us to investigate whether the presence of endocytic entry may reduce the efficacy of membrane-impermeable drugs of HIV-1. To test this hypothesis, we examined the effect of T20 on the internalization of HIV-1 and the impact of endocytosis on T20 efficacy. These experiments show that endocytosis has no apparent effect on T20 efficacy, suggesting that endocytosis does not offer measurable advantage for the virus to escape from membrane-impermeable T20. Taken together, these studies suggest that endocytosis contributes to the productive entry of HIV-1, however, the efficacy of T20 is not affected by viral endocytosis.

Chapter 1.

Introduction

1.1. Background

1.1.1. HIV

The human immunodeficiency virus (HIV) is a member of genus *Lentivirus*, part of family, *Retroviridae* (1). They are single-stranded, positive-sense, enveloped RNA viruses. The viral RNA genome is converted into double-stranded DNA by a viral reverse transcriptase (RT) that is transported along with the viral genome in the virus particle upon entry into the target cell. The resulting viral DNA is then integrated into the cellular DNA inside cell nucleus by a viral integrase and host cofactors (2). Once integrated, the virus can be transcribed, producing new viral RNA genomes and viral proteins. Those are packaged and released from the cell and a new viral particles begin the replication cycle. Alternatively, the virus may become latent, allowing the virus and its host cell to evade from the immune system (2, 3).

As shown in Figure 1.1A, it is roughly spherical with a diameter of about from 120 to 150 nm (4, 5). It is composed of two copies of positive single-stranded RNA that codes for both structural proteins that are found in all retroviruses and several nonstructural proteins unique to HIV (4). The HIV genome contains three genes, *gag*, *pol*, and *env*, encoding major structural proteins as well as essential enzymes for viral replication cycle as shown in Figure 1.1B, (6). These are synthesized as polyproteins which produce proteins for virion interior, called Gag (7), the viral enzymes (Pol) or the envelope glycoproteins (Env). In addition to these, HIV encodes certain regulatory (Tat, Rev) and auxiliary (Nef, Vif, Vpr, Vpu) proteins as well (8, 9). HIV has a 9.2 kb unspliced genomic transcript encoding for Gag and Pol precursors; a singly spliced, 4.5 kb encoding for Env, Vif, Vpr and Vpu and a multiply spliced, 2 kb mRNA encoding for Tat, Rev and Nef. Gag is processed into matrix (MA), capsid (CA), and nucleocapsid (NC) by a viral protease during virion maturation process. Pol is also initially expressed as a polyprotein that is cleaved into functional enzymes reverse transcriptase (RT), integrase, and protease. Envelope (Env) is expressed as a 160 kilodalton (kDa) polyprotein (gp160), which is cleaved into gp41 and gp120 within the Golgi of the infected cell. gp120 directly interacts with CD4, the viral receptor, while gp41 is required for virus fusion with the host cell (10). Env consists of a cap made of three glycoprotein gp 120 and three transmembrane gp41molecules anchoring the structure into the viral envelope (11, 12). This glycoprotein complex present as a trimer enables the virus to attach to and fuse with target cells to initiate the viral infection cycle (13, 14).

1.1.2. Acquired immunodeficiency syndrome (AIDS)

HIV causes the acquired immunodeficiency syndrome (AIDS). Infected humans progressively fail their immune system allowing life-threatening opportunistic infections and cancers (15). Without treatment, average survival time after infection with HIV is estimated to be 7 to 9 years, depending on the HIV subtype (16). Infection with HIV occurs by transfering blood, semen, vaginal fluid, or breast milk (17). HIV is present as both free virus particles and virus within infected cells in body. HIV infects immune cells including $CD4^+$ T cells, macrophages, and dendritic cells (18). Viral infection lowers the level of $CD4^+$ T cells via various mechanisms, such as apoptosis of uninfected cells, direct killing infected cells, and killing of infected $CD4^+$ T cells by $CD8^+$ cytotoxic T lymphocytes that can recognize infected cells (19, 20). When the number of $CD4^+$ T cell decreases below a critical level, the body becomes more susceptible to opportunistic infections due to the loss of cell-mediated immune system (21, 22).

1.1.3. HIV pandemic

Despite major advances in our scientific understanding of HIV, HIV/AIDS continues to persist as a globally pandemic (23). Approximately 35.3 million people are living with HIV globally in 2012 (24). There were about 1.8 million deaths from AIDS in 2010 (24). Two types of HIV have been characterized: HIV-1 and HIV-2. HIV-1 is related to viruses found in chimpanzees and gorillas living in Western Africa, while HIV-2 is related to viruses found in West African primate sooty mangabey (25). HIV-1 is more virulent and more infective causing the majority of HIV infections globally (26). HIV-2 has the lower infectivity compared to HIV-1 and HIV-2 is largely confined to West Africa due to its relatively poor transmission rate (27).

1.1.4. HIV-1 life cycle

The infection begins when the envelope glycoprotein spikes interact with the receptor CD4 on viral target cells. The envelope glycoprotein of HIV-1 consists of two non-covalently associated subunits, gp120 and gp41. The engagement of gp120 and CD4 receptor initiates a series of conformational changes in gp41 and gp120 that lead to the insertion of a region of gp41 into the membrane of the host cell, and the formation of a pre-hairpin intermediate. Further changes in the conformation of gp41 bring the viral and cellular membranes into close enough proximity for membrane fusion (28). Partial core shell uncoating facilitates reverse transcription, resulting in the pre-integration complex (PIC) (29). Upon import of PIC into the cell nucleus, viral DNA is then integrated into the cellular DNA inside cell nucleus by a viral integrase and host cell cofactors (2). The host RNA polymerase II (RNA Pol II) mediates the proviral transcription and viral mRNAs serve as templates for protein production. The viral RNA is incorporated into viral particles with viral protein components transcribed from host cells. A newly formed viral particle bud and release from the cell, which is mediated by endosomal sorting complex required for transport (ESCRT) complexes (30). Virus is then maturated during or after budding process to create an infectious viral particle (31). Each step in the HIV-1 life cycle is a potential target for antiviral intervention.

1.1.5. Current antiviral drugs for HIV-1

1.1.5.1. Reverse transcriptase inhibitors

Nucleoside or Nucleotide reverse transcriptase inhibitors are analogues of nucleoside or nucleotide which inhibit reverse transcription. The reverse transcriptase (RT) is necessary for HIV to become integrated into DNA in the nucleus of the human cell because it must be reversely transcribed into DNA from RNA viral genome. Since RT is a viral protein, which is not present in mammalian cells, it can be a selective target for viral inhibition. Nucleoside or Nucleotide reverse transcriptase inhibitors are chain terminators preventing other nucleosides or nucleotides from being incorporated into the DNA chain because of the absence of a 3' OH group (32). Non-nucleoside reverse transcriptase inhibitors inhibit reverse transcriptase by binding to an allosteric site of the enzyme (33).

1.1.5.2. Integrase inhibitors

Integrase inhibitors block the viral integrase, which is necessary for integration of viral DNA into the host DNA (34). Since integration is a critical and distinct step in retroviral replication, these inhibitor can prevent further spread of the virus and may be taken in combination with other types of anti HIV drugs to minimize resistance by the virus. Integrase inhibitors were initially developed for the treatment of HIV infection, but they could be applied to other retroviruses.

1.1.5.3. Protease inhibitors

Protease inhibitors block the viral protease enzyme necessary to produce mature virions upon budding from the host cells. Viral protease cleaves Gag and Gag/Pol precursor proteins and this cleavage is critical when immature virions proceed maturation process

(35, 36). Proteolytic maturation is essential for the production of infectious HIV-1 virus (31). Virus particles produced in the presence of protease inhibitors are defective and mostly non-infectious.

1.1.5.4. Highly active antiretroviral therapy (HAART)

HIV has very high genetic variability resulting from its fast replication cycle, a high mutation rate of replication, and recombinogenic properties of reverse transcriptase (37-39). Most of the mutations doesn't offer any advantage to virus, but some of them have a natural selection, which triggers virus to have superiority compared to their parent and enable them to evade from the human immune system and antiretroviral drugs (40-42). When antiretroviral drugs are used improperly, multidrug resistant strains can become the dominant genotypes and spread very rapidly. Antiretroviral combination therapy can suppress HIV replication, reduce the potential spontaneous resistance mutations, and defend against resistance. HAART is the name given to combinational treatment regimens used to suppress HIV viral replication and the progression of HIV disease. The usual HAART regimen combines three or more different mechanistic drugs such as two nucleoside reverse transcriptase inhibitors and a protease inhibitor, two nucleoside reverse transcriptase inhibitors and a non-nucleoside reverse transcriptase inhibitor or other such combinations. These HAART regimens have shown decreased amount of active virus and are able to lower the number of active virus in some cases until it is undetectable by current blood testing techniques. This combinational approach makes multiple blocks to HIV replication and reduce the possibility of a superior mutation. If a mutation that carries resistance to one of the drugs being taken induces, the other drugs continue to suppress

reproduction of that mutation (43, 44). However, there is persistent viral replication carrying HIV-1 resistance, which causes subsequent failure with treatment. This phenomena still occurs in a substantial proportion of patients, due to genetic variability or other factors related to individual patients (45). HIV resistance is continuously evolving, making difficulties to treat HIV permanently (46).

1.1.5.5. Entry inhibitor

The envelope glycoprotein complex is indispensable to HIV-1 entry into cells by mediating attachment to target cells and subsequent membrane fusion. Receptor antagonists prevent attachment of gp120 to the receptor or coreceptor and conformational changes within gp41 required for membrane fusion can be blocked by fusion inhibitors. The first fusion inhibitor developed was peptide mimics of the HR2 (heptad repeat domain 2) sequence of gp41 that act by competitively binding to HR1 (heptad repeat domain 1). T20 (Enfuvirtide/Fuzeon, Roche/Trimeris) is a 36 amino acid synthetic peptide corresponding to the part of gp41 amino acid sequences from the HXB2 isolate, shifted several residues along the HR2 sequence with respect to each other (47-53). This peptide inhibits virus entry by binding to the HR1 core that is formed after binding of gp120 to CD4 and the coreceptor, thereby blocking the subsequent formation of the six-helix bundle (47, 53-55). It is active in the nanomolar range against diverse HIV strains and blocks virus infection of cells and viral spread via cell-to-cell contact, which may be the more physiological route (47-53, 56). T20 has been used as a salvage therapy for patients who have developed a resistance issue with highly active antiretroviral therapy (HARRT), which is a combination of several medicines that aims to control the amount of virus in

patients' body (57, 58). It was approved for clinical use in March 2003 by the US Food and Drug Administration (FDA) and the European Medicines Agency (EMEA).

T20 is subcutaneously administered at the recommended dose of 90 mg twice daily with optimized background antiretroviral therapy, reducing the level of HIV-1 RNA in plasma up to 48 weeks compared with optimized background therapy alone. It shows a small volume of distribution (5.48L), low systemic clearance (1.4 L/h) and high plasma protein binding (92%). Following subcutaneous administration, it is almost completely absorbed, and exposure correlates almost linearly with dose over the range 45–180 mg. Since bioavailability is high (84.3%) and the elimination half-life (3.8 hours), it is recommended as twice-daily administration. The pharmacokinetic-pharmacodynamic relationship supports its combination therapy with other antiretroviral drugs at the recommended dose (59).

The other approved entry inhibitor is Maraviroc (Selzentry, Pfizer) (60, 61). Maraviroc works by targeting CCR5, a coreceptor located on human helper T lymphocytes (62, 63). The chemokine receptor CCR5 is an essential coreceptor for most HIV strains and necessary for viral entry into the host cell. Maraviroc binds to CCR5, to enter human macrophages and T cells. Because there is another coreceptor, CXCR4, which was used for viral entry, an HIV tropism test should be performed to determine if this drug will be effective (64).

1.1.6. T20 mechanism, resistance, and ongoing research

1.1.6.1. Viral fusion machinery and proposed/potential mechanisms of T20 action

The envelope glycoprotein of HIV-1 consists of two non-covalently associated

subunits, gp120 and gp41. The interaction between gp120 and the CD4 receptor initiates a series of conformational changes in gp41 and gp120, which leads to the insertion of a region of gp41 into the host cellular membrane, and the formation of a pre-hairpin intermediate. Further conformation changes in gp41 make the viral and cellular membranes be close enough for membrane fusion process. Based on the fact that T20 has a homologous sequence to a part of C terminal heptad region (CHR) in gp41 (65), the mechanism of T20 was proposed that it can bind to a region of gp41 that mediates this conformational change from pre-hairpin intermediate to the fusion-active structure, therefore preventing membrane fusion and viral entry (58).

However, T20 mechanism has not been fully revealed. There are studies showing that T20 can target multiple sites of gp41 and gp120, which was proved by several experiments. First, T20 didn't form a stable six-helix bundle with N-peptides homologous to N-terminal heptad region (NHR) in gp41. Also, it didn't inhibit the formation of a stable six-helix bundle. Finally, T20 efficacy was significantly lowered by peptides derived from the membrane-spanning domain in gp41 and coreceptor binding site in gp120 (66, 67).

1.1.6.2. Potential mechanisms of T20-resistance and ongoing and future development of antiviral drugs targeting HIV-1 entry

Although T20 has been used as a salvage therapy for patients who had developed a resistance from HAART, the fast resistance with T20 has been also reported (68). Also different clinical isolates showed variation in susceptibility to T20 (69, 70). T20 is still one of the promising antiretroviral drugs since primary resistance has not been observed, and thus T20-naive isolates remain clinically sensitive, leading people to investigate the

mechanisms of T20 resistance. Understanding of T20 resistance mechanism helps develop more potent and less resistant T20-like antiviral drugs.

One of the potential mechanism is that resistance to T20 is governed by changes in the HR1 region of gp41, specifically in a stretch of amino acids in and adjacent to the GIV motif, which is amino acids 36–45 of gp41 that forms part of the binding site of T20 (69). The 10 amino acid motif is critical for viral fusion, and T20-resistant mutants show poor replication compared with wild type. There are evidences that other domains in envelope glycoprotein outside the HR1 domain also play a role, including HR2 domain of gp41 (69, 71). Based on sequence analysis, mutation GIV to GIA in HR1, SNY to SKY in HR2 domain, and double mutation in HR1 and HR2 caused T20 resistance (69, 70). Thus, there has been many ongoing trials to develop T20-like peptide which is designed to impact on the resistance phenotype as well as not to influence viral fitness based on the above mechanistic studies.

Furthermore, another approach as ongoing research is improving stability and formulation. Although T20 is one of the potent anti HIV-1 drugs, it needs to be subcutaneously injected to reach a sufficiently high blood level for inhibiting viral infection and also causes common symptoms on the injection site (72-76). Also it has a short shelf-life and causes a high cost of production (58).

Researches on the next generation of fusion inhibitors, which optimally have enhanced efficacy, a higher genetic barrier to resistance issue, less frequent subcutaneous administration, and combined with the use of new formulation methods will enlighten to prevent both chronic and acute viral infections (77, 78). Besides T20 and derivatives, other fusion inhibitors have been developed that target different domains of gp41 (65, 78, 79).

1.1.7. Mechanisms of HIV-1 entry

The productive entry of HIV-1 is still controversial with different experimental approaches and research groups (80, 81). Productive entry of HIV-1 into CD4+ T cells is initiated by binding of the viral envelope gp120 to CD4 receptor. This binding causes a cascade of conformational changes in both the gp120 and gp41 that eventually lead to virus-cell membrane fusion and HIV-1 entry (28, 82). Endocytosis is an required entry step for enveloped viruses whose fusion proteins are activated by acidic pH (83). In contrast, viruses that undergo fusion upon interacting with corresponding cellular receptors regardless of the pH have been believed to fuse directly with a plasma membrane. Consistently, it was revealed that HIV-1 entry and viral membrane fusion do not require exposure to low pH (84).

Early studies of HIV-1 entry have focused on the identification of receptors on T cell surface mediating viral productive entry. These have revealed that CD4 and chemokine coreceptors (CCR5 or CXCR4) are necessary for HIV entry to $CD4^+$ T cells (85). Although it has not been observed directly, HIV-1 entry is long thought to be a direct fusion between viral membrane and T cell membrane (28, 83, 86). There are several studies supporting this mechanism: first of all, interaction between CD4 and envelope protein gp120 can trigger conformational changes to fusion-active structure (28); second, cell-cell fusion can be mediated by HIV envelope proteins expressed on one cell surface and receptors (87); third, viral entry does not require the endocytosis of its receptor CD4 nor does it depend on low pH, which may be necessary for viral endocytosis (88, 89); finally, electron microscopy (EM) images have shown the intermediates of a direct fusion between virus and cell membrane (90-92).

However, recent study using real time fluorescence imaging technology at single molecule level has directly shown that HIV-1 enter its target cells via dynamin-dependent endocytosis instead of direct fusion in TZM-bl cells (81). Consistently, viral fusion with endosomes and micropinosomes has been observed by EM (93, 94). Second, viral infection increases with blocking the acidification of endosomal compartments and apparently by sparing the virus from degradation in lysosomes (95-97). Third, efficient infection by Vesicular stomatitis virus G protein (VSV-G) pseudotyped virus (98) shows that there are no significant limitations associated with viral endocytosis. Lastly, inhibition of clathrin-mediated endocytosis decreases the efficacy of virus-cell fusion and infection in HeLa-derived cells (99).

Possible scenarios for productive viral entry are direct fusion at cellular plasma membrane, endocytosis, or both. Although direct fusion is thought to be the pathway for HIV-1 entry (82, 83, 86), this has been challenged recently by various studies (81, 100). This question is fundamentally important for molecular understanding of HIV-1 infection. Understanding of productive HIV-1 entry will help elucidate viral pathogenesis and further develop therapeutics that is aimed to block HIV entry to $CD4^+$ T cells.

1.1.8. Single-cycle replicative HIV-1

Non-capable of multiple rounds of infections but antigenic HIV-1 particles are essential tool for the research on many topics associated with this virus. This molecularly cloned HIV-1 that is capable of only a single round of infection (101, 102), e.g. single-

cycle replicative virions, offers a unique tool to address important questions related viral entry and infectivity. The production of these virions in cell culture involves the use of a mutant provirus clone together with a separate plasmid that drives the expression of viral envelope glycoproteins. Because viral proteins are expressed from cloned DNA instead of the provirus reversed transcribed from a RNA genome by RT, mutations in viral proteins that arise from RT errors or APOBEC3 activity are virtually eliminated. Since cells infected by these single-cycle virions result exclusively from the initial input virus, the efficiency of provirus integration can be correlated with the efficiency of viral entry without complications from multiple rounds of infection (103). Although single-cycle HIV-1 virions have been widely used for viral neutralization assays (104) and evaluation of antiviral drugs (105), the features of virions in terms of size, intensity, or infectivity have not been extensively studied. Those will be further characterized and optimized in chapter 1.

1.2. Rationale and Significance

1.2.1. Characterizing single-cycle replicative, fluorescently-labeled HIV-1

Although single-cycle HIV-1 virions have been extensively used for viral neutralization assays (104) and evaluation of antiviral drugs (105), conditions to optimize their infectivity in cell culture have not been fully reported. The intensity profiles and labeling efficiency of fluorescently-labeled virions during virion manipulation have not been also extensively studied, which has been used to track the behavior of HIV-1 in the cytoplasm of infected cells. Because the expression of provirus, envelope glycoproteins,

and fluorescent proteins is separate in three plasmids and there is a possibility that not all three plasmids can transfect the same at equal quantity, intensity profiles of fluorescent-tagged HIV-1 virion may show heterogeneous phenomena. Although EGFP-Vpr fusion protein in virions allows direct visualization, the potential presence of virions without EGFP may significantly complicate the study of imaging virus. Consistently, a recent study revealed that there is heterogeneity of HIV-1 virions in terms of viral protein composition with single-molecule sensitivity (5). This heterogeneity might lead to a broad spectrum of infectivity for individual HIV-1 virions (103), which was hypothesized in the literature (106). Thus, characterizing the infectivity and intensity profiles of single-cycle replicative, fluorescently-labeled HIV-1 will help further investigate the mechanism of viral entry as well as develop deep understanding of HIV-1 virions.

1.2.2. HIV-1 productive entry pathway

Productive entry of HIV-1 into $CD4^+$ T cells has not been clearly investigated yet. This question is fundamentally important for molecular understanding of HIV-1 infection. Early studies have suggested that HIV-1 can enter target cells via direct fusion at the plasma membrane (96, 107, 108). In contrast, recent studies have suggested that the direct fusion at the plasma membrane is not productive. Instead, HIV-1 may enter cells via dynamin-dependent endocytosis (81, 100) and lead to a productive infection. Possible mechanisms for productive viral entry are direct fusion at the plasma membrane, endocytosis, or both. In this study, in order to determine if virion endocytosis can lead to productive infection, we seek to correlate the inhibition of endocytosis and inhibition of infection. Understanding of productive HIV-1 entry will help elucidate viral pathogenesis

and further develop anti HIV-1 drugs that are aimed to block HIV entry to $CD4^+$ T cells.

1.2.3. Mechanism of entry inhibitor, T20

Both antibodies and T20 can block viral infections close to 100%, indicating that these drugs are efficacious enough *in vitro*. T20 has been used as a salvage therapy for patients who have developed a resistance issue with highly active antiretroviral therapy (HARRT), which is a combination of several medicines that aims to control the amount of virus in patients' body (57, 58). Although T20 needs to be subcutaneously injected to reach a sufficiently high blood level for inhibiting viral infection and also causes common symptoms on the injection site (72-76), T20 was the first new class of HIV inhibitors targeting the viral entry step. T20 was therefore a promising ingredient of a therapeutic salvage regimen (79) since T20 action is not affected by the presence of resistance mutations against protease and reverse transcriptase inhibitors.

The mechanism of T20 has been proposed that it binds to a region of gp41 that mediates the conformational change from pre-hairpin intermediate to the fusion-active structure based on its sequences homologous to C-terminal heptad repeat (CHR) region. Contrary to this belief, there have been several studies suggesting T20 inhibits HIV-1 entry by targeting multiple sites in gp41 and gp120 (57, 65). Although T20 is one of the promising and potent drugs, the mechanism and behavior of T20 has not been fully understood. Furthermore, in comparison to direct fusion at the plasma membrane, some studies have suggested that endocytosis may allow virions to escape from the action of membrane-impermeable drugs (109, 110). Thus, investigating the impact of endocytosis

on membrane-impermeable T20 and its mechanism is fundamentally important for molecular understanding of HIV-1 entry as well as developing new generations of T20-like anti HIV-1 drugs with improved potency and stability.

1.3. Specific aims and Hypotheses

1.3.1. Specific aim 1: Preparation and characterization of single-cycle replicative, fluorescently-labeled HIV-1 virions

1.3.1.1. Varying virus culture conditions improves the infectivity of HIV-1.

We defined infectivity as the fraction of virions that can establish a productive infection in a host indicator cell line by establishing how to measure the concentration of infectious virus particles (Ci.p.) by taking an advantage of viral protein, Vpr, suppressing cell cycle. We then varied virus culture conditions, such as EGFP-Vpr plasmid input, virion harvest time, media replacement after transfection, and envelope plasmid input**.**

1.3.1.2. There is a trade-off effect between virion infectivity and fluorescent intensity. How heterogenous are the fluorescent intensities of virions?

We tested the correlation between the number of virion particles and the concentration of physical particles (Cp.p.) by using custom-written MATLAB due to the potential presence of virions without EGFP. The labeling efficiency of HIV-1 carrying EGFP-Vpr was also determined. We then characterized HIV-1 tagged with EGFP-Vpr in

terms of size, mean intensity, and sum intensity distributions by varying EGFP-Vpr inputs. This would give us a rationale to pick a certain input of EGFP-Vpr, which results in the highest infectivity and reasonable intensity profiles for further imaging and infection studies.

1.3.2. Specific aim 2: Determine entry pathways that lead to productive HIV-1 infection

1.3.2.1. Endocytosis contributes to productive viral entry.

We tested whether there is a correlation between the inhibition on viral infection and the inhibition of cell endocytosis. First of all, we can clearly visualize HIV-1 virions colocalized with early endosomes. For the specific inhibition on dynamin-dependent endocytosis, we used dynamin I K44A mutant (111), which acts as a dominant-negative fashion to block the formation of functional dynamin oligomers required for dynamin-dependent endocytosis (112-114). The specificity of inhibition on endocytosis was checked by measuring transferrin uptake (115, 116). Also, to determine if virion endocytosis can lead to productive infection, various inhibitors that are known to block various steps of endocytosis were used. These studies were compared with VSV-G pseudotyped virions, which are known to enter cells through receptor-dependent endocytosis (117).

1.3.2.2. Productive viral entry depends on cell types, viral envelopes from different strain, or facilitating virus binding method.

We used different cell lines, such as TZM-bl, Rev-CEM, or, SupT1 cell lines with dynasore and T20 to determine if virion endocytosis/fusion can lead to productive infection. Also, envelope glycoproteins from both NL4-3 and HXB2 strains were tested in TZM-bl cell line with dynasore treatment. To exclude the possibility that the inhibitory effect of dynasore on viral infection in the presence of DEAE-dextran or spinoculation to facilitate virus binding to a cell and increasing apparent infectivity (103, 118) might have nonspecific effect, the parallel experiments without either facilitating method were also tested in TZM-bl cells.

1.3.3. Specific aim 3: Impact of virion endocytosis on membrane-impermeable HIV-1 drugs

1.3.3.1. Does T20 affect virion internalization?

We quantitated virion internalization with different inoculation time points and compared its fraction between in the absence and presence of T20, whose concentration is able to block viral infection close to 100%. We also tested the hypothesis that we might be able to see the higher fraction of virion internalization with saturation concentration of T20 due to no fusion events available.

1.3.3.2. Some events of viral endocytosis come from receptor-independent endocytosis, which is cellular proteins-specific on virion surface.

We compared the fraction of virion endocytosis between HIV-1 carrying envelope

glycoprotein and gag particles, which doesn't have viral envelope on virion surface. We also tested whether the receptor-independent phenomena come from the difference in host proteins on virion surface by producing virions from 293T or Jurkat T cells.

1.3.3.3. Endocytosis offers an advantage for virus to escape from membrane-impermeable peptidic inhibitor, T20.

Endocytosis may allow virus to escape from membrane-impermeable inhibitors. Otherwise, fusion inhibitor, T-20, may exert its inhibitory effect inside endosome as bound to endocytosed HIV-1 based on the assumption that endocytosis may contribute to viral infection. To test the effect of endoytosis on T20 efficacy, we titrated T20 in TZM-bl cells, whose endocytosis had been inhibited by dynasore or dyn I K44A. We then varied time points T20 added during virion inoculation to see whether T20 efficacy would be different.

1.4. Figures

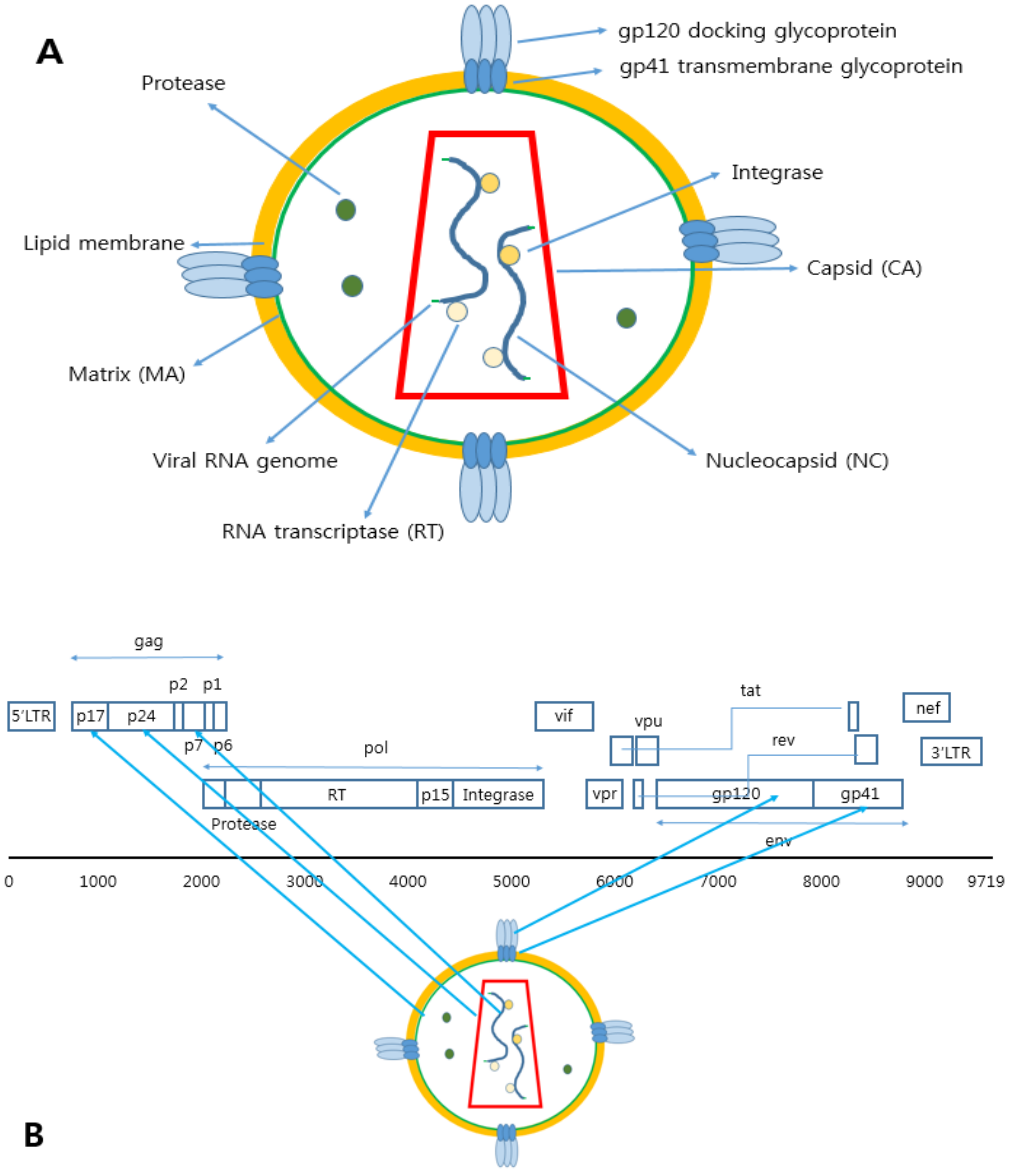

Figure 1.1. Diagram and structure of viral RNA genome.

(A) Diagram of HIV. This figure was from (119). (B) RNA genome structure of HIV-1. HIV has a 9.2kb unspliced genomic transcript which encodes for gag and pol precursors; a singly spliced, 4.5 kb encoding for env, Vif, Vpr and Vpu and a multiply spliced, 2 kb mRNA encoding for Tat, Rev and Nef. This figure was modified from (120).

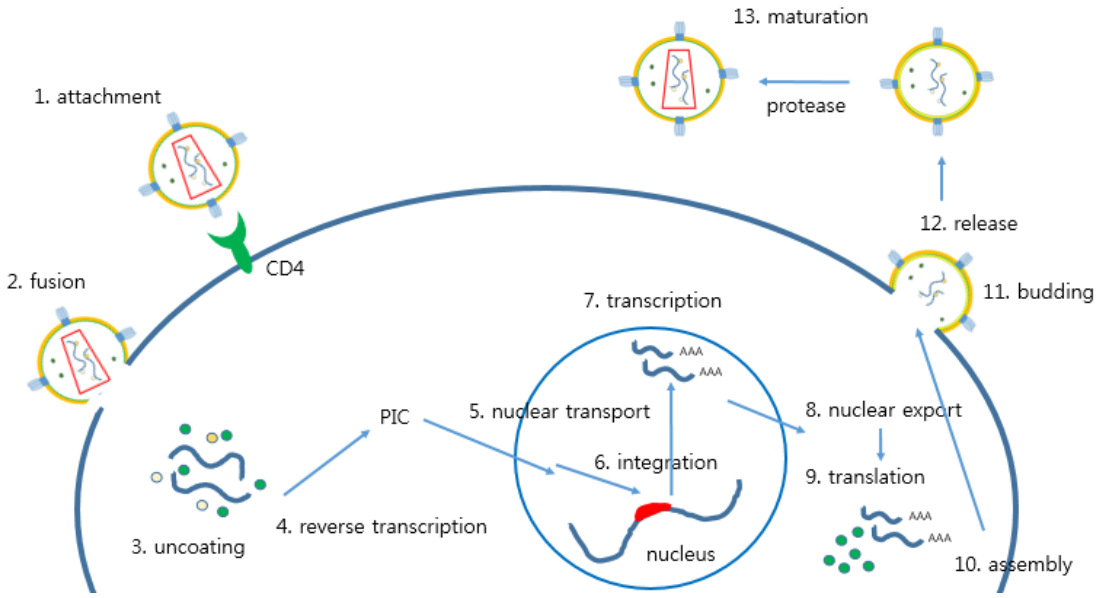

Figure 1.2. HIV-1 life cycle and potential targets (modified from (121)).

Step 1: Viral attachment with the engagement between viral gp120 and cellular CD4.

Step 2: Membrane fusion between viral membrane and cellular membrane.

Step 3: Viral uncoating resulting in the release of viral genome to cytoplasm.

Step 4: Viral RNA is converted into DNA by a viral reverse transcriptase.

Step 5: Pre-integration complex (PIC) is imported to cell nucleus.

Step 6: Viral genome is integrated into host cell DNA by a viral integrase.

Step 7-9: Host cell transcribes viral mRNAs, which are exported to cytosol and translated in cytosol

Step 10-13: Viral genome and proteins are packaged and budded out from cellular membrane with maturation process by a viral protease.

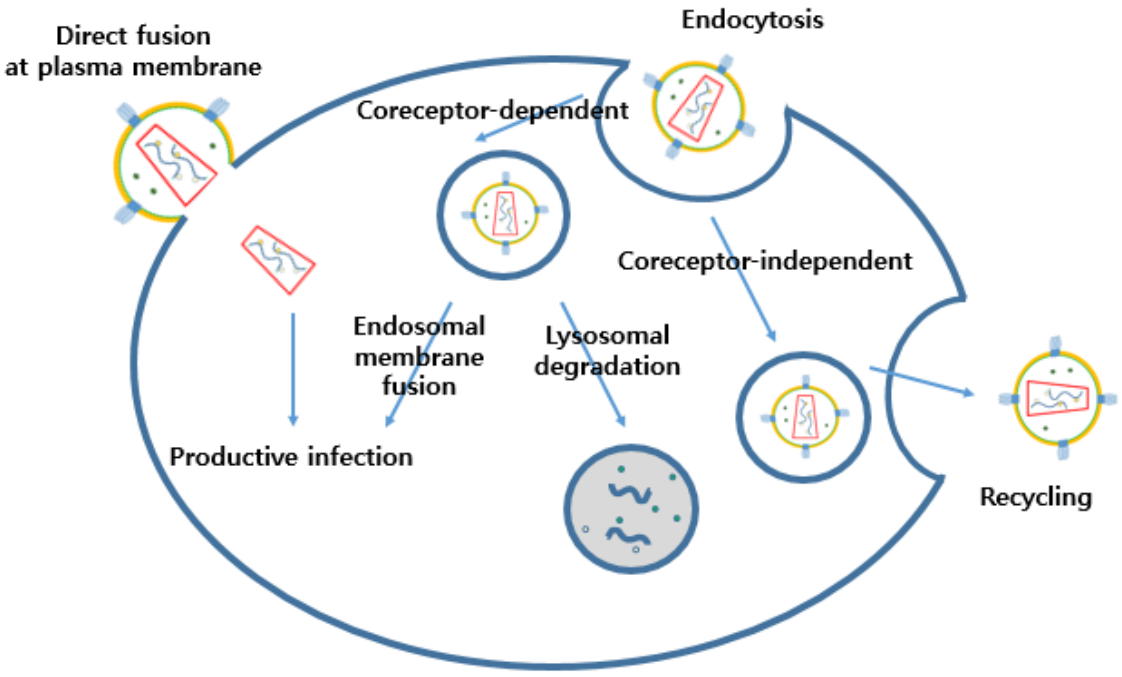

Figure 1.3. Possible productive HIV-1 entry.

Upon the engagement between HIV and CD4 receptor on cell surface, the virus can enter target cells through three non-exclusive pathways. The first pathway is the direct fusion of HIV particles at the plasma membrane. Second, HIV enters cells via receptor-dependent endocytosis and leads to HIV fusion with an endosome membrane, or this could lead to endosome maturation and lysosomal degradation of the virus particle. In the third pathway, coreceptor engagement might lead to virus membrane and endosome membrane fusion and release of the viral genome into the cytosol; alternatively, in the absence of the appropriate coreceptor or coreceptor independent transfer, viruses might be recycled back to the extracellular medium as infectious particles capable of mediating a productive infection. This figure was modified from (122).

1.5. References

1. Fenner F. 1975. International Committee on Taxonomy of Viruses: official names for viral families. Acta virologica 19:93.
2. Smith JA, Daniel R. 2006. Following the path of the virus: the exploitation of host DNA repair mechanisms by retroviruses. ACS chemical biology 1:217-226.
3. Telesnitsky A. 2010. Retroviruses: Molecular Biology, Genomics and Pathogenesis. Future virology 5:539-543.
4. Lu K, Heng X, Summers MF. 2011. Structural determinants and mechanism of HIV-1 genome packaging. Journal of molecular biology 410:609-633.
5. Pang Y, Song H, Kim JH, Hou X, Cheng W. 2014. Optical trapping of individual human immunodeficiency viruses in culture fluid reveals heterogeneity with single-molecule resolution. Nature nanotechnology 9:624-630.
6. Gelderblom HR, Hausmann EH, Ozel M, Pauli G, Koch MA. 1987. Fine structure of human immunodeficiency virus (HIV) and immunolocalization of structural proteins. Virology 156:171-176.
7. Freed EO. 1998. HIV-1 gag proteins: diverse functions in the virus life cycle. Virology 251:1-15.
8. Robert-Guroff M. 2002. HIV regulatory and accessory proteins: new targets for vaccine development. DNA and cell biology 21:597-598.
9. Bour S, Strebel K. 2000. HIV accessory proteins: multifunctional components of a complex system. Advances in pharmacology 48:75-120.
10. Lasky LA, Nakamura G, Smith DH, Fennie C, Shimasaki C, Patzer E, Berman P, Gregory T, Capon DJ. 1987. Delineation of a region of the human immunodeficiency virus type 1 gp120 glycoprotein critical for interaction with the CD4 receptor. Cell 50:975-985.
11. Lyumkis D, Julien JP, de Val N, Cupo A, Potter CS, Klasse PJ, Burton DR, Sanders RW, Moore JP, Carragher B, Wilson IA, Ward AB. 2013. Cryo-EM structure of a fully glycosylated soluble cleaved HIV-1 envelope trimer. Science 342:1484-1490.
12. Julien JP, Cupo A, Sok D, Stanfield RL, Lyumkis D, Deller MC, Klasse PJ, Burton DR, Sanders RW, Moore JP, Ward AB, Wilson IA. 2013. Crystal structure of a soluble cleaved HIV-1 envelope trimer. Science 342:1477-1483.
13. Layne SP, Merges MJ, Dembo M, Spouge JL, Nara PL. 1990. HIV requires multiple gp120 molecules for CD4-mediated infection. Nature 346:277-279.
14. Crowe SM, Mills J, Kirihara J, Boothman J, Marshall JA, McGrath MS. 1990. Full-length recombinant CD4 and recombinant gp120 inhibit fusion between HIV infected macrophages and uninfected CD4-expressing T-lymphoblastoid cells. AIDS research and human retroviruses 6:1031-1037.
15. Weiss RA. 1993. How does HIV cause AIDS? Science 260:1273-1279.
16. Lutalo T, Gray RH, Wawer M, Sewankambo N, Serwadda D, Laeyendecker O, Kiwanuka N, Nalugoda F, Kigozi G, Ndyanabo A, Bwanika JB, Reynolds SJ, Quinn T, Opendi P. 2007. Survival of HIV-infected treatment-naive individuals with documented dates of seroconversion in Rakai, Uganda. Aids 21 Suppl 6:S15-19.
17. van der Graaf M, Diepersloot RJ. 1986. Transmission of human immunodeficiency virus (HIV/HTLV-III/LAV): a review. Infection 14:203-211.

18. Kurimura T. 1993. [Target cells for HIV and the mechanism of its penetration into the cells]. Nihon rinsho. Japanese journal of clinical medicine 51 Suppl:73-75.
19. Finkel TH, Banda NK. 1994. Indirect mechanisms of HIV pathogenesis: how does HIV kill T cells? Current opinion in immunology 6:605-615.
20. Dyrhol-Riise AM, Ohlsson M, Skarstein K, Nygaard SJ, Olofsson J, Jonsson R, Asjo B. 2001. T cell proliferation and apoptosis in HIV-1-infected lymphoid tissue: impact of highly active antiretroviral therapy. Clinical immunology 101:180-191.
21. Mofenson LM, Korelitz J, Meyer WA, 3rd, Bethel J, Rich K, Pahwa S, Moye J, Jr., Nugent R, Read J. 1997. The relationship between serum human immunodeficiency virus type 1 (HIV-1) RNA level, CD4 lymphocyte percent, and long-term mortality risk in HIV-1-infected children. National Institute of Child Health and Human Development Intravenous Immunoglobulin Clinical Trial Study Group. The Journal of infectious diseases 175:1029-1038.
22. Alcabes P, Schoenbaum EE, Klein RS. 1993. CD4+ lymphocyte level and rate of decline as predictors of AIDS in intravenous drug users with HIV infection. Aids 7:513-517.
23. Cohen MS, Hellmann N, Levy JA, DeCock K, Lange J. 2008. The spread, treatment, and prevention of HIV-1: evolution of a global pandemic. The Journal of clinical investigation 118:1244-1254.
24. 2013. "Fact Sheet". UNAIDS.org.
25. Kanki PJ, Hopper JR, Essex M. 1987. The origins of HIV-1 and HTLV-4/HIV-2. Annals of the New York Academy of Sciences 511:370-375.
26. Sharp PM, Hahn BH. 2011. Origins of HIV and the AIDS pandemic. Cold Spring Harbor perspectives in medicine 1:a006841.
27. Gilbert PB, McKeague IW, Eisen G, Mullins C, Gueye NA, Mboup S, Kanki PJ. 2003. Comparison of HIV-1 and HIV-2 infectivity from a prospective cohort study in Senegal. Statistics in medicine 22:573-593.
28. Chan DC, Kim PS. 1998. HIV entry and its inhibition. Cell 93:681-684.
29. Auewarakul P, Wacharapornin P, Srichatrapimuk S, Chutipongtanate S, Puthavathana P. 2005. Uncoating of HIV-1 requires cellular activation. Virology 337:93-101.
30. Usami Y, Popov S, Popova E, Inoue M, Weissenhorn W, H GG. 2009. The ESCRT pathway and HIV-1 budding. Biochemical Society transactions 37:181-184.
31. Bukrinskaya AG. 2004. HIV-1 assembly and maturation. Archives of virology 149:1067-1082.
32. Das K, Arnold E. 2013. HIV-1 reverse transcriptase and antiviral drug resistance. Part 1. Current opinion in virology 3:111-118.
33. Das K, Arnold E. 2013. HIV-1 reverse transcriptase and antiviral drug resistance. Part 2. Current opinion in virology 3:119-128.
34. Metifiot M, Marchand C, Pommier Y. 2013. HIV integrase inhibitors: 20-year landmark and challenges. Advances in pharmacology 67:75-105.
35. Wensing AM, van Maarseveen NM, Nijhuis M. 2010. Fifteen years of HIV Protease Inhibitors: raising the barrier to resistance. Antiviral research 85:59-74.
36. Ashorn P, McQuade TJ, Thaisrivongs S, Tomasselli AG, Tarpley WG, Moss B. 1990. An inhibitor of the protease blocks maturation of human and simian immunodeficiency viruses and spread of infection. Proceedings of the National

Academy of Sciences of the United States of America 87:7472-7476.
37. Perelson AS, Ribeiro RM. 2008. Estimating drug efficacy and viral dynamic parameters: HIV and HCV. Statistics in medicine 27:4647-4657.
38. Rambaut A, Posada D, Crandall KA, Holmes EC. 2004. The causes and consequences of HIV evolution. Nature reviews. Genetics 5:52-61.
39. Robertson DL, Hahn BH, Sharp PM. 1995. Recombination in AIDS viruses. Journal of molecular evolution 40:249-259.
40. Tozzi V, Bellagamba R, Castiglione F, Amendola A, Ivanovic J, Nicastri E, Libertone R, D'Offizi G, Liuzzi G, Gori C, Forbici F, D'Arrigo R, Bertoli A, Salvatori MF, Capobianchi MR, Antinori A, Perno CF, Narciso P. 2008. Plasma HIV RNA decline and emergence of drug resistance mutations among patients with multiple virologic failures receiving resistance testing-guided HAART. AIDS research and human retroviruses 24:787-796.
41. Loveday C, Devereux H, Huckett L, Johnson M. 1999. High prevalence of multiple drug resistance mutations in a UK HIV/AIDS patient population. Aids 13:627-628.
42. Schmit JC, Cogniaux J, Hermans P, Van Vaeck C, Sprecher S, Van Remoortel B, Witvrouw M, Balzarini J, Desmyter J, De Clercq E, Vandamme AM. 1996. Multiple drug resistance to nucleoside analogues and nonnucleoside reverse transcriptase inhibitors in an efficiently replicating human immunodeficiency virus type 1 patient strain. The Journal of infectious diseases 174:962-968.
43. Brinkman K, Delnoy PP, de Pauw B. 1998. Highly active antiretroviral therapy (HAART) and prolonged survival of a patient with an HIV-related Burkitt lymphoma, despite an intracardiac relapse. International journal of STD & AIDS 9:773-775.
44. Morris K. 1998. HAART and host: balancing the response to HIV-1. Highly active antiretroviral therapy. Lancet 352:1686.
45. Telenti A, Aubert V, Spertini F. 2002. Individualising HIV treatment--pharmacogenetics and immunogenetics. Lancet 359:722-723.
46. Fumero E, Podzamczer D. 2003. New patterns of HIV-1 resistance during HAART. Clinical microbiology and infection : the official publication of the European Society of Clinical Microbiology and Infectious Diseases 9:1077-1084.
47. Chan DC, Fass D, Berger JM, Kim PS. 1997. Core structure of gp41 from the HIV envelope glycoprotein. Cell 89:263-273.
48. Wild C, Oas T, McDanal C, Bolognesi D, Matthews T. 1992. A synthetic peptide inhibitor of human immunodeficiency virus replication: correlation between solution structure and viral inhibition. Proceedings of the National Academy of Sciences of the United States of America 89:10537-10541.
49. Wild CT, Shugars DC, Greenwell TK, McDanal CB, Matthews TJ. 1994. Peptides corresponding to a predictive alpha-helical domain of human immunodeficiency virus type 1 gp41 are potent inhibitors of virus infection. Proceedings of the National Academy of Sciences of the United States of America 91:9770-9774.
50. Kilby JM, Hopkins S, Venetta TM, DiMassimo B, Cloud GA, Lee JY, Alldredge L, Hunter E, Lambert D, Bolognesi D, Matthews T, Johnson MR, Nowak MA, Shaw GM, Saag MS. 1998. Potent suppression of HIV-1 replication in humans by T-20, a peptide inhibitor of gp41-mediated virus entry. Nature medicine 4:1302-1307.
51. Armand-Ugon M, Gutierrez A, Clotet B, Este JA. 2003. HIV-1 resistance to the

gp41-dependent fusion inhibitor C-34. Antiviral research 59:137-142.
52. Jiang S, Lin K, Strick N, Neurath AR. 1993. HIV-1 inhibition by a peptide. Nature 365:113.
53. Lu M, Blacklow SC, Kim PS. 1995. A trimeric structural domain of the HIV-1 transmembrane glycoprotein. Nature structural biology 2:1075-1082.
54. Munoz-Barroso I, Durell S, Sakaguchi K, Appella E, Blumenthal R. 1998. Dilation of the human immunodeficiency virus-1 envelope glycoprotein fusion pore revealed by the inhibitory action of a synthetic peptide from gp41. The Journal of cell biology 140:315-323.
55. Gallo SA, Puri A, Blumenthal R. 2001. HIV-1 gp41 six-helix bundle formation occurs rapidly after the engagement of gp120 by CXCR4 in the HIV-1 Env-mediated fusion process. Biochemistry 40:12231-12236.
56. Martin N, Welsch S, Jolly C, Briggs JA, Vaux D, Sattentau QJ. 2010. Virological synapse-mediated spread of human immunodeficiency virus type 1 between T cells is sensitive to entry inhibition. Journal of virology 84:3516-3527.
57. Liu S, Lu H, Niu J, Xu Y, Wu S, Jiang S. 2005. Different from the HIV fusion inhibitor C34, the anti-HIV drug Fuzeon (T-20) inhibits HIV-1 entry by targeting multiple sites in gp41 and gp120. The Journal of biological chemistry 280:11259-11273.
58. LaBonte J, Lebbos J, Kirkpatrick P. 2003. Enfuvirtide. Nature reviews. Drug discovery 2:345-346.
59. Patel IH, Zhang X, Nieforth K, Salgo M, Buss N. 2005. Pharmacokinetics, pharmacodynamics and drug interaction potential of enfuvirtide. Clinical pharmacokinetics 44:175-186.
60. Carr A. 2003. Enfuvirtide, an HIV-1 fusion inhibitor. The New England journal of medicine 349:1770-1771; author reply 1770-1771.
61. Burton A. 2003. Enfuvirtide approved for defusing HIV. The Lancet. Infectious diseases 3:260.
62. Cipriani S, Francisci D, Mencarelli A, Renga B, Schiaroli E, D'Amore C, Baldelli F, Fiorucci S. 2013. Efficacy of the CCR5 antagonist maraviroc in reducing early, ritonavir-induced atherogenesis and advanced plaque progression in mice. Circulation 127:2114-2124.
63. Asin-Milan O, Chamberland A, Wei Y, Haidara A, Sylla M, Tremblay CL. 2013. Mutations in variable domains of the HIV-1 envelope gene can have a significant impact on maraviroc and vicriviroc resistance. AIDS research and therapy 10:15.
64. Biswas P, Tambussi G, Lazzarin A. 2007. Access denied? The status of co-receptor inhibition to counter HIV entry. Expert opinion on pharmacotherapy 8:923-933.
65. Liu S, Jing W, Cheung B, Lu H, Sun J, Yan X, Niu J, Farmar J, Wu S, Jiang S. 2007. HIV gp41 C-terminal heptad repeat contains multifunctional domains. Relation to mechanisms of action of anti-HIV peptides. The Journal of biological chemistry 282:9612-9620.
66. Liu S, Jiang S. 2004. High throughput screening and characterization of HIV-1 entry inhibitors targeting gp41: theories and techniques. Current pharmaceutical design 10:1827-1843.
67. Liu S, Wu S, Jiang S. 2007. HIV entry inhibitors targeting gp41: from polypeptides to small-molecule compounds. Current pharmaceutical design 13:143-162.

68. Xu L, Pozniak A, Wildfire A, Stanfield-Oakley SA, Mosier SM, Ratcliffe D, Workman J, Joall A, Myers R, Smit E, Cane PA, Greenberg ML, Pillay D. 2005. Emergence and evolution of enfuvirtide resistance following long-term therapy involves heptad repeat 2 mutations within gp41. Antimicrobial agents and chemotherapy 49:1113-1119.
69. Greenberg ML, Cammack N. 2004. Resistance to enfuvirtide, the first HIV fusion inhibitor. The Journal of antimicrobial chemotherapy 54:333-340.
70. Baldwin C, Berkhout B. 2007. HIV-1 drug-resistance and drug-dependence. Retrovirology 4:78.
71. Poveda E, Rodes B, Toro C, Martin-Carbonero L, Gonzalez-Lahoz J, Soriano V. 2002. Evolution of the gp41 env region in HIV-infected patients receiving T-20, a fusion inhibitor. Aids 16:1959-1961.
72. Reynes J, Arasteh K, Clotet B, Cohen C, Cooper DA, Delfraissy JF, Eron JJ, Henry K, Katlama C, Kuritzkes DR, Lalezari JP, Lange J, Lazzarin A, Montaner JS, Nelson M, M OH, Stellbrink HJ, Trottier B, Walmsley SL, Buss NE, Demasi R, Chung J, Donatacci L, Guimaraes D, Rowell L, Valentine A, Wilkinson M, Salgo MP. 2007. TORO: ninety-six-week virologic and immunologic response and safety evaluation of enfuvirtide with an optimized background of antiretrovirals. AIDS patient care and STDs 21:533-543.
73. Trottier B, Walmsley S, Reynes J, Piliero P, O'Hearn M, Nelson M, Montaner J, Lazzarin A, Lalezari J, Katlama C, Henry K, Cooper D, Clotet B, Arasteh K, Delfraissy JF, Stellbrink HJ, Lange J, Kuritzkes D, Eron JJ, Jr., Cohen C, Kinchelow T, Bertasso A, Labriola-Tompkins E, Shikhman A, Atkins B, Bourdeau L, Natale C, Hughes F, Chung J, Guimaraes D, Drobnes C, Bader-Weder S, Demasi R, Smiley L, Salgo MP. 2005. Safety of enfuvirtide in combination with an optimized background of antiretrovirals in treatment-experienced HIV-1-infected adults over 48 weeks. Journal of acquired immune deficiency syndromes 40:413-421.
74. Lalezari JP, DeJesus E, Northfelt DW, Richmond G, Wolfe P, Haubrich R, Henry D, Powderly W, Becker S, Thompson M, Valentine F, Wright D, Carlson M, Riddler S, Haas FF, DeMasi R, Sista PR, Salgo M, Delehanty J. 2003. A controlled Phase II trial assessing three doses of enfuvirtide (T-20) in combination with abacavir, amprenavir, ritonavir and efavirenz in non-nucleoside reverse transcriptase inhibitor-naive HIV-infected adults. Antiviral therapy 8:279-287.
75. Lalezari JP, Eron JJ, Carlson M, Cohen C, DeJesus E, Arduino RC, Gallant JE, Volberding P, Murphy RL, Valentine F, Nelson EL, Sista PR, Dusek A, Kilby JM. 2003. A phase II clinical study of the long-term safety and antiviral activity of enfuvirtide-based antiretroviral therapy. Aids 17:691-698.
76. Kilby JM, Lalezari JP, Eron JJ, Carlson M, Cohen C, Arduino RC, Goodgame JC, Gallant JE, Volberding P, Murphy RL, Valentine F, Saag MS, Nelson EL, Sista PR, Dusek A. 2002. The safety, plasma pharmacokinetics, and antiviral activity of subcutaneous enfuvirtide (T-20), a peptide inhibitor of gp41-mediated virus fusion, in HIV-infected adults. AIDS research and human retroviruses 18:685-693.
77. Ni L, Gao GF, Tien P. 2005. Rational design of highly potent HIV-1 fusion inhibitory proteins: implication for developing antiviral therapeutics. Biochemical and biophysical research communications 332:831-836.

78. Qi Z, Shi W, Xue N, Pan C, Jing W, Liu K, Jiang S. 2008. Rationally designed anti-HIV peptides containing multifunctional domains as molecule probes for studying the mechanisms of action of the first and second generation HIV fusion inhibitors. The Journal of biological chemistry 283:30376-30384.
79. Eggink D, Berkhout B, Sanders RW. 2010. Inhibition of HIV-1 by fusion inhibitors. Current pharmaceutical design 16:3716-3728.
80. Herold N, Anders-Osswein M, Glass B, Eckhardt M, Muller B, Krausslich HG. 2014. HIV-1 entry in SupT1-R5, CEM-ss, and primary CD4+ T cells occurs at the plasma membrane and does not require endocytosis. Journal of virology 88:13956-13970.
81. Miyauchi K, Kim Y, Latinovic O, Morozov V, Melikyan GB. 2009. HIV enters cells via endocytosis and dynamin-dependent fusion with endosomes. Cell 137:433-444.
82. Eckert DM, Kim PS. 2001. Mechanisms of viral membrane fusion and its inhibition. Annual review of biochemistry 70:777-810.
83. Marsh M, Helenius A. 2006. Virus entry: open sesame. Cell 124:729-740.
84. McClure MO, Marsh M, Weiss RA. 1988. Human immunodeficiency virus infection of CD4-bearing cells occurs by a pH-independent mechanism. The EMBO journal 7:513-518.
85. Wyatt R, Sodroski J. 1998. The HIV-1 envelope glycoproteins: fusogens, antigens, and immunogens. Science 280:1884-1888.
86. Gallo SA, Finnegan CM, Viard M, Raviv Y, Dimitrov A, Rawat SS, Puri A, Durell S, Blumenthal R. 2003. The HIV Env-mediated fusion reaction. Biochimica et biophysica acta 1614:36-50.
87. Bieniasz PD, Fridell RA, Aramori I, Ferguson SS, Caron MG, Cullen BR. 1997. HIV-1-induced cell fusion is mediated by multiple regions within both the viral envelope and the CCR-5 co-receptor. The EMBO journal 16:2599-2609.
88. Brandt SM, Mariani R, Holland AU, Hope TJ, Landau NR. 2002. Association of chemokine-mediated block to HIV entry with coreceptor internalization. The Journal of biological chemistry 277:17291-17299.
89. Maddon PJ, McDougal JS, Clapham PR, Dalgleish AG, Jamal S, Weiss RA, Axel R. 1988. HIV infection does not require endocytosis of its receptor, CD4. Cell 54:865-874.
90. Stein BS, Gowda SD, Lifson JD, Penhallow RC, Bensch KG, Engleman EG. 1987. pH-independent HIV entry into CD4-positive T cells via virus envelope fusion to the plasma membrane. Cell 49:659-668.
91. Hladik F, Sakchalathorn P, Ballweber L, Lentz G, Fialkow M, Eschenbach D, McElrath MJ. 2007. Initial events in establishing vaginal entry and infection by human immunodeficiency virus type-1. Immunity 26:257-270.
92. Sougrat R, Bartesaghi A, Lifson JD, Bennett AE, Bess JW, Zabransky DJ, Subramaniam S. 2007. Electron tomography of the contact between T cells and SIV/HIV-1: implications for viral entry. PLoS pathogens 3:e63.
93. Marechal V, Prevost MC, Petit C, Perret E, Heard JM, Schwartz O. 2001. Human immunodeficiency virus type 1 entry into macrophages mediated by macropinocytosis. Journal of virology 75:11166-11177.
94. Pauza CD, Price TM. 1988. Human immunodeficiency virus infection of T cells and monocytes proceeds via receptor-mediated endocytosis. The Journal of cell

biology 107:959-968.
95. Fredericksen BL, Wei BL, Yao J, Luo T, Garcia JV. 2002. Inhibition of endosomal/lysosomal degradation increases the infectivity of human immunodeficiency virus. Journal of virology 76:11440-11446.
96. Schaeffer E, Soros VB, Greene WC. 2004. Compensatory link between fusion and endocytosis of human immunodeficiency virus type 1 in human CD4 T lymphocytes. Journal of virology 78:1375-1383.
97. Wei BL, Denton PW, O'Neill E, Luo T, Foster JL, Garcia JV. 2005. Inhibition of lysosome and proteasome function enhances human immunodeficiency virus type 1 infection. Journal of virology 79:5705-5712.
98. Aiken C. 1997. Pseudotyping human immunodeficiency virus type 1 (HIV-1) by the glycoprotein of vesicular stomatitis virus targets HIV-1 entry to an endocytic pathway and suppresses both the requirement for Nef and the sensitivity to cyclosporin A. Journal of virology 71:5871-5877.
99. Daecke J, Fackler OT, Dittmar MT, Krausslich HG. 2005. Involvement of clathrin-mediated endocytosis in human immunodeficiency virus type 1 entry. Journal of virology 79:1581-1594.
100. Sloan RD, Kuhl BD, Mesplede T, Munch J, Donahue DA, Wainberg MA. 2013. Productive entry of HIV-1 during cell-to-cell transmission via dynamin-dependent endocytosis. Journal of virology 87:8110-8123.
101. Munk C, Landau NR. 2003. Production and use of HIV-1 luciferase reporter viruses. Current protocols in pharmacology / editorial board, S.J. Enna Chapter 12:Unit12 15.
102. Richards KH, Clapham PR. 2006. Human immunodeficiency viruses: propagation, quantification, and storage. Current protocols in microbiology Chapter 15:Unit15J 11.
103. Kim JH, Song H, Austin JL, Cheng W. 2013. Optimized Infectivity of the Cell-Free Single-Cycle Human Immunodeficiency Viruses Type 1 (HIV-1) and Its Restriction by Host Cells. PloS one 8:e67170.
104. Montefiori DC. 2005. Evaluating neutralizing antibodies against HIV, SIV, and SHIV in luciferase reporter gene assays. Current protocols in immunology / edited by John E. Coligan ... [et al.] Chapter 12:Unit 12 11.
105. McMahon MA, Shen L, Siliciano RF. 2009. New approaches for quantitating the inhibition of HIV-1 replication by antiviral drugs in vitro and in vivo. Current opinion in infectious diseases 22:574-582.
106. Klasse PJ. 2012. The molecular basis of HIV entry. Cellular microbiology 14:1183-1192.
107. Marechal V, Clavel F, Heard JM, Schwartz O. 1998. Cytosolic Gag p24 as an index of productive entry of human immunodeficiency virus type 1. Journal of virology 72:2208-2212.
108. Vidricaire G, Tardif MR, Tremblay MJ. 2003. The low viral production in trophoblastic cells is due to a high endocytic internalization of the human immunodeficiency virus type 1 and can be overcome by the pro-inflammatory cytokines tumor necrosis factor-alpha and interleukin-1. The Journal of biological chemistry 278:15832-15841.
109. Roberts PC, Kipperman T, Compans RW. 1999. Vesicular stomatitis virus G protein

acquires pH-independent fusion activity during transport in a polarized endometrial cell line. Journal of virology 73:10447-10457.
110. de la Vega M, Marin M, Kondo N, Miyauchi K, Kim Y, Epand RF, Epand RM, Melikyan GB. 2011. Inhibition of HIV-1 endocytosis allows lipid mixing at the plasma membrane, but not complete fusion. Retrovirology 8:99.
111. McClure SJ, Robinson PJ. 1996. Dynamin, endocytosis and intracellular signalling (review). Molecular membrane biology 13:189-215.
112. Pucadyil TJ, Schmid SL. 2008. Real-time visualization of dynamin-catalyzed membrane fission and vesicle release. Cell 135:1263-1275.
113. Zhang P, Hinshaw JE. 2001. Three-dimensional reconstruction of dynamin in the constricted state. Nature cell biology 3:922-926.
114. Roux A, Uyhazi K, Frost A, De Camilli P. 2006. GTP-dependent twisting of dynamin implicates constriction and tension in membrane fission. Nature 441:528-531.
115. Klausner RD, Van Renswoude J, Ashwell G, Kempf C, Schechter AN, Dean A, Bridges KR. 1983. Receptor-mediated endocytosis of transferrin in K562 cells. The Journal of biological chemistry 258:4715-4724.
116. Dautry-Varsat A, Ciechanover A, Lodish HF. 1983. pH and the recycling of transferrin during receptor-mediated endocytosis. Proceedings of the National Academy of Sciences of the United States of America 80:2258-2262.
117. Sun XJ, Yau VK, Briggs BJ, Whittaker GR. 2005. Role of clathrin-mediated endocytosis during vesicular stomatitis virus entry into host cells. Virology 338:53-60.
118. O'Doherty U, Swiggard WJ, Malim MH. 2000. Human immunodeficiency virus type 1 spinoculation enhances infection through virus binding. Journal of virology 74:10074-10080.
119. US National Institute of Health (redrawn by en:User:Carl Henderson). http://web.archive.org/web/20050531012945/http://www.niaid.nih.gov/factsheets/howhiv.htm.
120. HIV sequence database. http://www.hiv.lanl.gov/.
121. Engelman A, Cherepanov P. 2012. The structural biology of HIV-1: mechanistic and therapeutic insights. Nature reviews. Microbiology 10:279-290.
122. Permanyer M, Ballana E, Este JA. 2010. Endocytosis of HIV: anything goes. Trends in microbiology 18:543-551.

Chapter 2.

Preparation and Characterization of Single-cycle Replicative, Fluorescently-labeled HIV-1 Virions

2.1. Abstract

Molecularly cloned HIV-1 that is capable of only a single round of infection (1, 2), called single-cycle replicative virion, offers a unique tool to address important questions related to the early event of viral infection, such as viral entry. In this study, we established how to measure the concentration of infectious particles (Ci.p.) for measuring infectivity by taking an advantage of viral protein, Vpr, suppressing G2 cell cycle (3). The infectivity was then optimized by varying several virus culture conditions. Among these culture variables, EGFP-Vpr plasmid input, virion harvest time, media replacement after transfection, and envelope plasmid input can all improve HIV-1 infectivity by reducing the number of defective virions.

In order to investigate viral entry, we visualized virions by tagging Vpr, a viral accessory protein physically associated with the virus core, with EGFP (4-6). Although the imaging method cannot provide a direct conversion between the number of virion particles

and the concentration of physical particles (Cp.p.) due to the potential presence of virions without EGFP, they were strongly correlated supporting p24 values as a measurement of viral Cp.p. in our imaging method. Furthermore, we characterized HIV-1 tagged with EGFP-Vpr in terms of size, mean intensity, and sum intensity distributions. Even though there was a trade-off effect between fluorescent intensity and infectivity, we were able to pick 0.15 μg/ml of EGFP-Vpr plasmid input which results in the highest infectivity and reasonable intensity profiles amid the broad distribution of intensities. This will help further investigate the mechanism of viral entry as well as develop deep understanding of HIV-1 virions.

2.2. Introduction

The infectivity of retroviruses such as HIV-1 in plasma or cultured media is generally less than 0.1% (7-12). Although there have been extensive studies about this virus over the past 30 years (13-19), the molecular mechanisms that underlie this apparent low infectivity are not fully understood. Broadly defined, two different mechanisms have been proposed to explain this phenomenon.

One possible mechanism is that a large proportion of virions are inherently defective, with only a small portion of virions highly infectious. In other words, the average infectivity of a virus pool is low because of the presence of defective virions. Alternatively, virions are intrinsically infectious but the viral-cell interactions lead to a major barrier for HIV-1 infection, which limits the apparent infectivity of HIV-1 virions. Overall, recent studies suggested that HIV-1 virion attachment to host cells is an inefficient process, but once virions enter a host cell, subsequent steps can occur with a relatively high efficiency.

Consistently, polycations or spinoculation has been used for facilitating and increasing virus binding to a cell and apparent infectivity. (20, 21). This model argues against the presence of defective virions in a virus pool, but supports the hypothesis that HIV-1 virions are intrinsically infectious. However, the high infectivity of HIV-1 virions revealed from the above studies was for viruses that were either pre-adsorbed on host cell surface or which had already initiated reverse transcription. In the virus pool, there were still large populations of unadsorbed virions or virions that had not initiated reverse transcription. Whether they are defective virions, i.e., virions that are deficient in receptor engagement or initiation of reverse transcription remains unknown. The production of defective virions due to mutations results in the heterogeneity of a virus pool, which may significantly complicate the study of viral infectivity.

Alternatively, single-cycle replicative HIV-1 (1, 2) allows to address these important questions. The production of these virions in cell culture use a mutant provirus clone together with a separate plasmid that drives the expression of viral envelope glycoproteins. Because viral proteins are expressed from cloned DNA instead of the provirus reversed transcribed from a RNA genome by reverse transcriptase (RT), mutations in viral proteins that arise from RT errors or APOBEC3 activity are virtually excluded. By varying culture conditions used to produce these virions, one can potentially optimize the infectivity of HIV-1 and address the intrinsic infectivity of these virions. Moreover, because cells infected by these single-cycle virions result exclusively from the initial input virus, the efficiency of provirus integration and that of viral entry can be correlated without complications from multiple rounds of infection.

Although single-cycle HIV-1 virions have been extensively used for viral

neutralization assays (22) and evaluation of antiviral drugs (23), conditions to optimize their infectivity in cell culture have not been fully reported. The typical procedures use an equal weight mixture of provirus and envelope plasmids for transfection in 293 or 293T cells, and virions are harvested 48 hours post transfection (1). Because the expression of provirus and envelope glycoproteins is separate in two plasmids, the ratio between the two plasmids may pose the expression of Gag and envelope glycoproteins at different levels. As a result, the overall infectivity of virions may be different depending on the level of envelope protein incorporation (24, 25). Also, there has been no rationale for harvesting virions 48 hours post transfection. Biophysical instability of virion proteins is known to cause virus inactivation with time (7). This inactivation can occur simultaneously with virion production and thus an optimal time frame for harvesting virion from cell culture may be expected. Indeed, recent studies on replicative HIV-1 virions revealed that virions harvested at early time points from culture media have higher infectivity on a per particle basis (12), suggesting that HIV-1 virion infectivity may be optimized through variation in their culture conditions.

To track the behavior of HIV-1 in the cytoplasm of infected cells, virions derived from the X4-tropic NL4-3 provirus clone were tagged internally with EGFP fused to Vpr (4, 5). Vpr is an accessory protein of HIV that physically associates with the virion core (6) and thus this fusion protein serves as a fluorescent marker (5) for virion manipulation. Control experiments showed that EGFP–Vpr also distinguishes virions from microvesicles (26). Alternatively, HIV virions carrying free EGFPs were generated by constructing the provirus clone that carries EGFPs between matrix and capsid proteins through two linkers that can be cleaved by HIV protease during the virion maturation process (27). Viral

membrane and free EGFPs should disappear resulting from virla fusion with the plasma membrane due to their virtually infinite dilution within the plasma membrane and the cytosol (27).

However, a recent study revealed that there is heterogeneity of HIV-1 in terms of protein composition with single-molecule sensitivity (26). For gp120, its copy number varied over one order of magnitude, despite the fact that all these virions were derived from a single clone. This heterogeneity might lead to a broad spectrum of infectivity for individual HIV-1 virions (21), which was hypothesized in the literature (28). Indeed, recent studies have shown that the transmitted 'founder' virus that establishes infection in AIDS patients corresponds to virions with a higher envelope glycoprotein content (29). Because the expression of provirus, envelope glycoproteins, and EGFP-Vpr is separate in three plasmids and there is a possibility that not all three plasmids can transfect each cell, intensity profiles of fluorescent-tagged HIV-1 virion may show heterogeneous phenomena. Although EGFP-Vpr fusion protein in virions allows direct visualization, the potential presence of virions without EGFP may significantly complicate the study of imaging virus.

Thus, characterizing the infectivity and intensity profiles of single-cycle replicative, fluorescently-labeled HIV-1 will help further investigate the mechanism of viral entry as well as develop deep understanding of HIV-1 virions.

2.3. Materials and Methods

Construction of plasmids

NL4-3 is an HIV-1 strain widely used for production of cloned HIV-1 virions (30-32). To produce single-cycle virus, we introduced a frameshift mutation within the

envelope coding region of the NL4-3 provirus, which resulted in premature stop codons in the open reading frame (ORF) for the envelope glycoprotein (31). Cotransfection of the mutant provirus together with envelope expression plasmid in 293T cells allows production of single-cycle virus. Three plasmids, pNL4-3 (cat#114), pEGFP-Vpr (cat#11386), and pNL4-3.Luc3.R^{-}E^{-} (cat#3418) were obtained through the NIH AIDS Research and Reference Reagent Program. Briefly, to construct the provirus DNA that harbors the frameshift mutation in the ORF of the envelope glycoprotein, a 1509-bp DNA fragment between EcoRI and NheI in pNL4-3 was replaced with the corresponding region in pNL4-3.Luc3.R^{-}E^{-}. The resulting plasmid was designated as pNL4-3E^{-}.

To construct the envelope glycoprotein expression plasmid, the Rev/Env expression cassette in pNL4-3 was PCR amplified and subcloned into the vector pcDNA3.1(-) using BamHI and XbaI restriction enzymes. The resulting plasmid was designated as pcDNA3.1REC.

To construct the provirus clone that carries mutations in both Vpr and envelope glycoproteins, the ORF of Vpr in pNL4-3E^{-} was replaced with that of pNL4-3.Luc3.R^{-}E^{-} using two restriction enzymes, PflMI and NheI. The resulting plasmid was designated as pNL4-3R^{-}E^{-}.

To construct the provirus clone that carries enhanced green fluorescent proteins (EGFPs) between matrix and capsid proteins through two linkers that can be cleaved by HIV protease during the virion maturation process (27), three DNA fragments were first PCR-amplified. Fragment 1 uses pNL4-3 as a template, with forward and reverse primers as follows, 5'-GCCAGAGGAGATCTCTCGACG-3', 5'-CCATCGTACGCTGGAGGTTCTGCACTATAGGGTAATTTTGG-3'. Fragment 2 uses

pEGFP-Vpr as a template, with forward and reverse primers as follows, 5'-CTCCAGCGTACGATGGTGAGCAAGGGCGAGGAGC-3', 5'-CTGGCTCGGCCGCTTGTACAGCTCGTCCATGCCGAGAGTG-3'. Fragment 3 uses pNL4-3 as a template, with forward and reverse primers as follows, 5'-GCGGCCGAGCCAGGTCAGCCAAAATTACCCTATAGTG-3', 5'-CACTTCCCCTTGGTTCTCTCATC-3'. These three DNA fragments were digested by BssHII/BsiWI, BsiWI/EagI, or EagI/SphI, respectively, and then sequentially ligated and cloned into pNL4-3E$^-$ using BssHII and SphI restriction sites. The resulting plasmid was designated as pNL4-3E$^-$ MA-EGFP-CA. All of the plasmids constructed above were subjected to sequencing to confirm their identity before their use in cell culture and transfection procedures.

Production of single-cycle replicative, fluorescently-labeled HIV-1 virions

HEK 293T/17 cells (ATCC, Manassas, VA) were cultured at 37°C with 5% CO_2 in DMEM supplemented with 10% FBS (HyClone Laboratories, Logan, UT). Throughout, all cell lines were discarded after ten passages and new aliquots of frozen cells were thawed to improve reproducibility of virion production and infection experiments. To produce single-cycle virions tagged with EGFP, 10^6 293T cells in a 2-ml culture volume were seeded overnight in a 35-mm dish before transfection using the TransIT LT-1 transfection reagent (Mirus Bio, Madison, WI). For each dish, 1 μg of the provirus-containing plasmid pNL4-3R$^-$E$^-$ was used to make the transfection reagent mixture, together with various amount of envelope expression plasmid pcDNA3.1REC and pEGFP-Vpr as indicated throughout the text. The transfection reagent mixture was incubated at room temperature

for 15 min before drop wise addition to the culture media. At designated time points post transfection, the culture media together with the transfection reagents was replaced with fresh complete media and the incubation was continued at 37°C with 5% CO_2. At various time points post transfection, the entire culture media containing single-cycle HIV-1 viruses was collected and filtered through a 0.45-µm syringe filter (Millex-HV PVDF, Millipore) in less than 10 minutes on average. The filtrate was then aliquoted on ice, flash-frozen in either liquid nitrogen or dry ice/ethanol bath and stored in a -80°C freezer. HIV virions carrying free EGFPs were generated by transfection of 293T cells with 1 µg pNL4-3E^{-}MA-EGFP-CA plasmid and 0.1 µg pcDNA3.1REC in 2-ml volume in a 35-mm dish.

Infection assay in TZM-bl cell line

TZM-bl cells (cat#8129, NIH AIDS Research and Reference Reagent Program) were cultured at 37°C with 5% CO_2 in DMEM supplemented with 10% FBS. To determine the concentration of infectious HIV-1 particles, Ci.p., $8X10^4$ TZM-bl cells in a 1-ml culture volume were seeded in each well of a 12-well plate one day prior to infection. On the next day, virus stocks taken out of -80°C freezer were placed in a room temperature water bath until just thawed, and serially diluted in complete media containing 20 µg/ml DEAE-dextran. 100 µl of viruses at each dilution were layered on top of the cell and the infection was continued for two hours at 37°C with gentle rocking every 30 min. At the end of two hours, 1 ml of complete media was added to each well and the incubation was continued at 37°C for 48 hours with 5% CO_2. At the end of 48 hours, cells were fixed in 2% gluteraldehyde at room temperature for five minutes. After fixation, the cells were washed three times with PBS, and stained for 50 min at 37°C using cell staining solution provided

in the beta-galactosidase staining kit (Mirus Bio, Madison, WI). After incubation, the cells were washed three times with milliQ water and the number of blue cells in each well was counted with a Nikon TS100-F inverted microscope.

p24 ELISA Assay

To determine the concentration of physical particles for each virion preparations, Cp.p., we measured p24 values for each virion preparation using p24 ELISA and converted p24 values to concentrations of physical particles. The p24 values were measured using HIV-1 p24 Antigen Capture Kit (Advanced Bioscience Laboratories, Rockville, MD) following the manufacturer's instructions. Briefly, properly diluted virus samples were lysed and captured in a micro-ELISA plate at 37°C for one hour. The wells were then washed and the specifically captured p24 antigen was incubated with human anti-p24 polyclonal antibodies conjugated with peroxidase at 37°C for one hour. At the end of incubation, peroxidase substrate was added and the reaction was continued for 30 minutes at room temperature. The reaction was stopped by adding 2N Sulfuric acid. The absorbance at 450 nm was measured using a SynergyTM HT multi-mode microplate reader. The stoichiometry of Gag protein in HIV-1 has been determined to be approximately 2,500 (33, 34). Using a molecular weight of 24 kD for p24, this yields 10^7 particles per ng of p24. Thus one can estimate the number of physical particles based on p24 ELISA measurement for each virion preparation. Independently, we also validated this method using confocal imaging and direct counting of virion particles. The infectivity of single-cycle HIV-1 was calculated by taking the ratio between infectious particle concentration (Ci.p.) and physical particle concentration (Cp.p.).

Confocal imaging and counting of virions

HIV Virions carrying EGFP-Vpr or free EGFPs at various dilutions in 200 µl complete media (90% DMEM with 10% FBS) were deposited onto a Poly-L-Lysine (PLL) -coated coverslip, and incubated at room temperature for 30 minutes (35). The media was then removed and virions on the surface were fixed with 4% paraformaldehyde (PFA) for 10 minutes at room temperature. The coverslip was then washed with PBS and mounted onto a glass cover slide with 3 µl mounting media, sealed with nail polish and imaged using an Olympus FluoView 500 Laser Scanning Confocal Microscope. The virion particles in a fluorescence image were identified and quantitated using a custom-written MATLAB script. In this script, the virion particles were identified based on a global threshold automatically established by maximizing the inter-class variance between the foreground and background (Otsu's method) (36), which eliminates the use of any subjective parameters during image analysis. Several different areas on a single coverslip sample as noted in each figure were imaged and the resulting particle numbers in each area were averaged and plotted in Figure 2.5A. Each particle size was measured based on the identification of virion particles. Sum intensity was defined as the total intensity from each pixel in one virion. Mean intensity was defined as a ratio of sum intensity to each particle size.

2.4. Results

2.4.1. Measurement of infectious particle concentration (Ci.p.) for single-cycle viruses

Throughout this work, we define infectivity as the fraction of virions that can establish a productive infection in a host indicator cell line. To establish a quantitative

framework for measurement of infectivity, we generated single-cycle virions using NL4-3 virus and infected TZM-bl cell lines (37) using virions produced under various conditions. This cell line has been one of the popular cell lines for HIV-1 infection and thus comparison among labs is possible (38-41). Cells were infected for two hours at 37°C and further incubated for 48 hours to allow production of β-galactosidase in infected cells. We then used X-Gal staining to visualize these infected cells, which appeared in blue color (42). It is worth noting that un-integrated provirus DNA can also turn on Tat transcription (43) and cells may turn blue in the absence of the provirus integration (44). However, this integration-independent infectivity is only 5% of total infectivity observed for NL4-3 virus in TZM-bl cells (45). Thus, counting stained cells under a microscope (Figure 2.1A and B) measures the number of cells that have been productively infected by NL4-3 virus, i.e., provirus has been integrated into cellular chromosomes, which upon transcriptional activation, produces Tat protein that subsequently activates the expression of β-galactosidase.

In the presence of viral Vpr protein (3, 46-48), majorities of blue cells were singles and each blue cell was counted as resulting from one infectious particle under current Multiplicity of Infection (MOI) conditions (0.005). Occasionally, blue cells appeared as clusters due to cell division and the cluster of blue cells was counted as resulting from one infectious particle. This counting method was supported by our observations shown in Figure 2.1C, where the number of clustered blue cells was correlated with the progression of cell cycle. HIV-1 virions carrying Vpr proteins resulted in less clusters of blue cells due to cell cycle arrest by Vpr proteins (3, 46-48). To examine the linearity of this assay, we varied the dilution factors for the input virions and the resulting blue cells were counted. A

typical result is shown in Figure 2.1D, where the number of blue cells was plotted as a function of the dilution factor for each 100 µl of virus. Linear regression of this plot yields a straight line with an intercept close to zero (-5.4±2.5) and a slope of (4.30±0.05) X10^6/ml with adjusted R-square of 0.998. Because MOI were less than 1 under these conditions (the highest MOI = 0.005), this dependence strongly suggests that a single HIV-1 virion is capable of establishing an infection, and each blue cell resulted from infection by a single virus, with 95% chance of being an integrated provirus. In fact, for even the most concentrated virus in these experiments, the total number of viral physical particles as determined using p24 ELISA was less than the total number of starting cells. Thus, the slope in Figure 2.1D directly measures the concentration of infectious particles, Ci.p.. Based on the strong linear correlation, we have used blue-cell counting to determine Ci.p. in TZM-bl cells throughout, and compare them for virions produced under various conditions.

2.4.2. Infectivity improvement of EGFP-Vpr HIV-1 virions

Inhibitory effect of EGFP tagging on virion infectivity

The infectivity for both EGFP-tagged virions, HIV-1 carrying EGFP-Vpr or free EGFPs, is lower than those untagged viruses (21), likely due to the inhibitory effect of EGFP tagging on HIV-1 virion infectivity. This effect of inhibition is clear from Figure 2.2C, where we varied the input pEGFP-Vpr plasmid systematically and measured the infectivity of resulting virions. A similar trend of inhibition was also observed for free EGFP virions, where an increasing fraction of EGFP-tagged mutant provirus decreases virion infectivity (21). There is a trade-off effect between infectivity and fluorescent

intensity, thus the optimized infectivity with low fluorescent intensity may be challenging to observe fluorescent virions. We then decided to measure fluorescent intensities with different inputs of EGFP-Vpr and the result will be discussed in chapter 2.4.4.

Harvest time dependence of virion infectivity

Recent studies on replicative HIV-1 virions revealed that virions harvested at early times from culture media have higher infectivity (12). To explore this phenomenon for single-cycle HIV virions, we produced virions carrying EGFP-Vpr and collected HIV-1 virions at different times post transfection. As revealed in earlier study, infectious particles can be detected as early as six hours post transfection (21), reaching a peak value around 24 hours and the Ci.p. starts to be at a plateau (Figure 2.3A). In contrast, the concentration of physical particles Cp.p. continues to increase until 72 hours (Figure 2.3B). As a result, the infectivity of virions collected at different times shows a pronounced dependence on harvest time, reaching a maximum at 24 hours and dropping off thereafter (Figure 2.3C). The difference in infectivity can be as large as fourfold for virions collected at different time points post transfection. This time dependence has interesting implications for the production of HIV-1 virions by 293T cells; either the virions produced at early times lose infectivity with time, or more defective virions are produced at later times after transfection. The infectivity decay of HIV-1 virions has been reported previously (7), which is attributable to loss of reverse transcriptase activity, biophysical instability of virion particles and possibly gp120 shedding, although the shedding of gp120 was later shown to be insignificant for NL4-3 virus (49). It was revealed that the infectivity decay is not solely due to spontaneous inactivation of these virions in culture media, but rather, production of

defective or less infectious virions occurs at the same time so that the overall rate of infectivity decay speeds up (21).

Media change post transfection increases HIV-1 infectivity

The transfection reagent we used, TransIT-LT1, is a low toxicity reagent that is comprised of a lipid and protein/polyamine mixture. Although media change is not required after transfection using this reagent, we decided to replace the media to test if infectivity of HIV-1 virions changes. As shown in Figure 2.3C, media change has a positive impact on virion infectivity. The infectivity of EGFP-Vpr virions at early harvest times is higher than later ones, similar to the untagged virus (21). Notably, the infectivity of virions generated with media change six hours post transfection (open circles) is three or fourfold higher than those without (filled squares). This increase in infectivity is due to a slight increase in Ci.p. and a concomitant decrease in Cp.p., as shown in Figure 2.3A and B. These results confirm that media change after transfection increases HIV-1 virion infectivity.

Dependence of HIV infectivity on envelope plasmid input

Viral envelope glycoproteins are necessary for virus to productive infect cells (50, 51). Recent studies claims that the low number of envelope spikes on HIV-1 compared to other viruses might be the one of reasons for the inefficient transmission of HIV. (17, 24, 52-54). Based on these observations, a constant mutant provirus DNA (1 µg) was used throughout but the envelope plasmid was varied from 0.1 to 4 µg. Thus, the molar ratio between the two plasmids, provirus and envelope, varied over two orders of magnitude.

Virions were collected at 24 hours post transfection with media change at six hours post transfection. Notably, the infectivity of HIV virions changes with increasing envelope plasmid and shows a plateau at 1 μg envelope plasmid.

However, we have used DEAE-dextran for facilitating virus binding to cells for all infection assays, which may pose a possibility that the increase in infectivity with more input of envelop plasmid is not due solely to higher expression of envelope glycoprotein. DEAE-dextran may increase viral infectivity although the expression of envelope glycoprotein reaches to a plateau. The infectivity of HIV-1 virions prepared from varied inputs of pEnv was assayed as described previously (21) but in the absence of DEAE-dextran. The infectivity increases with increasing pEnv and shows a peak at 2 μg pEnv (Figure 2.4D). The subsequent decrease in virion infectivity may be due to incorporation of gp160 at high pEnv (21), which inhibits productive infection of virions (55, 56). Figure 2.4E shows the fold enhancement of HIV-1 virion infectivity as a function of pEnv due to the inclusion of 20 μg/ml DEAE-dextran in the infectivity assay. The fold enhancement was calculated as the ratio of virion infectivities measured in the presence and absence of DEAE-dextran for the same batch of virions. Thus, the infectivity of HIV virions changes with increasing envelope plasmid.

2.4.3. Measurement of physical particle concentration for single-cycle viruses

The stoichiometry of Gag protein in HIV-1 has been determined to be approximately 2,500 per virion (33, 34). Using a molecular weight of 24 kD for p24, this yields 10^7 particles per ng of p24. One can thus estimate the number of physical particles based on p24 ELISA measurement. To support this approach for measurement of Cp.p., the

concentration of physical particles, we have developed a confocal imaging and quantitation procedure to count the number of virions and examine its correlation with p24 values. This procedure uses virions labeled with EGFP fused to Vpr, which allows direct visualization of virions encapsulating EGFP-Vpr under a confocal fluorescence microscope (Figure 2.5A). To objectively quantitate the number of virions in a field of view (FOV), we developed a custom-written MATLAB script, which could identify fluorescent particles automatically and also output fluorescence intensity associated with each particle for statistical purposes. To examine the correlation between the number of particles and p24 measurement, EGFP-Vpr virions with various p24 values were deposited onto PLL-coated coverslips and the resulting particle numbers in a FOV were measured as described in Experimental Procedures. Figure 2.5B plots one such result, where the number of fluorescent particles identified in a FOV is linearly correlated with their p24 values, with adjusted R-square of 0.992 and intercept on y-axis close to zero. Although this imaging method cannot provide a direct conversion between the number of virion particles and p24 values due to the potential presence of virions without EGFP, this correlation supports p24 values as a measurement of viral Cp.p..

2.4.4. Distributions of virion size and intensity profile

By converting an original fluorescent confocal image to a binary image based on Otsu's method (36), the size in pixels of each virion can be identified. As shown in Figure 2.6A, the distributions of particle size were skewed with all five different virus concentrations from 20 to 100 ng/ml based on p24 values. The majority of particle was 1 or 2 size in pixels, resulting in 1.81 or 2.00 as center values with Gaussian fitting (Figure

2.6A). Based on this observation, particle which are 1 and 2 pixels may be background since the distribution of them was very different compared to that of rest of particles. Therefore, we reanalyzed the data with removing 1 and 2 pixels and fitted Gaussian (Figure 2.6B). The center values were from 7.16 to 8.18 and the average particle sizes with Gaussian fitting were similar with different dilutions of virus, probably implying the majority of particles imaged was a single virion.

With identified virus particles, we further conducted virion intensity mapping by varying pEGFP-Vpr amount from 0.05 to 1 μg/ml. The apparent intensity peak increases with more input of EGFP-Vpr plasmid regardless of the assumption that 1 and 2 pixels are background. Thus, there is a trade-off effect between fluorescent intensity and infectivity based on our previous observation of the highest infectivity with 0.3 μg EGFP-Vpr input, which concentration is 0.15 μg/ml. However, the distributions of intensity, both mean and sum intensities, showed pretty broad (Figure 2.7), meaning virions in culture media were heterogeneous in terms of fluorescent intensity, which was also revealed in our recent work (26). Thus, we were able to pick 0.15 μg/ml of EGFP-Vpr plasmid input which results in the highest infectivity and reasonable intensity profiles amid the broad distribution of intensities for further studies.

2.4.5. Labeling efficiency of EGFP-Vpr

Although EGFP-Vpr fusion protein allows direct visualization of virions encapsulating EGFP-Vpr and the number of virion particles and p24 values were strongly correlated (Figure 2.5B), the potential presence of virions without EGFP may significantly complicate the study of investigating viral entry by imaging them. We compared the

number of HIV-1 carrying EGFP-Vpr and free EGFPs under the same p24 conditions. In this experiment, we produced HIV-1 carrying free EGFPs by transfecting 293T cells with pNL4-3E¯MA-EGFP-CA and pc.DNA3.1REC, resulting in all virus particles identified by p24 ELISA should carry EGFPs. With five different p24 values from 33.3 to 100 ng/ml, about 50% HIV-1 virions have EGPF-Vpr fusion proteins (Figure 2.8). It means the rest of virions without EGFP signal cannot be observed with an approach using fluorescence even though they can still infect cells.

2.5. Discussion

The goal of this study was to characterize HIV-1 carrying EGFP-Vpr in terms of infectivity, fluorescent intensity, and labeling efficiency. The apparent low infectivity of cell-free HIV virions in culture media has not been fully understood. Whether this is due to virions themselves having intrinsically low infectivity or because of viral-cell interactions that limit HIV-1 infection remains to be elucidated. The assumption behind intrinsic low infectivity for these virions is that a large proportion of virion particles are defective, the fraction of which may change in the viral life cycle. The overall infectivity of fluorescently-tagged HIV-1 virions can be improved through variation in culture conditions, suggesting that these conditions work by reducing defective or less infectious virions (Figure 2.2, 2.3, and 2.4). Nevertheless, these improvements are not as dramatic as the impact of host cells on HIV-1 infectivity (21). These results indicate that host cells may cause a major barrier for HIV-1 infectivity even though the intrinsic infectivity of HIV-1 virions can be optimized. Also, the viral-cell interactions likely restrict the infectivity of HIV-1 virions. For all these events, the single-cycle HIV-1 virions are ideal materials to

further address these questions because the single replication cycle allows to dissect individual steps in the viral life cycle and their contribution to the overall infectivity of the virion. For instance, the impact of early events in virus life cycle on infection, such as the kinetics of virion attachment or internalization can be measured and quantitated, which will be further discussed in chapter 3. HIV virions with optimized infectivity can be used in these mechanistic studies to understand the molecular mechanisms of the apparent low infectivity.

With our transfection system, which used two or three plasmid for producing virions, there is a possibility that not all plasmids can transfect each cell. This may contribute to the heterogeneity of HIV-1 in virus pool, resulting in the potential presence of virions without EGFP. Although our imaging method cannot provide a direct conversion between the number of virion particles and p24 values due to the potential presence of virions without EGFP, the strong correlation supports p24 values as a measurement of viral Cp.p.. Furthermore, we were able to choose 0.15 μg/ml EGFP-Vpr which results in the highest infectivity and reasonable intensity profiles amid the broad distribution of intensities for further studies even though there is a trade-off effect between fluorescent intensity and infectivity.

Taken together, molecularly cloned HIV-1 that is capable of only a single round of infection (1, 2) offers a unique tool to address important questions related to the early event of viral infection. In this study, we established how to measure the concentration of infectious particles (Ci.p.) for measuring infectivity (Figure 2.1) by taking an advantage of Vpr function suppressing G2 cell cycle (3). The infectivity was then optimized by varying several virus culture conditions, such as, EGFP-Vpr plasmid input (Figure 2.2), virion

harvest time (Figure 2.3), media replacement after transfection (Figure 2.3), and envelope plasmid input (Figure 2.4). Also, fluorescent-tagged virion using EGFP-Vpr fusion protein, which showed ~50% labeling efficiency (Figure 2.8), allows direct visualization of HIV-1 encapsulating EGFP-Vpr based on the strong correlation between the number of virion particles and the concentration of physical particles (Cp.p.) (Figure 2.5B). Furthermore, we were able to pick 0.15 μg/ml of EGFP-Vpr plasmid input which results in the highest infectivity (Figure 2.2C) and reasonable intensity profiles amid the broad distribution of intensities (Figure 2.7) for further imaging studies although there was a trade-off effect between fluorescent intensity and infectivity.

2.6 Acknowledgements

This work was supported by NIH grant 1DP2OD008693-01 to Dr. Wei Cheng and also in part by Research Grant No. 5-FY10-490 to W.C. from the March of Dimes Foundation. The following reagents were obtained through the AIDS Research and Reference Reagent Program, Division of AIDS, National Institute of Allergy and Infectious Diseases (NIAID), National Institutes of Health (NIH): pNL4-3 from Dr. Malcolm Martin; pNL4-3.Luc.R^- E^- from Dr. Nathaniel Landau; pEGFP-Vpr from Warner C. Greene; TZM-bl cells from Dr. John C. Kappes, Dr. Xiaoyun Wu and Tranzyme Inc. Authors thank Dr. Wei Cheng for custom-written MATLAB, Dr. Jin H. Kim for plasmids construction including pNL4-3.E^-, pcDNA3.1REC, and pNL4-3E^- MA-EGFP-CA, Microscopy and Image Analysis Laboratory for Olympus FluoView 500 Laser Scanning Confocal Microscope, and DNA sequencing core for all sequencing results in the University of Michigan.

2.7 Figures

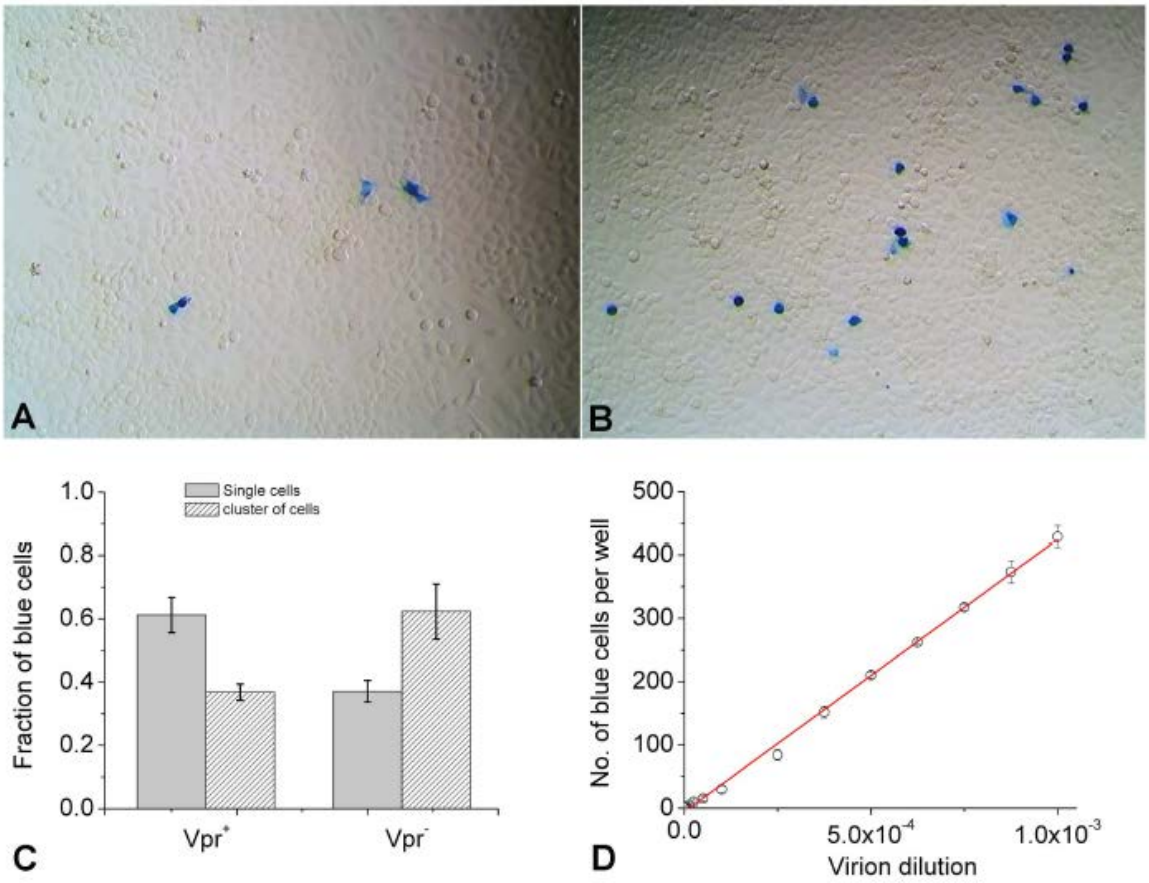

Figure 2.1. Measurement of infectious HIV-1 virions by blue-cell counting in TZM-bl cells.

(A) and (B), representative images of blue TZM-bl cells in 12-well plates for quantitation of infectious particles showing well-resolved single cells and clusters of cells such as doublets. (C) Fraction of single or clustered blue cells depends on the presence of Vpr in single-cycle HIV-1 virions. Vpr^+ virions were generated from transfection of 293T cells with 1 µg pNL4-$3E^-$ and 0.1 µg pcDNA3.1REC. Vpr^- virions were generated from transfection of 293T cells with 1 mg pNL4-$3R^-$ E^- and 0.1 µg pcDNA3.1REC. Both virions were harvested 48 hours post transfection without media change. TZM-bl cells were infected by either of these two virions and the resulting single or clustered blue cells were counted. Error bars are standard deviations from six independent replicates of the same experiments. (D) The number of blue cells was plotted as a function of virion dilution factor per 100 µl of virus. The red line shows its linear regression. The virus was produced by transfection of 293T cells using 1.0 µg pNL4-$3E^-$ plasmid and 0.2 µg pcDNA3.1REC, followed by collection 48 hours post transfection without media change. Error bars are standard deviations from six independent replicates of the same experiments.

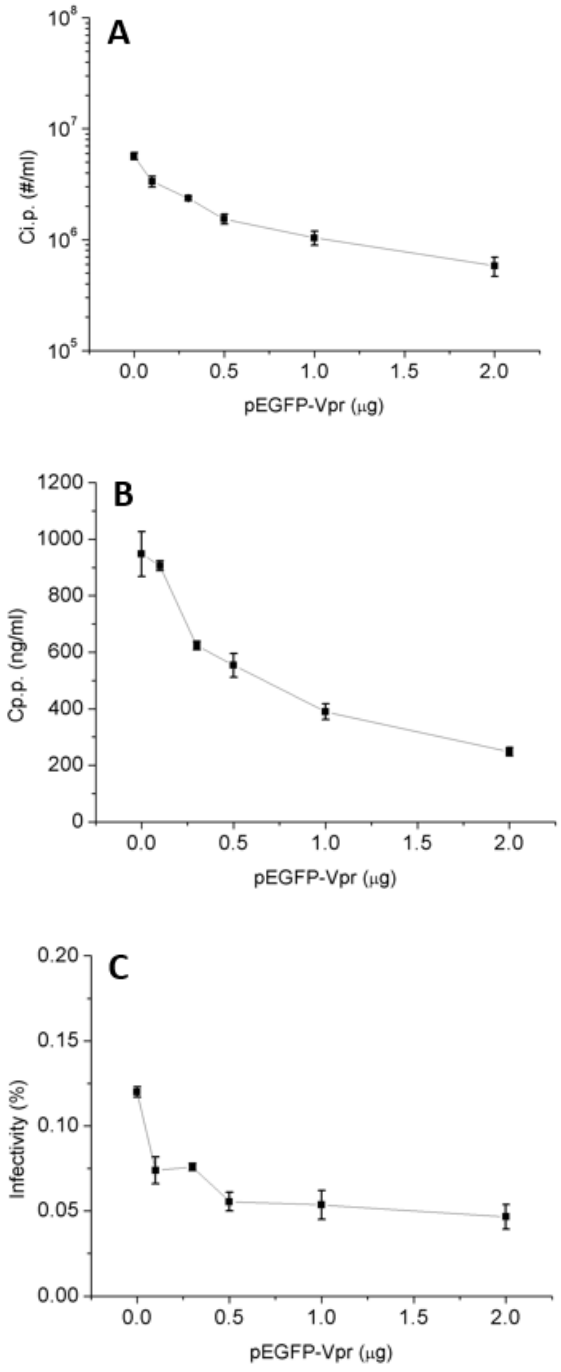

Figure 2.2. Infectivity of EGFP-tagged single-cycle virions as a function of input EGFP.

Panels (A), (B) and (C) show Ci.p., Cp.p., and infectivity of HIV-1 virions tagged with EGFP-Vpr, as a function of input pEGFP-Vpr plasmid. The viruses were collected 48 hours post transfection without media change. Error bars are standard deviations from three independent replicates of the same experiments.

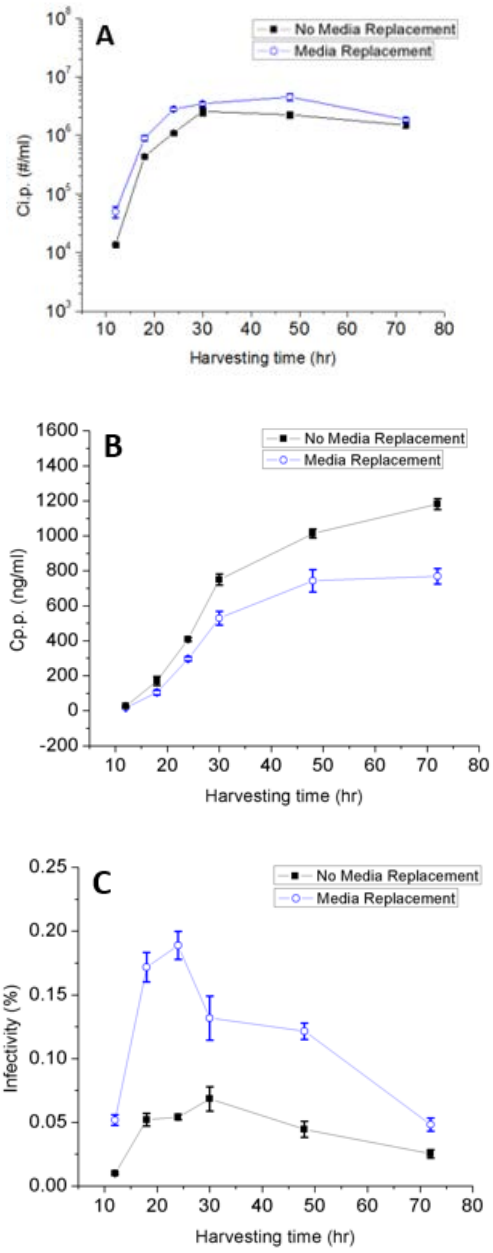

Figure 2.3. Ci.p., Cp.p., and infectivity of HIV-1 virions as a function of harvest time post transfection and media change at 6h PT.

Panels (A), (B) and (C) show Ci.p., Cp.p., and infectivity of HIV-1 virions tagged with EGFP-Vpr, as a function of harvest time post transfection, with media change six hours post transfection (open circles) and without (filled squares). Virions were produced using 1.0 µg pNL4-3R^{-}E^{-} plasmid, 0.3 µg pEGFp-Vpr and 0.1 µg pcDNA3.1REC. Error bars are standard deviations from three independent replicates of the same experiments.

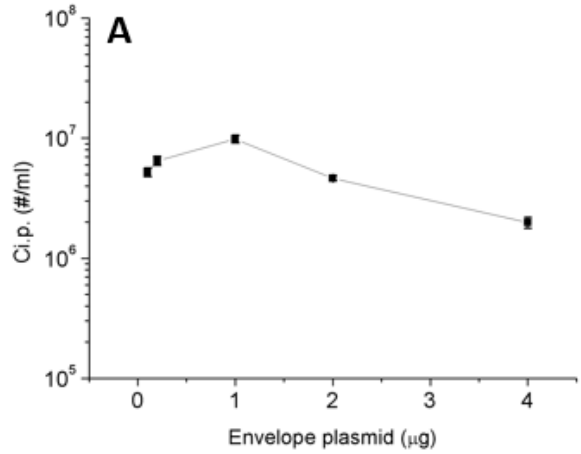
A
Ci.p. (#/ml)
10^8
10^7
10^6
10^5
0
1
2
3
4
Envelope plasmid (μg)

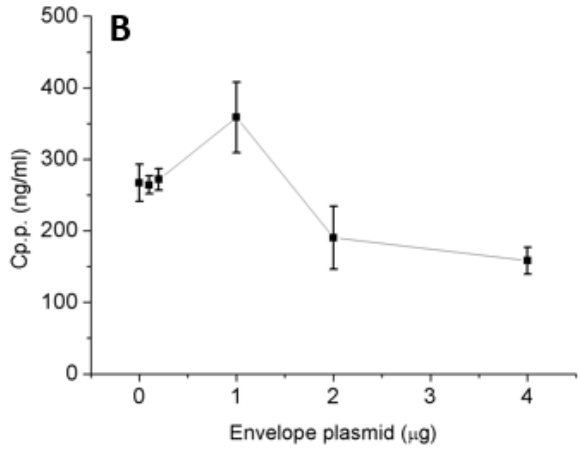
B
Cp.p. (ng/ml)
500
400
300
200
100
0
0
1
2
3
4
Envelope plasmid (μg)

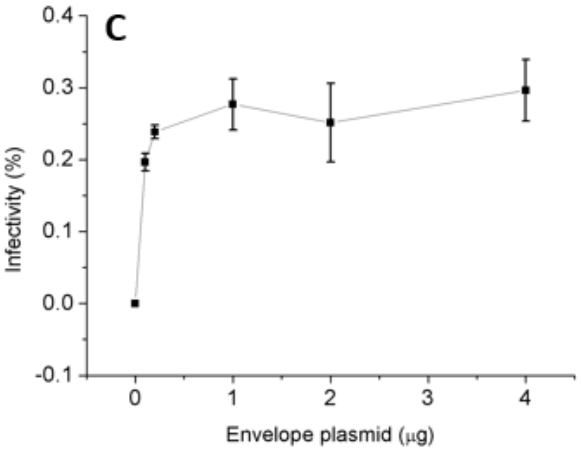
C
Infectivity (%)
0.4
0.3
0.2
0.1
0.0
-0.1
0
1
2
3
4
Envelope plasmid (μg)

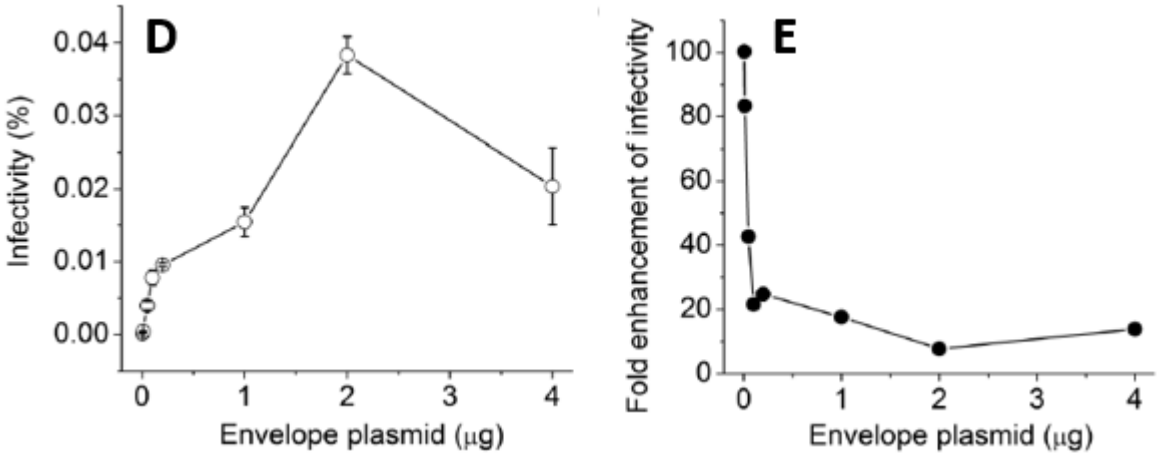

Figure 2.4. Dependence of HIV-1 virion infectivity on envelope plasmid input during transfection.

(A), (B) and (C) show Ci.p., Cp.p. and infectivity for HIV-1 virions tagged with EGFP-Vpr produced with various inputs of envelope plasmid pcDNA3.1REC. The viruses were collected 24 hours post transfection with media change at 6h post transfection. Ci.p. was zero with no envelope. Error bars are standard deviations from three independent replicates of the same experiments. (D) Infectivity of HIV-1 virions as a function of pEnv in the absence of DEAE-dextran and the quantitative effect of DEAE-dextran in enhancing HIV-1 infectivity. The error bars are standard deviations from three independent repeats of the same experiments for 0.005, 0.01, 0.05, 0.1, 2, 4 μg pEnv, and from two independent repeats of the same experiments for 0.2 and 1 μg pEnv due to the shortage of virus stocks. (E) Fold enhancement of HIV-1 virion infectivity as a function of pEnv due to the inclusion of 20 μg/ml DEAE-dextran in the infectivity assay. The fold enhancement was calculated as the ratio of virion infectivities measured in the presence and absence of DEAE-dextran for the same batch of virions.

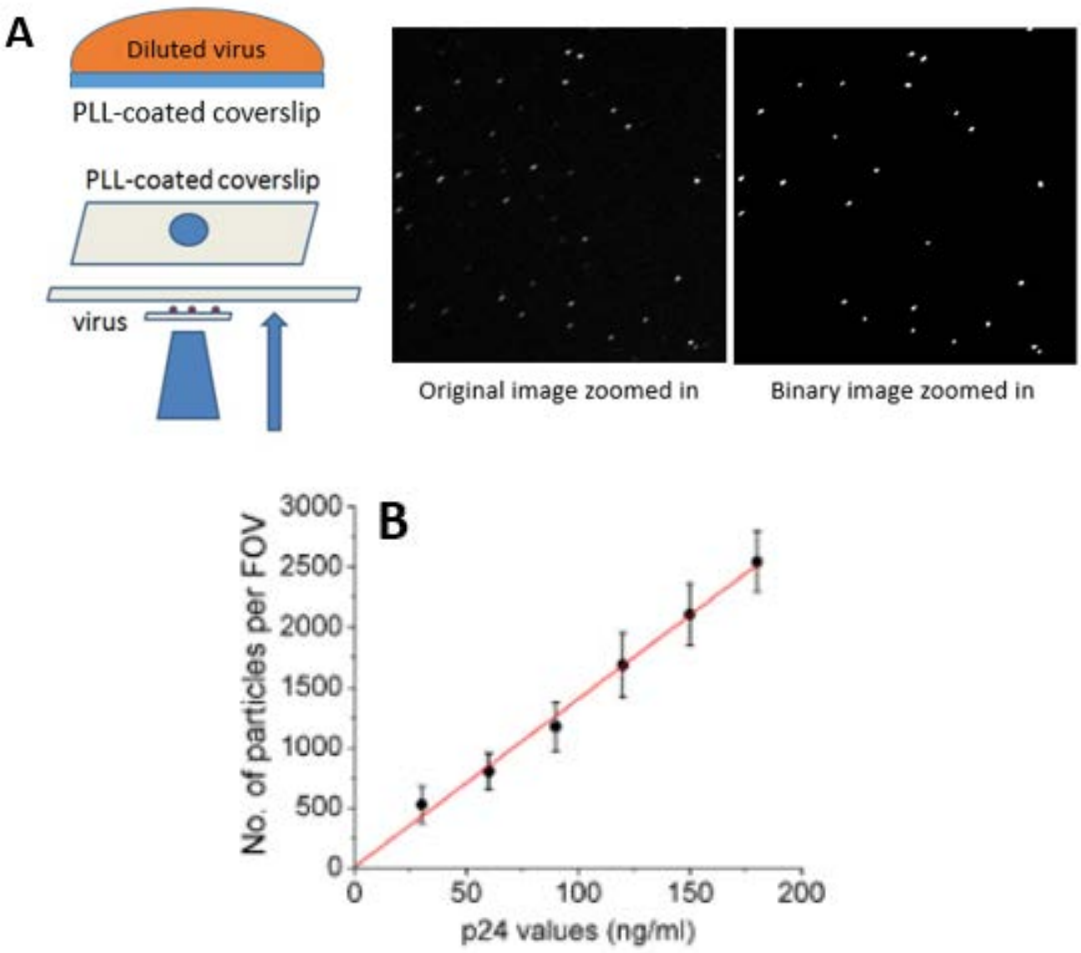

Figure 2.5. Confocal imaging of EGFP-Vpr virions and particle quantitation.

(A) A schematic figure showing how to deposit and image virions on PLL-coated coverslip. With custom-written MATLAB, an original confocal image was converted into a binary image for identifying each virion. With identified virions, the intensity can be measured with an original image. The image is 1024 by 1024 pixels with a physical size of 124 by 122 nm in x and y dimensions. (B) The correlation between numbers of fluorescent particles identified from a FOV and the input p24 values measured using ELISA. The linear regression is shown in red line. HIV-1 virions tagged with EGFP-Vpr was produced by transfecting 293T cells with 1 µg pNL4-3R^{-}E^{-}, 0.1 µg pcDNA3.1REC, and 0.3 µg pEGFP-Vpr. The viruses were collected 24 hours post transfection with media change at 6h post transfection. Error bars for each sample are standard deviations from at least nine different areas analyzed on a coverslip surface.

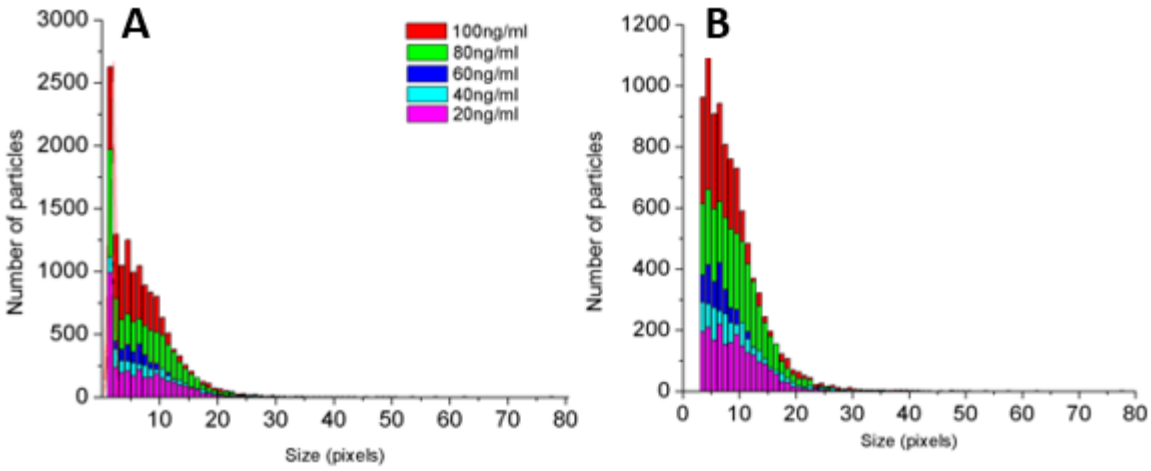

	All particles		Removing 1 and 2 pixels	
Virus amount	Xc	SE	Xc	SE
20ng/ml	1.81	0.13	7.16	0.21
40	1.81	0.21	7.95	0.22
60	2.00	0.72	6.99	0.18
80	1.81	0.26	7.92	0.24
100	1.81	0.64	8.18	0.25

$$y = y_0 + \frac{A}{w\sqrt{\pi/2}} e^{-2\frac{(x-x_c)^2}{w^2}}$$

Figure 2.6. Size distribution of EGFP-Vpr virion.

(A) Size distribution of all fluorescent particles identified by custom-written MATLAB with five different Cp.p. values. (B) Size distribution of fluorescent particle except 1 and 2 pixels identified by custom-written MATLAB with five different Cp.p. values. The table shows center and standard error values from each Gaussian fitting. HIV-1 virions tagged with EGFP-Vpr was produced by transfecting 293T cells with 1 µg pNL4-3R$^-$E$^-$, 0.1 µg pcDNA3.1REC, and 0.3 µg pEGFP-Vpr. The viruses were collected 24 hours post transfection with media change at 6h post transfection. Error bars for each sample are standard deviations from five different areas analyzed on a coverslip surface.

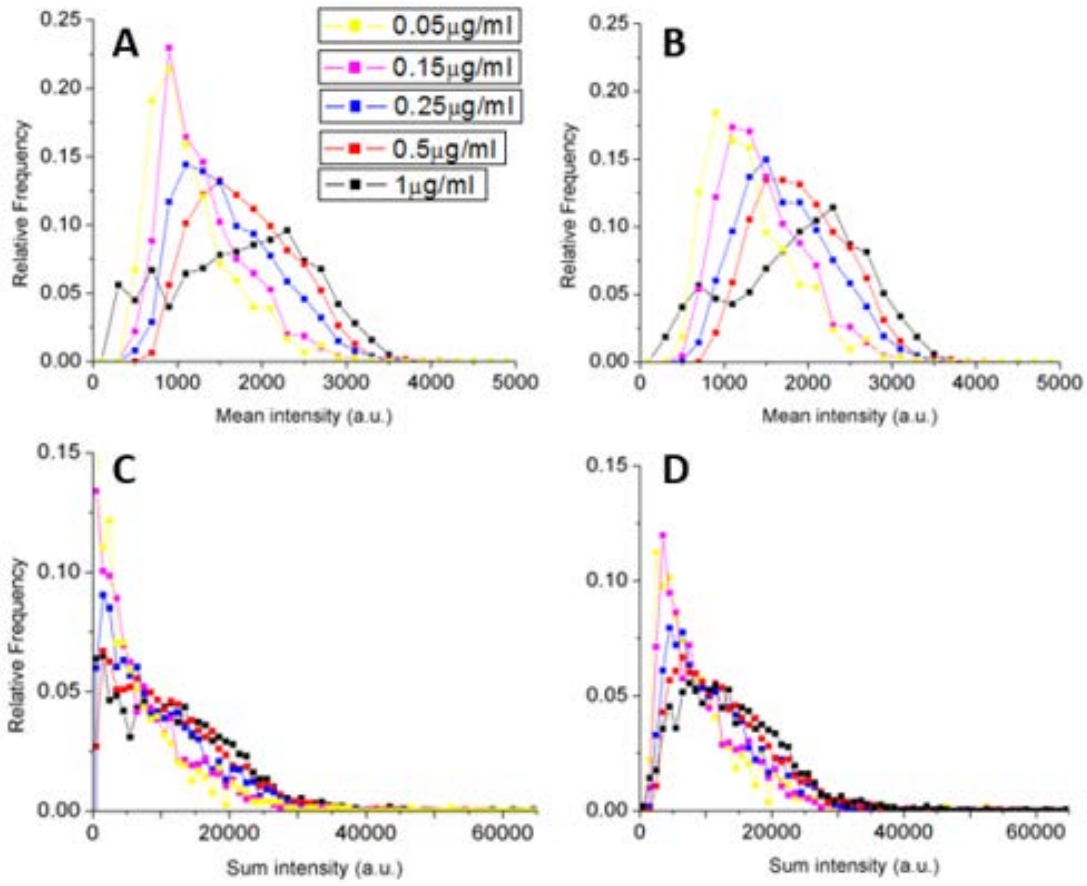

Figure 2.7. Intensity distribution of EGFP-Vpr virions with different inputs of EGFP-Vpr.

(A) Mean intensity distribution of all EGFP-Vpr virions identified and measured by MATLAB used in Figure 2.2. (B) Mean intensity distribution of EGFP-Vpr virions excluding 1 and 2 pixels. (C) Sum intensity distribution of all EGFP-Vpr virions. (D) Sum intensity distribution of EGFP-Vpr virions excluding 1 and 2 pixels. Mean intensity can be calculated as the ratio of sum intensity to particle size. Sum intensity of each virion was defined as the total intensity of each virion. HIV-1 virions tagged with EGFP-Vpr produced with various inputs of pEGFP-Vpr from 0.05 to 1 μg/ml. The viruses were collected 24 hours post transfection with media change at 6h post transfection. Error bars for each sample are standard deviations from ten different areas analyzed on a coverslip surface.

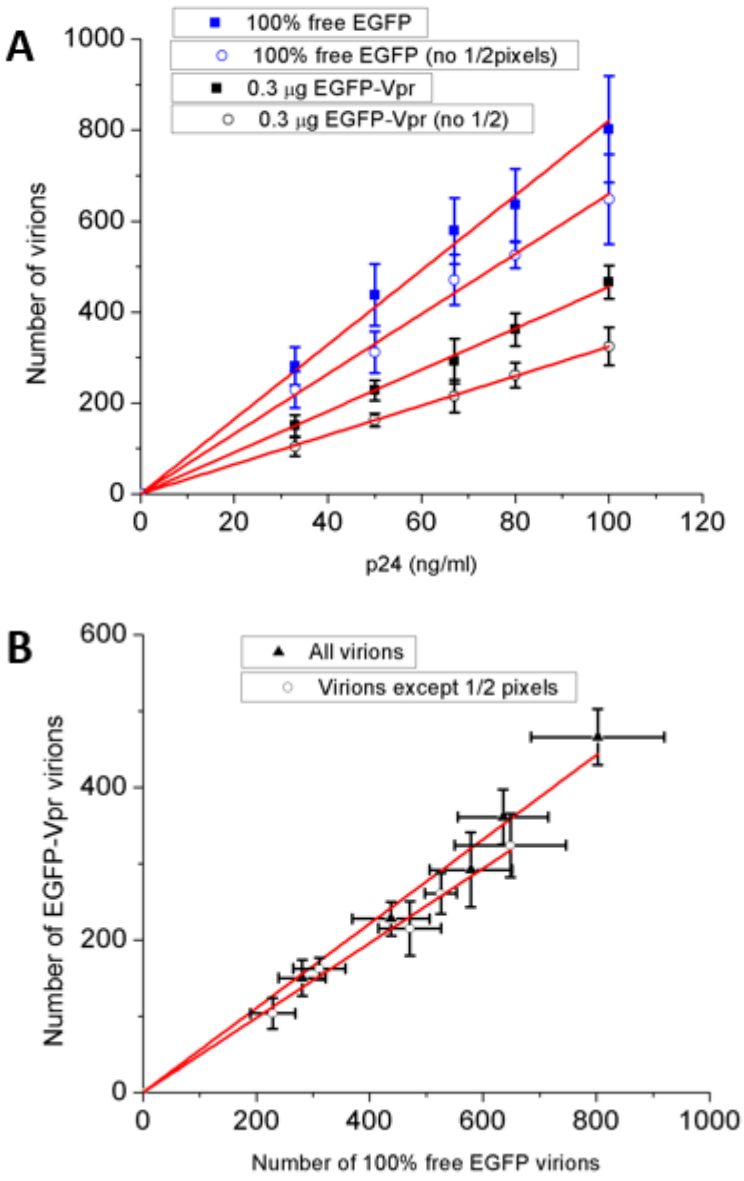

Figure 2.8. Labeling efficiency of HIV-1 tagged with EGFP-Vpr.

(A) The correlation between numbers of fluorescent particles identified in a FOV and the input p24 values measured using ELISA. The linear regression is shown in red line. All adjusted R square values are above 0.99. (B) The slope shows the labeling efficiency of EGFP-Vpr HIV-1 virions. HIV-1 virions tagged with EGFP-Vpr was produced by transfecting 293T cells with 1 μg pNL4-3R^{-}E^{-}, 0.1 μg pcDNA3.1REC, and 0.3 μg pEGFP-Vpr. HIV-1 virion carrying free EGFPs was produced with 1 μg pNL4-3E^{-}MA-EGFP-CA 0.1 μg pcDNA3.1REC. The viruses were collected 24 hours (EGFP-Vpr) or 18 hours (free EGFPs) post transfection with media change at 6h post transfection. Error bars for each sample are standard deviations from at least ten different areas analyzed on a coverslip surface except the lowest p24 values from three areas.

2.8 References

1. Munk C, Landau NR. 2003. Production and use of HIV-1 luciferase reporter viruses. Current protocols in pharmacology / editorial board, S.J. Enna Chapter 12:Unit12 15.
2. Richards KH, Clapham PR. 2006. Human immunodeficiency viruses: propagation, quantification, and storage. Current protocols in microbiology Chapter 15:Unit15J 11.
3. He J, Choe S, Walker R, Di Marzio P, Morgan DO, Landau NR. 1995. Human immunodeficiency virus type 1 viral protein R (Vpr) arrests cells in the G2 phase of the cell cycle by inhibiting p34cdc2 activity. Journal of virology 69:6705-6711.
4. Schaeffer E, Geleziunas R, Greene WC. 2001. Human immunodeficiency virus type 1 Nef functions at the level of virus entry by enhancing cytoplasmic delivery of virions. Journal of virology 75:2993-3000.
5. McDonald D, Vodicka MA, Lucero G, Svitkina TM, Borisy GG, Emerman M, Hope TJ. 2002. Visualization of the intracellular behavior of HIV in living cells. The Journal of cell biology 159:441-452.
6. Accola MA, Ohagen A, Gottlinger HG. 2000. Isolation of human immunodeficiency virus type 1 cores: retention of Vpr in the absence of p6(gag). Journal of virology 74:6198-6202.
7. Layne SP, Merges MJ, Dembo M, Spouge JL, Conley SR, Moore JP, Raina JL, Renz H, Gelderblom HR, Nara PL. 1992. Factors underlying spontaneous inactivation and susceptibility to neutralization of human immunodeficiency virus. Virology 189:695-714.
8. Bourinbaiar AS. 1994. The ratio of defective HIV-1 particles to replication-competent infectious virions. Acta virologica 38:59-61.
9. Kwon YJ, Hung G, Anderson WF, Peng CA, Yu H. 2003. Determination of infectious retrovirus concentration from colony-forming assay with quantitative analysis. Journal of virology 77:5712-5720.
10. Rusert P, Fischer M, Joos B, Leemann C, Kuster H, Flepp M, Bonhoeffer S, Gunthard HF, Trkola A. 2004. Quantification of infectious HIV-1 plasma viral load using a boosted in vitro infection protocol. Virology 326:113-129.
11. Thomas JA, Ott DE, Gorelick RJ. 2007. Efficiency of human immunodeficiency virus type 1 postentry infection processes: evidence against disproportionate numbers of defective virions. Journal of virology 81:4367-4370.
12. Platt EJ, Kozak SL, Durnin JP, Hope TJ, Kabat D. 2010. Rapid dissociation of HIV-1 from cultured cells severely limits infectivity assays, causes the inactivation ascribed to entry inhibitors, and masks the inherently high level of infectivity of virions. Journal of virology 84:3106-3110.
13. Wyatt R, Sodroski J. 1998. The HIV-1 envelope glycoproteins: fusogens, antigens, and immunogens. Science 280:1884-1888.
14. Greene WC, Peterlin BM. 2002. Charting HIV's remarkable voyage through the cell: Basic science as a passport to future therapy. Nature medicine 8:673-680.
15. Cavrois M, Neidleman J, Greene WC. 2008. The achilles heel of the trojan horse model of HIV-1 trans-infection. PLoS pathogens 4:e1000051.

16. Binley J. 2009. Specificities of broadly neutralizing anti-HIV-1 sera. Current opinion in HIV and AIDS 4:364-372.
17. Klein JS, Bjorkman PJ. 2010. Few and far between: how HIV may be evading antibody avidity. PLoS pathogens 6:e1000908.
18. Blumenthal R, Durell S, Viard M. 2012. HIV entry and envelope glycoprotein-mediated fusion. The Journal of biological chemistry 287:40841-40849.
19. Thali M. 2011. Tetraspanin functions during HIV-1 and influenza virus replication. Biochemical Society transactions 39:529-531.
20. O'Doherty U, Swiggard WJ, Malim MH. 2000. Human immunodeficiency virus type 1 spinoculation enhances infection through virus binding. Journal of virology 74:10074-10080.
21. Kim JH, Song H, Austin JL, Cheng W. 2013. Optimized Infectivity of the Cell-Free Single-Cycle Human Immunodeficiency Viruses Type 1 (HIV-1) and Its Restriction by Host Cells. PloS one 8:e67170.
22. Montefiori DC. 2005. Evaluating neutralizing antibodies against HIV, SIV, and SHIV in luciferase reporter gene assays. Current protocols in immunology / edited by John E. Coligan ... [et al.] Chapter 12:Unit 12 11.
23. McMahon MA, Shen L, Siliciano RF. 2009. New approaches for quantitating the inhibition of HIV-1 replication by antiviral drugs in vitro and in vivo. Current opinion in infectious diseases 22:574-582.
24. Yuste E, Reeves JD, Doms RW, Desrosiers RC. 2004. Modulation of Env content in virions of simian immunodeficiency virus: correlation with cell surface expression and virion infectivity. Journal of virology 78:6775-6785.
25. Poon B, Hsu JF, Gudeman V, Chen IS, Grovit-Ferbas K. 2005. Formaldehyde-treated, heat-inactivated virions with increased human immunodeficiency virus type 1 env can be used to induce high-titer neutralizing antibody responses. Journal of virology 79:10210-10217.
26. Pang Y, Song H, Kim JH, Hou X, Cheng W. 2014. Optical trapping of individual human immunodeficiency viruses in culture fluid reveals heterogeneity with single-molecule resolution. Nature nanotechnology 9:624-630.
27. Miyauchi K, Kim Y, Latinovic O, Morozov V, Melikyan GB. 2009. HIV enters cells via endocytosis and dynamin-dependent fusion with endosomes. Cell 137:433-444.
28. Klasse PJ. 2012. The molecular basis of HIV entry. Cellular microbiology 14:1183-1192.
29. Parrish NF, Gao F, Li H, Giorgi EE, Barbian HJ, Parrish EH, Zajic L, Iyer SS, Decker JM, Kumar A, Hora B, Berg A, Cai F, Hopper J, Denny TN, Ding H, Ochsenbauer C, Kappes JC, Galimidi RP, West AP, Jr., Bjorkman PJ, Wilen CB, Doms RW, O'Brien M, Bhardwaj N, Borrow P, Haynes BF, Muldoon M, Theiler JP, Korber B, Shaw GM, Hahn BH. 2013. Phenotypic properties of transmitted founder HIV-1. Proceedings of the National Academy of Sciences of the United States of America 110:6626-6633.
30. Adachi A, Gendelman HE, Koenig S, Folks T, Willey R, Rabson A, Martin MA. 1986. Production of acquired immunodeficiency syndrome-associated retrovirus in human and nonhuman cells transfected with an infectious molecular clone. Journal of virology 59:284-291.

31. Connor RI, Chen BK, Choe S, Landau NR. 1995. Vpr is required for efficient replication of human immunodeficiency virus type-1 in mononuclear phagocytes. Virology 206:935-944.
32. Cavrois M, Neidleman J, Bigos M, Greene WC. 2004. Fluorescence resonance energy transfer-based HIV-1 virion fusion assay. Methods in molecular biology 263:333-344.
33. Carlson LA, Briggs JA, Glass B, Riches JD, Simon MN, Johnson MC, Muller B, Grunewald K, Krausslich HG. 2008. Three-dimensional analysis of budding sites and released virus suggests a revised model for HIV-1 morphogenesis. Cell host & microbe 4:592-599.
34. Briggs JA, Krausslich HG. 2011. The molecular architecture of HIV. Journal of molecular biology 410:491-500.
35. Joyner AS, Willis JR, Crowe JE, Jr., Aiken C. 2011. Maturation-induced cloaking of neutralization epitopes on HIV-1 particles. PLoS pathogens 7:e1002234.
36. Nobuyuki Otsu (1979). "A threshold selection method from gray-level histograms". IEEE Trans. Sys., Man., Cyber. 9 (1): 62–66
37. Platt EJ, Wehrly K, Kuhmann SE, Chesebro B, Kabat D. 1998. Effects of CCR5 and CD4 cell surface concentrations on infections by macrophagetropic isolates of human immunodeficiency virus type 1. Journal of virology 72:2855-2864.
38. Derdeyn CA, Decker JM, Sfakianos JN, Wu X, O'Brien WA, Ratner L, Kappes JC, Shaw GM, Hunter E. 2000. Sensitivity of human immunodeficiency virus type 1 to the fusion inhibitor T-20 is modulated by coreceptor specificity defined by the V3 loop of gp120. Journal of virology 74:8358-8367.
39. Baldanti F, Paolucci S, Parisi A, Meroni L, Gerna G. 2002. Emergence of multiple drug-resistant human cytomegalovirus variants in 2 patients with human immunodeficiency virus infection unresponsive to highly active antiretroviral therapy. Clinical infectious diseases : an official publication of the Infectious Diseases Society of America 34:1146-1149.
40. Brass AL, Dykxhoorn DM, Benita Y, Yan N, Engelman A, Xavier RJ, Lieberman J, Elledge SJ. 2008. Identification of host proteins required for HIV infection through a functional genomic screen. Science 319:921-926.
41. Platt EJ, Bilska M, Kozak SL, Kabat D, Montefiori DC. 2009. Evidence that ecotropic murine leukemia virus contamination in TZM-bl cells does not affect the outcome of neutralizing antibody assays with human immunodeficiency virus type 1. Journal of virology 83:8289-8292.
42. Kimpton J, Emerman M. 1992. Detection of Replication-Competent and Pseudotyped Human-Immunodeficiency-Virus with a Sensitive Cell-Line on the Basis of Activation of an Integrated Beta-Galactosidase Gene. Journal of virology 66:2232-2239.
43. Wu Y, Marsh JW. 2001. Selective transcription and modulation of resting T cell activity by preintegrated HIV DNA. Science 293:1503-1506.
44. Wiskerchen M, Muesing MA. 1995. Human immunodeficiency virus type 1 integrase: effects of mutations on viral ability to integrate, direct viral gene expression from unintegrated viral DNA templates, and sustain viral propagation in primary cells. Journal of virology 69:376-386.

45. Padow M, Lai L, Deivanayagam C, DeLucas LJ, Weiss RB, Dunn DM, Wu X, Kappes JC. 2003. Replication of chimeric human immunodeficiency virus type 1 (HIV-1) containing HIV-2 integrase (IN): naturally selected mutations in IN augment DNA synthesis. Journal of virology 77:11050-11059.
46. Rogel ME, Wu LI, Emerman M. 1995. The human immunodeficiency virus type 1 vpr gene prevents cell proliferation during chronic infection. Journal of virology 69:882-888.
47. Re F, Braaten D, Franke EK, Luban J. 1995. Human immunodeficiency virus type 1 Vpr arrests the cell cycle in G2 by inhibiting the activation of p34cdc2-cyclin B. Journal of virology 69:6859-6864.
48. Jowett JB, Planelles V, Poon B, Shah NP, Chen ML, Chen IS. 1995. The human immunodeficiency virus type 1 vpr gene arrests infected T cells in the $G2^+$ M phase of the cell cycle. Journal of virology 69:6304-6313.
49. Chertova E, Bess JW, Jr., Crise BJ, Sowder IR, Schaden TM, Hilburn JM, Hoxie JA, Benveniste RE, Lifson JD, Henderson LE, Arthur LO. 2002. Envelope glycoprotein incorporation, not shedding of surface envelope glycoprotein (gp120/SU), Is the primary determinant of SU content of purified human immunodeficiency virus type 1 and simian immunodeficiency virus. Journal of virology 76:5315-5325.
50. Chan DC, Kim PS. 1998. HIV entry and its inhibition. Cell 93:681-684.
51. Eckert DM, Kim PS. 2001. Mechanisms of viral membrane fusion and its inhibition. Annual review of biochemistry 70:777-810.
52. Zhu P, Liu J, Bess J, Jr., Chertova E, Lifson JD, Grise H, Ofek GA, Taylor KA, Roux KH. 2006. Distribution and three-dimensional structure of AIDS virus envelope spikes. Nature 441:847-852.
53. Powers KA, Poole C, Pettifor AE, Cohen MS. 2008. Rethinking the heterosexual infectivity of HIV-1: a systematic review and meta-analysis. The Lancet. Infectious diseases 8:553-563.
54. Schiller J, Chackerian B. 2014. Why HIV virions have low numbers of envelope spikes: implications for vaccine development. PLoS pathogens 10:e1004254.
55. Crooks ET, Tong T, Osawa K, Binley JM. 2011. Enzyme digests eliminate nonfunctional Env from HIV-1 particle surfaces, leaving native Env trimers intact and viral infectivity unaffected. Journal of virology 85:5825-5839.
56. McCune JM, Rabin LB, Feinberg MB, Lieberman M, Kosek JC, Reyes GR, Weissman IL. 1988. Endoproteolytic cleavage of gp160 is required for the activation of human immunodeficiency virus. Cell 53:55-67.

Chapter 3.

Determine Entry Pathways that Lead to Productive HIV-1 Infection

3.1. Abstract

Although it has been well established that HIV initiates a T cell infection by binding to CD4 and chemokine coreceptors on the cell surface, the fundamental mechanisms of receptor-mediated viral entry for a productive infection have not been completely understood. In this chapter, we determined to investigate entry pathways that lead to productive HIV-1 infection with the characterized and optimized fluorescently-labeled, single-cycle replicative HIV-1 in chapter 2. Possible scenarios for productive viral entry are direct fusion at the plasma membrane, endocytosis, or both. Although direct fusion has been long thought to be the pathway for HIV-1 entry, this notion has been challenged recently by various studies (1,2). This question is fundamentally important for molecular understanding of HIV-1 infection. To determine if virion endocytosis can lead to

productive infection, we seek to correlate the inhibition of endocytosis and inhibition of infection. First of all, we can clearly visualize HIV-1 virions colocalized in early endosomes, and the fraction of colocalization is similar between HIV-1 and VSV-G pseudotyped virions. Also, we used various inhibitors that are known to block various steps of endocytosis. The results from three different cell lines suggest that endocytosis can indeed lead to productive infection, as revealed by the specific inhibition of HIV-1 infectivity by the dynamin I K44A mutant. However, endocytosis may not be the only productive pathway for HIV-1 infection because all these inhibition data that we have observed appear to be partial, which is in sharp contrast to inhibition by T20. These results also suggest that endocytosed virions need to fuse with endosomal membrane for productive infection. Understanding of productive HIV-1 entry will help elucidate viral pathogenesis and further develop therapeutics that is aimed to block HIV entry to $CD4^+$ T cells.

3.2. Introduction

Endocytosis is an required entry step for enveloped viruses whose fusion proteins are activated by acidic pH (3). In contrast, viruses that undergo fusion upon interacting with corresponding cellular receptors regardless of the pH have been believed to fuse directly with cellular plasma membrane. Consistently, it was revealed that HIV-1 entry and viral membrane fusion do not require exposure to low pH (4). Productive entry of HIV-1 into $CD4^+$ T cells is initiated by binding of the viral envelope gp120 to CD4 receptor. This binding causes a cascade of conformational changes in both the gp120 and gp41 that

eventually lead to virus-cell membrane fusion and HIV-1 entry (5,6). Subsequently, transcription of the viral RNA by the viral reverse transcriptase generates a double-stranded DNA copy of the viral genome, which is transported to the nucleus and integrated into host chromosomes to establish a successful infection (7). Studies over the years have uncovered many important aspects of HIV entry into $CD4^+$ T cells and mechanisms of subsequent killing (8,9). Although inhibitors targeting viral entry have become the new generation of antiretroviral drugs, our understanding on the molecular basis of HIV entry has not been completely understood. Thus, it is critical to elucidate the mechanisms by which HIV enters $CD4^+$ T cells. Such knowledge will not only enlighten our understanding of HIV pathogenesis, but also help develop therapeutics that is aimed to block HIV entry to $CD4^+$ T cells.

Early studies of HIV-1 entry have focused on the identification of receptors on T cell surface mediating viral productive entry. These have revealed that CD4 and chemokine coreceptors (CCR5 or CXCR4) are necessary for HIV entry to $CD4^+$ T cells (10). Although it has not been observed directly, HIV-1 entry is long thought to be a direct fusion between viral membrane and T cell membrane (3,6,11). There are several studies supporting this mechanism: first of all, interaction between CD4 and envelope protein gp120 can trigger conformational changes to fusion-active structure (6); second, cell-cell fusion can be mediated by HIV envelope proteins expressed on one cell surface and receptors (12); third, viral entry does not require the endocytosis of its receptor CD4 nor does it depend on low pH, which may be necessary for viral endocytosis (13,14); finally, electron microscopy (EM) images have shown the intermediates of a direct fusion between virus and cell membrane (15-17).

However, a recent study using real time fluorescence imaging technology at single molecule level has directly shown that HIV-1 enter its target cells via dynamin-dependent endocytosis instead of direct fusion in TZM-bl cells (1). Consistently, viral fusion with endosomes and micropinosomes has been observed by EM (18,19). Second, viral infection increases with blocking the acidification of endosomal compartments and apparently by sparing the virus from degradation in lysosomes (20-22). Third, efficient infection by VSV-G pseudotyped virus (23) shows that there are no significant limitations associated with viral endocytosis. Lastly, the inhibition of clathrin-mediated endocytosis decreases the efficacy of virus-cell fusion and infection in HeLa-derived cells (24).

Dynamin is distinguished from regulatory GTPases by its low affinity for GTP and high turnover rate of GTP hydrolysis (25,26). It is necessary for clathrin-dependent coated vesicle formation during the process of vesicles pinching off from a plasma membrane (27). Dynamin is organized into multiple domains. The N-terminal GTPase domain is structurally related to other GTPases (28), and mutations impairing GTP binding and/or hydrolysis block endocytosis (29,30).

Thus, for more specific inhibition on dynamin-dependent endocytosis, we used dynamin I K44A mutant (31), which acts as a dominant-negative fashion to block the formation of functional dynamin oligomers required for dynamin-dependent endocytosis (32-34). Also, to determine if virion endocytosis can lead to productive infection, various inhibitors that are known to block various steps of endocytosis were used. These studies were compared with VSV-G pseudotyped virions, which are known to enter cells through receptor-dependent endocytosis (35). Furthermore, one can postulate that viral entry might be different among cell lines since protein compositions on cellular surface and cellular

components in cytosol are different. $CD4^+$ T lymphocyte is naturally targeted by HIV-1 (10). Thus, several T cell lines, such as SupT1, Rev-CEM or Jurkat cells, were also used. However, endocytosis may not be the only productive pathway for HIV-1 infection. Either entry mechanism, direct fusion on plasma membrane or endocytosis, membrane fusion between viral and cellular membranes is required for virus to productively infect host cells (6). Thus, T20, which displayed outstanding effects of fusion inhibition (36,37), was used as a positive control for inhibition on viral infection. T20, the first clinically approved fusion inhibitor by FDA, is 36 amino acid synthetic peptide which is homologous to some parts of C terminal heptad repeat (CHR) and tryptophan-rich regions of gp41-encoded fusion machinery (38).

Possible scenarios for productive viral entry are direct fusion at cellular plasma membrane, endocytosis, or both. Although direct fusion is thought to be the pathway for HIV-1 entry (3,5,11), this has been challenged recently by various studies (1,2). This question is fundamentally important for molecular understanding of HIV-1 infection. In this study, in order to determine if virion endocytosis can lead to productive infection, we seek to correlate the inhibition of endocytosis and inhibition of infection.

3.3. Materials and Methods

Virus production

HEK 293T/17 cells (AYCC, Manassas, VA) were cultured at 37°C with 5% of CO_2 in media including 90% of DMEM and 10% of FBS (HyClone, Laboratories, Logan, UT). All cells for virus production were less than five times passaged. To produce single-cycle

HIV-1 virions, 10^6 293T cells in 2-ml were seeded, settled overnight in 6-well plate and transfected with necessary plasmids using TransIT LT-1 transfection reagent (Mirus Bio, Madison, WI). For each well, 1 µg of proviral DNA as pNL4-3R$^-$E$^-$ was used together with various amount of envelope expression plasmid, pcDNA3.1REC and 0.3 µg of pEGFP-Vpr. HIV-1 virions carrying 50% free EGFPs or mCherrys were produced with 0.5 µg of pNL4-3E$^-$ and 0.5 µg of pNL4-3E$^-$MA-EGFP-CA or pNL4-3E$^-$MA-mCherry-CA plasmids with 0.1 µg of pcDNA3.1REC. The amount of plasmids for EGFP tags was determined based on our previous work in chapter 2 (39). The entire culture media including virus was replaced at 6 hours post transfection, collected and filtered using a 0.45-µm syringe filter (Millex-HV PVDF, Millipore) at 24 post transfection for EGFP-Vpr. For free EGFP tags, 18 hours was used as a harvesting time. All virus samples were flash frozen and stored -80°C. All detailed transfection and virus preparation procedures followed the protocol described earlier in our work (39).

NL4-3 is an HIV-1 strain widely used for production of cloned HIV-1 virions (40-42), which was used for all our studies otherwise we noted. HXB2 strain (pIIIenv 3-1, cat 289, NIH AIDS Research and Reference Reagent Program) was used as envelope glycoprotein (43) only in Figure 3.10B,.

Construction of plasmids

The construction procedures of all plasmids except HXB2 envelope expression plasmid were described in chapter 2. To construct HXB2 envelope glycoprotein expression plasmid, the Rev/Env expression cassette in pIIIenv 3-1 was PCR amplified and subcloned

into the vector pcDNA3.1(-) using NotI and EcoRI restriction enzymes. The resulting plasmid was designated as pcDNA3.1REC/HXB2. pIIIenv 3-1 was used as a template, with forward and reverse primers as follows, 5'-NotI CACAGCGGCCGCGCCTTAGGCATCTCCTAT-3', 5'-EcoRI CACAGAATTCTAGCCCTTCCAGTCCCCCCTTTTCTTTTA-3'.

Preparation of dynasore, chlorpromazine, and T20

Dynasore (Sigma-Aldrich) was solubilized in DMSO, and chlorpromazine (Sigma-Aldrich) and T20 (Roche) were prepared in distilled water. All inhibitors were flash-frozen, aliquoted, and stored in -80°C freezer.

Optimization of DEAE-dextran concentration in each cell line

Productive infections with different concentrations of DEAE-dextran were quantitated by following each infection assay in TZM-bl and T cell lines, such as SupT1 or Jurkat cells. For Rev-CEM cells, 5 μg/ml was chosen in our previous work (39). Each concentration of DEAE-dextran was optimized based on the highest infectious virus concentration in each cell line. With all concentrations of DEAE-dextran, the fractions of live cells in terms of cellular permeability by trypan blue assay (44,45) were above 95% except 20 μg/ml with Jurkat cells, whose fraction was 73% (data not shown), resulting in picking up 10 μg/ml instead of 20 μg/ml.

Imaging and quantitating the localization of HIV-1 and VSV-G pseudotyped virion inside early endosomes

10^5 TZM-bl cells (cat#8129, NIH AIDS Research and Reference Reagent Program) were seeded on PLL-coated coverslip and incubated overnight at 37°C with 5% CO_2. Cells were inoculated with 2 ng (MOP 200) HIV-1 carrying free EGFPs for 15, 30 minutes or 2 hours with every 15 minutes rocking at 37°C with 5% CO_2. Virus inoculation included 20 μg/ml of DEAE-dextran, which has optimized infectivity in TZM-bl cell line. Complete media including free virions was removed. Cells on coverslip were washed with PBS three times, fixed with 4% paraformaldehyde for 10 minutes at room temperature, and washed with TBS. Cells were then permeabilized with 0.1% Triton X-100/TBS for 30 minutes at room temperature, and washed twice with TBS. For preventing nonspecific binding of antibodies, SuperBlock blocking buffer (Pierce Biotech) was incubated with samples for 30 minutes at room temperature. 1 μg/ml Rabbit polyclonal antibody to EEA1 (Invitrogen) was prepared using 90% TBS/10% SuperBlock and incubated with samples for 1 hours at room temperature. To remove unbound primary antibodies, cells were washed with 90% TBS/10% SuperBlock three times. 4 μg/ml Goat polyclonal secondary antibody to Rabbit IgG labeled with Alexa 594 (Invitrogen) was incubated and washed with the same condition as primary antibody. The coverslip was mounted on a glass cover slide with mounting media, sealed with nail polish, and imaged using an Olympus FluoView 500 Laser Scanning Confocal Microscope. Confocal images were collected with Argon and HeNe Red lasers using 100X objectives and 250 nm step size. Custom-written MATLAB was able to solve the issue that there were fluorescent viral particles present on several stacks of confocal images when quantitating the total number of virions in a FOV. Each

fluorescent virion was identified by recognizing all overlapping virion region based on centroid-to-centroid distances, globally finding the shortest distances, and correlating and relabeling particle regions. The number of colocalized virus particles showing yellow color was manually picked. The fraction of colocalization was from more than 5 areas up to 10 of confocal images.

Toxicity of inhibitors in terms of cellular membrane permeability and growth

TZM-bl, Rev-CEM, or SupT1 cells were pretreated with dynasore or chlorpromazine for 30 minutes at 37°C, and further incubated for 2 or 5 days, following the infection assay without virus infection. Cells were then collected and incubated with 0.4% w/v trypan blue dye for 5 minutes at room temperature and measured the fraction of non-permeabilized cells following the previous protocol (44,45). Heat-killed cells in 80°C for 10 minutes as a positive control showed more than 99% permeabilized cells showing blue colors in a microscope. T20 didn't show any apparent toxicity within the range of concentrations used for all cell lines, however, high concentrations of dynasore or chlorpromazine showed a toxicity. Based on our observation, we were able to use up to 200, 175, or 75 μM dynasore for TZM-bl, Rev-CEM, or SupT1, respectively for our further inhibition assays.

Measuring the inhibition on productive infection in TZM-bl cell line

For measuring inhibition on infections by dyn I K44A, we transfected TZM-bl cells for 24 hours with 1, 2, or 5 μg of each plasmid, pcDNA3.1(-), wild-type HA-dyn I, non-tagged dyn I K44A from rat, or HA-tagged dyn I K44A from human. We used TransIT LT-

1 as a transfection reagent (Mirus Bio, Madison, WI). Then, cells were trypsinized and $8x10^4$ cells in 1-ml were seeded in 12-well plate and settled at 37°C. After 6 hours, complete media was removed and cells were inoculated with 100 µl of diluted single-cycle HIV-1. Inoculation was done at 37°C for 2 hours with every 15 minutes rocking in the presence of 20 µg/ml DEAE-dextran. Cells were further incubated for 2 days at 37°C by adding 1-ml of complete media. Cells were then fixed with 2% gluteraldehyde for 5 minutes at room temperature, and stained using β-galactosidase staining kit (Mirus Bio, Madison, WI) for 50 minutes at 37°C. The number of blue cells were counted with a microscope. The inhibition data was calculated by normalizing the number of blue cells in each well with TZM-bl cells, which had transfected with pcDNA3.1(-).

In order to quantitate the inhibitory effect of several inhibitors on viral infection, $8x10^4$ cells in 1-ml were seeded in 12-well plate and incubated at 37°C. Complete media was removed and 100 µl of complete media containing each concentration of dynasore was pretreated with TZM-bl cells for 30 minutes at 37°C. With non-toxic concentration of dynasore in terms of membrane permeability and cell growth, we was able to use up to 200 µM dynasore in TZM-bl cells. Cells were then inoculated with 100 µl of free mCherry-labeled virus containing dynasore for reaching the same concentration during pretreatment step. There was no apparent difference in viral infection between the presence and absence of dynasore during inoculation (data not shown). In the case of T20, which acts on virus, cells were inoculated with a mixture of virus and certain concentration of T20 instead of pretreatment. Inoculation was done at 37°C for 2 hours with every 15 minutes rocking in the presence of 20 µg/ml DEAE-dextran. Inoculum was removed and cells were washed once with complete media. Cells were further incubated for 2 days at 37°C by adding 1-ml

of complete media. All further infection assay was the same as the above experiment. The inhibition data was calculated by normalizing the number of blue cells in each well with TZM-bl cells, which had not been pretreated with dynasore.

Measuring the transfection efficiency in TZM-bl cell line

10^6 TZM-bl cells in 2-ml were transfected with 2 µg of pcDNA 3.1(-), dyn I-EGFP, or dyn I K44A-EGFP by using 2 µl of TransIT LT-1 to 1 µg DNA. They were harvested for 24 hours, trypsinized, and washed with complete media. Cells were then fixed with 4% paraformaldehyde at room temperature for 10 minutes and washed with PBS. They were analyzed with a flow cytometer (FACS Canto II) using a 488 nm laser.

Measuring the inhibition on productive infection in Rev-CEM, and SupT1 cell lines

Rev-CEM (cat#11467, NIH AIDS Research and Reference Reagent Program), SupT1 (cat#100), or Jurkat cells (cat#177) were cultured at 37°C with 5% of CO_2 in medium including 90% of RPMI and 10% of FBS. $2X10^5$ of each T cell line in 200 µl were pretreated with a certain concentration of dynasore for 30 minutes at 37°C. With non-toxic concentration of dynasore in terms of membrane permeability and cell growth, we was able to use up to 200 µM for Rev-CEM and 75 µM for SupT1 cells. 200 µl of cells were inoculated with 100 µl of 50% free mCherry-labeled virus including dynasore for reaching the same concentration of dynasore in 300 µl volume of inoculum. There was no apparent difference in the inhibition on viral infection between the presence and absence of dynasore during inoculation (data not shown). Inoculation was done for 2 hours at 37°C with

automatic rocking in the presence of 5 or 10 µg/ml DEAE-dextran for Rev-CEM or SupT1 cells respectively. Free virions and dynasore were removed by washing with complete media. They further incubated for 5 days at 37°C in 2-ml of complete media. Cells were fixed with 2% paraformaldehyde for 5 minutes at room temperature and washed with PBS. mCherry or EGFP positive cells were quantitated with a flow cytometer (iCyt Synergy, Sony). With Rev-CEM cells, infected cells can be quantitated by mCherry or EGFP signal. Infected SupT1 cells showed mCherry signals. The fraction of infected cells were counted with a flow cytometer using 488 nm and 561 nm lasers.

Measuring the transferrin uptake in TZM-bl

$3X10^4$ TZM-bl cells in 1-ml were seeded in each well with a 12-well plate and settled for overnight. They were pretreated with 40, 80, 200 µM of dynasore for 30 minutes at 37°C and incubated with 20 µg/ml of Alexa 488 transferrin conjugate (Invitrogen) for 5 minutes at 37°C followed by at 4°C for 20 minutes. Controls were incubated with the same concentration of transferrin conjugates for 25 minutes at 4°C. Transferrin solutions were prepared with DMEM without FBS. Then, cells were washed with pre-chilled PBS six times and incubated with pre-chilled pH 2.0 buffer for 5 minutes at 4°C followed by pre-chilled PBS washing twice to remove transferrin bound on cell surface. pH 2.0 buffer was made using 500 mM NaCl and 0.2 N glacial acetic acid with distilled water (46). Cells were trypsinized, fixed with 4% paraformaldehyde for 10 minutes at room temperature, washed with PBS three times, and analyzed with a flow cytometer (FACS Canto II) using a 488 nm laser (47). For measuring the effect of dyn I K44A on transferrin uptake, all following procedures were the same as previous protocol other than using transfected

TZM-bl cells.

3.4. Results

3.4.1. Colocalization of HIV-1 virion with early endosomes

In order to start investigating whether HIV-1 can be internalized via receptor-dependent endocytosis, we visualized both HIV-1 virions carrying free EGFPs and early endosomes inside TZM-bl cells. Early endosome antigen 1 (EEA1) is well known to exclusively localize in early endosomes (48-50). We can clearly observe yellow spots from the colocalization of HIV-1 virions showing green color and EEA1, which was immunostained by Alexa 594 (Figure 3.2A). The fraction of colocalization was quantitated as a ratio of the number of fluorescent virions colocalized with EEA1 to the total number of virions recognized by custom-written MATLAB in all stacks of confocal images in a FOV.

Since endocytosis is a pretty fast event, virus was inoculated with TZM-bl cells for from 15 to 30 minutes, which are shorter than 2 hours generally used for checking a productive infection (39,51). Around 10% of fluorescent HIV-1 existed inside early endosomes with all different inoculation time points (Figure 3.2C). This would be one of the evidences that some extent of HIV-1 virions enter target cells via receptor-dependent endocytosis and the viral uptake is quite fast, taking less than 15 minutes. Since VSV-G has been known to enter cells through receptor-mediated endocytosis (35), we used VSV-G pseudotyped virions as a positive control. We compared the fraction of colocalization inside early endosomes between genuine HIV-1 virions carrying envelope glycoproteins

from NL4-3 strain and VSV-G pseudotyped one. Both HIV-1 and VSV-G pseudotyped virions were visualized by carrying free EGFPs by inserting EGFP in between MA and CA (1). Around 10% of fluorescent particles carrying either genuine viral envelope or VSV-G was localized inside early endosomes with all different inoculation time points from 15 minutes to 2 hours (Figure 3.2C).

Thus, HIV-1 was clearly present in early endosomes and the fraction of colocalized virions between HIV-1 and VSV-G pseudotyped virion was comparable. However, there is a possibility that all virions in early endosomes undergo lysosomal degradation. It is also feasible some portion of endocytosed virus particles in early endosomes may cause productive infection by further membrane fusion between virus and endosome. Furthermore, both direct fusion and endocytosis might be able to the way HIV-1 infects its target cell. Therefore, our following approache would be investigating the correlation between the inhibition of endocytosis and inhibition of productive infection.

3.4.2. Seeking correlation between inhibition of productive HIV-1 infection and inhibition of endocytosis

The above studies showed HIV-1 can be internalized into early endosomes via receptor-dependent endocytosis (Figure 3.2A). This is consistent with a recent study claiming HIV-1 enter TZM-bl cells via dynamin-dependent endocytosis in TZM-bl cells (1). Dynamin is necessary for clathrin-dependent coated vesicle formation during the process of vesicles pinching off from cellular plasma membrane (27). To determine if virion endocytosis can lead to productive infection, we used various inhibitors that are known to block various steps of endocytosis. For more specific inhibition on dynamin-

dependent endocytosis, we used dyn I K44A mutant (31), which acts as a dominant-negative fashion to block the formation of functional dynamin oligomers required for dynamin-dependent endocytosis (32-34). TZM-bl cell line, which is engineered to express CD4 receptors, CXCR4, and CCR coreceptors (52), has been widely used as an indicator cell line for measuring HIV-1 infection (39,53-56). TZM-bl cells were transfected with non-tagged dyn I K44A from rat or HA-tagged dyn I K44A from human. The homology of two plasmids' sequences was 91%. The inhibition on productive HIV-1 infection was then measured by counting blue cells that have been productively infected by NL4-3 virus, i.e., provirus has been integrated into cellular chromosomes, which upon transcriptional activation, produces Tat protein that subsequently activates the expression of β-galactosidase (51).

1, 2 or 5 µg of either dyn I K44A mutant or wild-type dyn I plasmid was transfected to TZM-bl cells for 24 hours and reseeded for measuring virus infection. Since the strong CMV promoter in dyn I K44A plasmid might cause beyond normal level of dynamin molecules inside cells, wild-type HA-tagged dyn I was used as a control. There were 30% inhibition on viral infection with dyn I K44A transfected TZM-bl cells compared to both pcDNA3.1(-) and wild-type dyn I transfected cells. Also, the fraction of inhibition on viral infection was similar among different amounts of each plasmid for both tagged and non-tagged, suggesting that 1 µg of transfection was sufficient to block dynamin I (Figure 3.3A).

3.4.3. Specificity of inhibition by dynamin I K44A on endocytosis

To provide further support for the role of dynamin-dependent endocytic pathway in productive HIV-1 infection, we meant to determine the phenotypic correlation between inhibition of dynamin-dependent endocytosis and inhibition of HIV-1 infection. Transferrin has been used as a conventional example for clathrin-dependent endocytosis with the fact that dynamin is necessary for clathrin-dependent coated vesicle formation during the process of vesicles pinching off from membrane (27). Transferrin binds at the cell surface to its corresponding receptor and is internalized by receptor-mediated endocytosis, a process that requires the formation of clathrin-coated pit (46,57-59).

We used Alexa 488-transferrin conjugates to determine whether there is a decrease in the uptake and trafficking of transferrin upon dynamin I inhibition. We incubated transferrin at 37°C for 5 minutes with dyn I-transfected TZM-bl cells, followed by PBS and acid wash to detach membrane-bound transferrin (46,59). Only endocytosed Alexa 488-transferrin conjugates were measured based on the intensity of each cell using a flow cytometer. Over the entire range of transfected amount of dyn I K44A investigated, we observed a similar decrease in the extent of endocytosed transferrin molecules (Figure 3.5B). The inhibition of dyn I K44A on productive viral entry correlated with the decrease by about 30% in the transferrin uptake. Furthermore, this inhibition on the extent of endocytosed transferrin due to dynamin I mutants persisted for at least 78 hours post transfection (60), which is necessary for checking viral productive infection based on TZM-bl indicator cells (Figure 3.5C). Transfection of TZM-bl indicator cells by dyn I K44A, the dominant-negative mutant of dynamin I, decreased HIV-1 infection by ~30% (Figure 3.3A), which correlated with the decrease of endocytosis as monitored via transferrin uptake, suggesting that dynamin-dependent endocytosis contributes to the

productive infection of HIV-1. These studies were compared with VSV-G pseudotyped virions, which are known to enter cells through endocytosis (35). VSV-G pseudotyped virions also showed ~30-40% inhibition on transferrin uptake by dyn I K44A (Figure 3.3B).

There was a correlation between the specific inhibition on dynamin-dependent endocytosis and the inhibition of viral infection (Figure 3.3A). Also, the extent of inhibition on viral infection by dyn I K44A was comparable between HIV-1 and VSV-G pseudotyped virion (Figure 3.3B). Moreover, not all TZM-bl cells were not transfected with dyn I K44A due to the limitation of transfection efficiency. The transfection efficiency might change the interpretation of data. Also, there were still residual fraction of endocytosis, as indicated by transferrin uptake, which was not blocked by dyn I K44A. Although less than 30% of TZM-bl cells were transfected and expressed dyn I or dyn I K44A (Figure 3.4B and C), we still saw the inhibition of viral infection by 30%. Thus, we concluded that about 30% of HIV-1 established productive infections via dynamin I -dependent endocytosis in our system using TZM-bl cells. This strongly suggests some extent of HIV-1 enter via dynamin-dependent endocytosis and leads to productive infections.

3.4.4. Blocking various steps of endocytosis by inhibitors with different cell lines

To investigate HIV-1 can enter and infect cells, several inhibitors related to different steps of entry were used with different cell lines. Dynasore interferes the GTPase activity of dynamin I and dynamin II, but not all other small GTPases (47). It has been used to claim HIV-1 can enter a cell via dynamin-dependent endocytosis (1). Chlorpromazine was also known to block the clathrin-dependent endocytosis, which is the major entry pathway

of VSV-G (35,61). Either entry mechanism, direct fusion on plasma membrane or endocytosis, membrane fusion between viral and cellular membranes is required for virus to productively infect host cells (6). Thus, T20, which displayed outstanding effects of fusion inhibition (36,37), was used as a positive control for inhibition on viral infection.

First, we optimized the concentration of DEAE-dextran in each cell line based on the highest infectious virus concentration and no apparent cellular toxicity. We used 20 μg/ml DEAE-dextran for TZM-bl, and 10 μg/ml for both SupT1 and Jurkat cell lines (Figure 3.1). The optimized concentration of DEAE-dextran for each cell line was used for further inhibition assay in this chapter 3. With all concentrations of DEAE-dextran, the fractions of live cells in terms of cellular permeability by trypan blue assay were above 95% except 20 μg/ml with Jurkat cells, which fraction was 73% (data not shown), resulting in picking up 10 μg/ml instead of 20 μg/ml.

We pretreated various concentrations of dynasore with TZM-bl, Rev-CEM, and SupT1 cell lines before virus infection. Each concentration of dynasore were pretreated with each cell line for 30 minutes at 37°C. Since our measurement of inhibitory effects might be overestimated due to the decreased number of cells analyzed with a flow cytometer, we checked the cytotoxicity of inhibitors, such as dynasore, chlorpromazine, and T20 with each cell line. It is also necessary to see inhibitory effect of each drug on viral entry with the normal condition of cells. Thus, we checked both membrane permeability using trypan blue dye and cell growth counting the total number of cells which have been treated with inhibitors and incubated further same as the infection assay. Within the range of concentrations used in all graphs, cellular membrane permeability was above 95% (data not shown).

With TZM-bl cell line, we observed up to 50% inhibition on productive viral infections within the range of concentrations without apparent cytotoxicity in terms of cellular growth and membrane permeability (Figure 3.7A). Also, we were able to measure viral infection with Rev-CEM and SupT1 cell lines based on a mCherry signal since mCherry-labeled HIV-1 was inoculated and there is a linear correlation between the number of mCherry-positive cells and virus input (Figure 3.6A and B). Rev-CEM, which is a rev-dependent indicator T cell line (62), also showed up to 50% inhibition on viral infection based on both GFP and mCherry signals (Figure 3.7B). SupT1 cells showed up to 30% inhibition based on a mCherry signal (Figure 3.7C). The residual 50% or above of viral productive infections might be either from direct fusion events or endocytosis that cannot be blocked by dynasore with non-toxic concentration. We concluded some portion of endocytosis is strongly related to viral productive infection even though there was a difference in the extent of inhibition among cell lines and inhibition approach.

Furthermore, VSV-G pseudotyped virions was also blocked by the similar extent with dynasore treatment in TZM-bl cell line (Figure 3.9B). Also, chlorpromazine, which is the molecule blocking clathrin-dependent endocytosis (61), was able to inhibit productive infection with both HIV-1 and VSV-G pseudotyped virions (Figure 3.9A). These results strongly suggest this inhibition of HIV-1 entry is related to inhibition on endocytosis.

However, endocytosis may not be the only productive pathway for HIV-1 infection because all these inhibitions that we have observed appear to be partial, which is in sharp contrast to inhibition by T20. T20 potently block almost all productive infections with three different cell lines (Figure 3.8A, B, and C). Even with the saturating concentration of T20 (1 μM), there were comparable endocytosed viral particles (data shown and discussed

in chapter 4), this may suggest that endocytosed virion needs to fuse with endosomal membrane for productive infection. Due to the partial inhibition on infection by blocking endocytosis, the specificity of inhibitors is critical for interpretation of these data.

3.4.5. Off-target inhibition by dynasore on endocytosis to viral infection

Both uptake and trafficking of transferrin were strongly blocked in cells preincubated for 30 minutes at 37°C with 80 μM of dynasore based on the studies (1,63) that first reported the discovery of dynasore molecule (47). However, there have been some studies showing that dynasore or other small molecules related to inhibition on receptor-mediated endocytosis was unable to antagonize transferrin uptake, suggesting a potential off-target effect of these inhibitors. To test the effect of dynasore on clathrin-dependent endocytosis, we incubated transferrin for various time periods at 37°C with TZM-bl cells pretreated with dynasore. First of all, we used 2 hours as incubation time for transferrin with cells, which was the same condition as inoculation when measuring viral infections (39). Over the entire range of concentrations of dynasore up to 200 μM investigated, we couldn't see a decrease or trend in the extent of endocytosed transferrin molecules (Figure 3.5A). One possibility that we couldn't detect the difference in intensity peak might be that 2 hours was too long to observe the difference that might be transient, as endocytosis could happen very fast. We have thus shortened the incubation time. However, even with 5 minutes as well as 30 minutes, there was no apparent change in the intensity peak. Dynasore, a noncompetitive inhibitor of dynamin, inhibited HIV-1 infection in various cell lines (Figure 3.7A, B, and C), but this inhibition is not correlated with the reduction in transferrin uptake, suggesting

that dynasore inhibits HIV-1 infection through an off-target effect. The other recent study also suggested the off-target effect of dynasore by showing that dynasore cannot impair fluid-phase endocytosis and peripheral membrane ruffling which was blocked by cells having the lack of all three dynamins (64).

3.4.6. Inhibitory effect of dynasore on viral infection in TZM-bl cells regardless of different facilitating methods for virus binding to cell surface and viral envelopes from different strains

In order to overcome the apparent low infectivity of HIV-1 (65-71), polycations or spinoculation has been used for facilitating virus binding to a cell and increasing apparent infectivity (39,72). However, there is a possibility that the inhibitory effect of dynasore on viral infection in the presence of DEAE-dextran, whose optimized concentration we have used for our all infection assay, might have nonspecific effect. To exclude this possibility, TZM-bl cells, which had been pretreated with dynasore, were infected with HIV-1 virions in the absence or presence of DEAE-dextran (Figure 3.10A). Regardless of the presence of DEAE-dextran, dynasore indeed inhibited productive viral infection up to 50%. The other method, Spinoculation, which has been used for facilitating virus binding to cellular surface in the literature (72), was also tested with the fixed concentration of dynasore, 80 μM. Figure 3.10B shows that dynasore inhibited viral infection by 20-30%, which is relatively consistent result with DEAE-dextran, in the presence of spinoculation in 1,200 g for 2 hours, whose condition was described in the earler study (72).

Furthermore, in our studies, we have extensively used NL4-3, which is an HIV-1

strain widely used for production of cloned HIV-1 virions (40-42). Since the inhibition on viral infection by dynasore might be envelope glycoprotein specific, we decided to test HXB2 envelope from different HIV strain (43). Indeed, dynasore can inhibit productive infection of HIV-1 carrying HXB2 envelope glycoproteins with either 20 μg/ml DEAE-dextran or spinoculation (Figure 3.10B). Therefore, we concluded the inhibitory effect of dynasore on productive viral infection is due to the inhibition on endocytosis, but not the nonspecific effect of DEAE-dextran or spinoculation.

3.5. Discussion

Productive entry of HIV-1 into $CD4^+$ T cells has not been clearly investigated yet. This question is fundamentally important for molecular understanding of HIV-1 infection. Early studies have suggested that HIV-1 can enter target cells via direct fusion at the plasma membrane (21,73,74). In contrast, recent studies have suggested that the direct fusion at the plasma membrane is not productive. Instead, HIV-1 may enter cells via dynamin-dependent endocytosis (1,2) and lead to a productive infection.

First of all, we can clearly visualize HIV-1 virions colocalized with early endosomes (Figure 3.2A). Also, the fraction of colocalization was comparable with VSV-G pseudotyped virions (Figure 3.2C). This suggests the localized HIV-1 inside early endosomes may go to further productive infections based on the fact that VSV-G is able to cause infections via receptor-dependent endocytosis (35).

To examine the extent to which endocytosis leads to productive infection of HIV-1, we have used several inhibitors of dynamin to investigate whether there is a correlation

between inhibition of HIV-1 infection and the inhibition of cell endocytosis. These studies were compared with VSV-G pseudotyped virions, which are known to enter cells through endocytosis (35). Transfection of TZM-bl indicator cells by dyn1 K44A, the dominant-negative mutant of dynamin I, decreased HIV-1 infection by ~30% (Figure 3.3), which correlated with the decrease of endocytosis as monitored via transferrin uptake (Figure 3.5B), suggesting that dynamin-dependent endocytosis contributes to the productive infection of HIV-1.

Furthermore, dynasore, a noncompetitive inhibitor of dynamin (47), inhibited HIV-1 infection in various cell lines (Figure 3.7A, B, and C), suggesting that endocytosis can indeed lead to productive infection, as revealed by the specific inhibition of HIV-1 infectivity by the dyn I K44A mutant (Figure 3.3). The specificity of inhibitors is critical for interpretation of these data, and through this study we uncovered the off-target effect of dynasore (Figure 3.5A). Our all inhibition data showed partial inhibition on viral infection by blocking endocytosis due to cellular cytotoxicity with high concentrations of dynasore and chlorpromazine. However, there was no apparent difference in the extent of inhibition on viral infection between HIV-1 and VSV-G pseudotyped virion (Figure 3.9A and B). This also suggests that endocytosis can indeed contribute to productive infection. It would be required to knock down all 3 dynamin isoforms in order to definitively assess the effect of dynamin-dependent endocytosis on viral infection (64).

Either direct fusion or endocytosis, there should be membrane fusion process between viral membrane and plasma/endosome membrane for viral productive infection (5,6). Interestingly, endocytosed HIV-1 can be clearly observed in SupT1 cells even in the presence of saturating T20 (data shown and discussed in chapter 4), suggesting that T20

may be endocytosed together with HIV-1 and exert its effect inside an endosome. However, endocytosis may not be the only productive pathway for HIV-1 infection because all these inhibitions that we have observed appear to be partial, which is in sharp contrast to inhibition by T20. T20, the membrane-impermeable inhibitor of HIV-1 entry, potently inhibited HIV-1 infection in all cell lines investigated (Figure 3.8A, B, and C). These results also suggest that endocytosed virions need to fuse with endosomal membrane for productive infection. Therefore, we concluded receptor-dependent endocytosis contributes to productive entry of HIV-1. Understanding of productive HIV-1 entry will help elucidate viral pathogenesis and further develop therapeutics that is aimed to block HIV entry to $CD4^+$ T cells.

3.6 Acknowledgements

This work was supported by NIH grant 1DP2OD008693-01 to Dr. Wei Cheng and also in part by Research Grant No. 5-FY10-490 to W.C. from the March of Dimes Foundation. The following reagents were obtained through the AIDS Research and Reference Reagent Program, Division of AIDS, National Institute of Allergy and Infectious Diseases (NIAID), National Institutes of Health (NIH): pNL4-3 from Dr. Malcolm Martin; pNL4-3.Luc.R^- E^- from Dr. Nathaniel Landau; pEGFP-Vpr from Warner C. Greene; TZM-bl cells from Dr. John C. Kappes, Dr. Xiaoyun Wu and Tranzyme Inc; Rev-CEM cells from Dr. Yuntao Wu and Dr. Jon W. Marsh; SupT1 cells from Dr. Dharam Ablashi; Jurkat cells from Dr. Arthur Weiss. Plasmids were obtained from Addgene, the nonprofit plasmid repository: HA-tagged dyn I K44A from human, wild-type dyn I, dyn I-EGFP, and dyn I K44A-EGFP from Dr. Sandra Schmid; non-tagged dyn I K44A from rat from Robert Lefkowitz. Authors thank Dr. Michael DeSantis for custom-written MATLAB, Microscopy and Image Analysis Laboratory for Olympus FluoView 500 Laser Scanning Confocal Microscope, flow cytometry core, DNA sequencing core for all sequencing results in the University of Michigan.

3.7 Figures

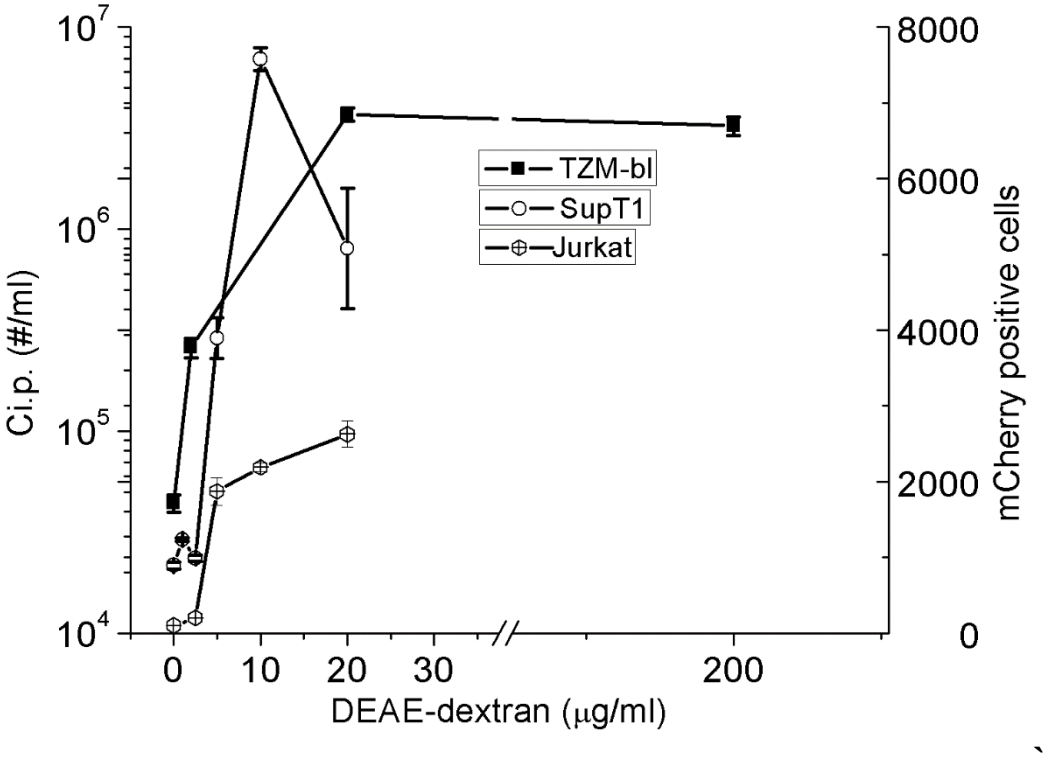

Figure 3.1. Optimization of DEAE-dextran concentration in TZM-bl, SupT1, and Jurkat cell lines.

The optimized concentration of DEAE-dextran for each cell line was used for all inhibition assay in this chapter 3. (A) Optimized concentration of DEAE-dextran in TZM-bl cell line is 20 µg/ml under MOP 0.14 condition. (B) Optimized concentration of DEAE-dextran in SupT1 cell line is 10 µg/ml under MOP 170 condition. (C) Optimized concentration of DEAE-dextran in Jurkat cell line is 10 µg/ml under MOP 170 condition. All procedures followed the infection assays with each cell line described in Material and Methods. With all concentrations of DEAE-dextran, the fractions of live cells in terms of cellular permeability by trypan blue assay were above 95% except 20 µg/ml with Jurkat cells, whose fraction was 73% (data not shown), resulting in picking up 10 µg/ml instead of 20 µg/ml.

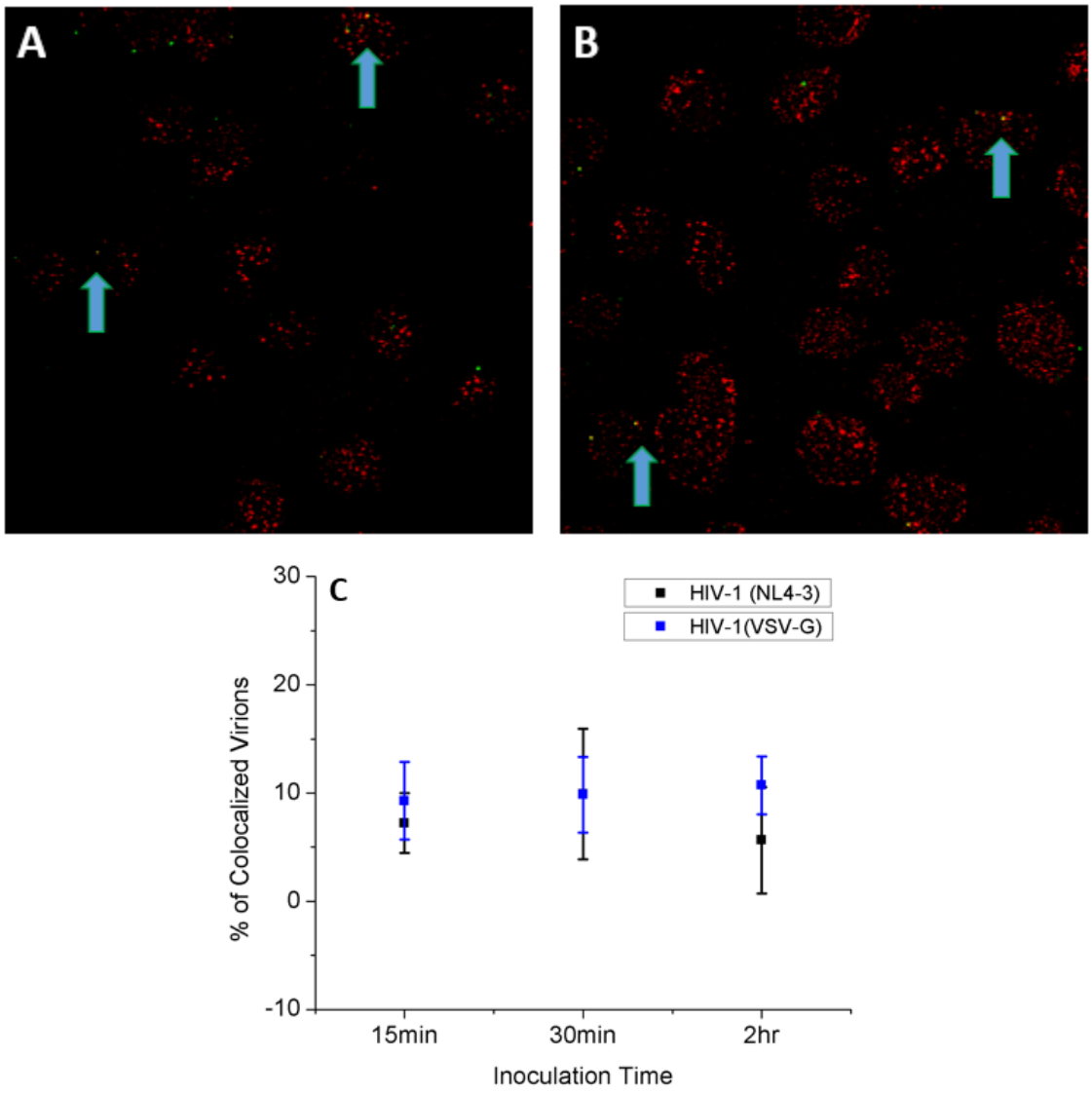

Figure 3.2. Colocalization of HIV-1 or VSV-G pseudotyped virion with early endosomes.

(A) Representative image for HIV-1 colocalization inside early endosomes. TZM-bl cells were inoculated with HIV-1 carrying free EGFPs for 30 minutes under MOP 200 condition. (B) Representative image for the colocalization of VSV-G pseudotyped virion inside early endosomes. TZM-bl cells were inoculated with VSV-G pseudotyped HIV-1 carrying free EGFPs for 30 minutes under MOP 200 condition. (C) Quantitation of colocalization with different inoculation time points was measured by the number of colocalized virions with early endosomes over the total number of fluorescent viral particles. Black squares (HIV-1 carrying free EGFPs with 1 µg of NL4-3 ENV). Blue squares (VSV-G pseudotyped virions carrying free EGFPs with 1 µg of VSV-G ENV). Error bars were from five areas of confocal images.

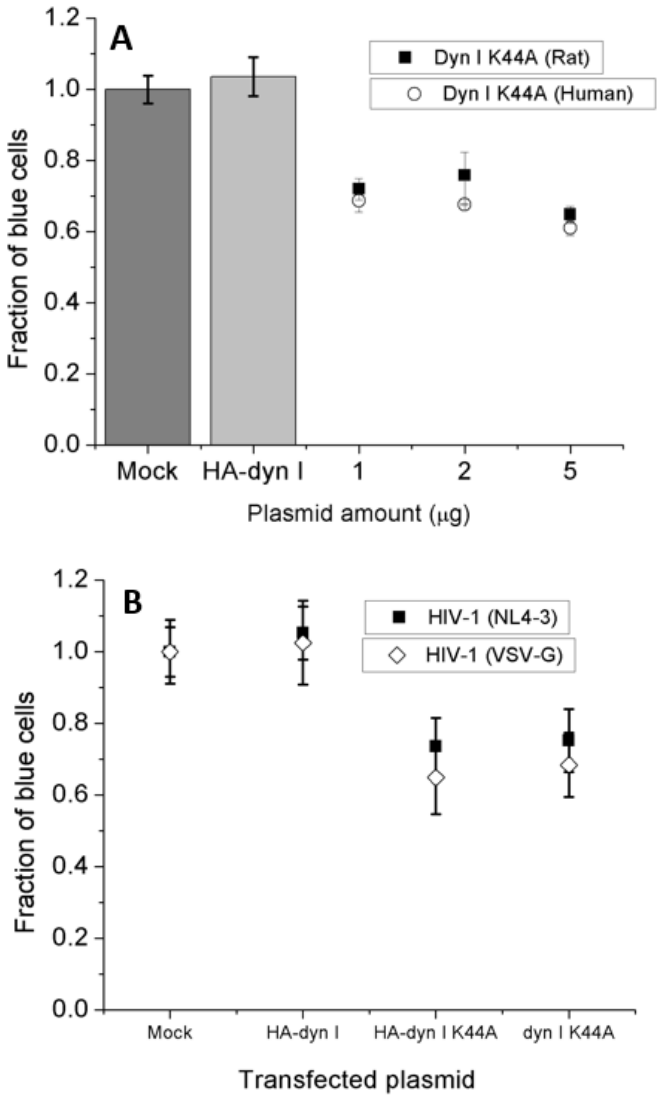

Figure 3.3. Correlation between inhibition on productive infection and dynamin-dependent endocytosis.

(A) Fraction of blue cells with transfection of different amounts of plasmids. Black bar (pcDNA 3.1(-), 2 μg). Gray bar (wild-type HA-tagged dyn I, 2 μg). Filled squares (HA-tagged dyn I K44A from rat). Open circles (Non-tagged dyn I K44A from human). (B) Fraction of blue cells in TZM-bl cells by using different viral envelope transfected with 2 μg of each plasmid. Filled squares (HIV-1 carrying free EGFPs with 1 μg of NL4-3 ENV). Open diamonds (VSV-G pseudotyped virions carrying free EGFPs with 1 μg of VSV-G ENV). Error bars were from duplicates of transfection and blue cell counting.

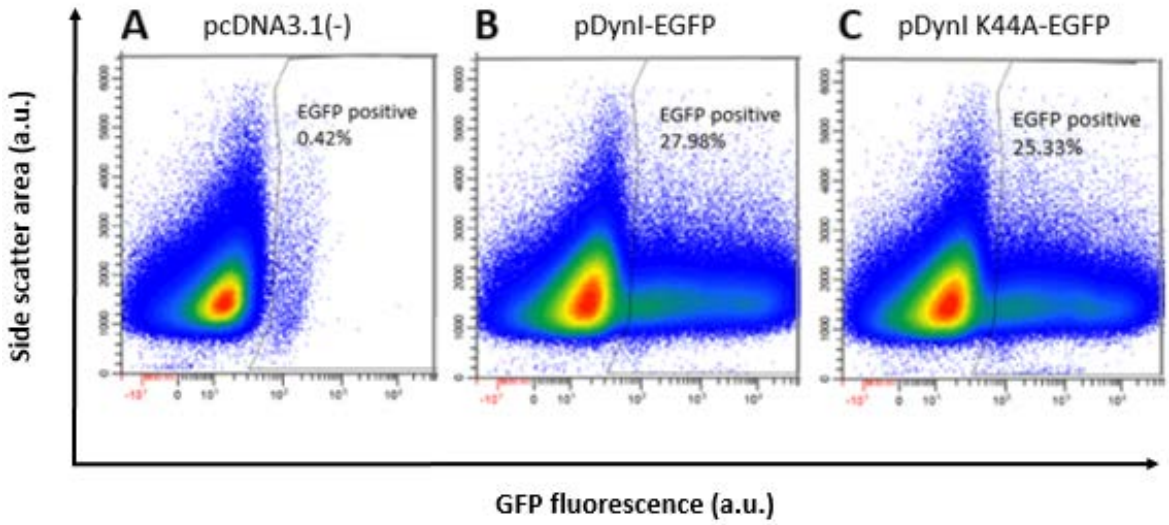

Figure 3.4. Transfection efficiency of dyn I-EGFP or dyn I K44A-EGFP in TZM-bl cells.

Representative images of flow cytometry (A) Negative control. TZM-bl cells were transfected for 24 hours with 2 µg of pcDNA 3.1(-). (B) 2 µg of dyn I-EGFP. (C) 2 µg of dyn I K44A-EGFP.

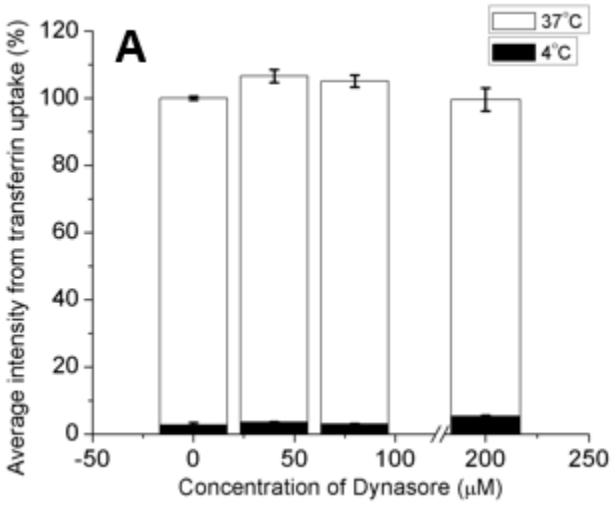
A
37°C
4°C
Average intensity from transferrin uptake (%)
120
100
80
60
40
20
0
-50
0
50
100
200
250
Concentration of Dynasore (μM)

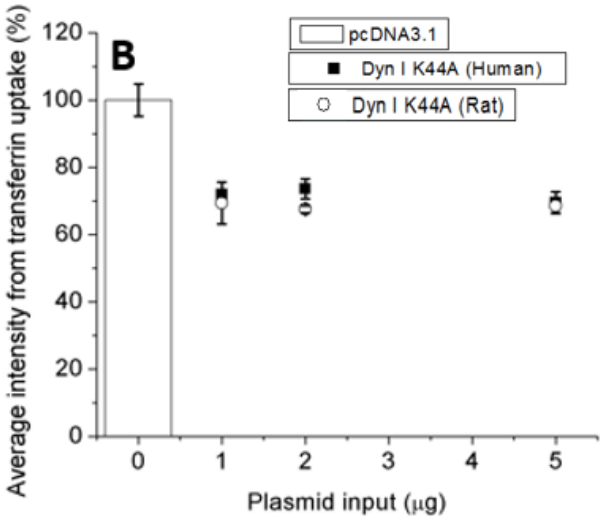
B
pcDNA3.1
Dyn I K44A (Human)
Dyn I K44A (Rat)
Average intensity from transferrin uptake (%)
120
100
80
60
40
20
0
0
1
2
3
4
5
Plasmid input (μg)

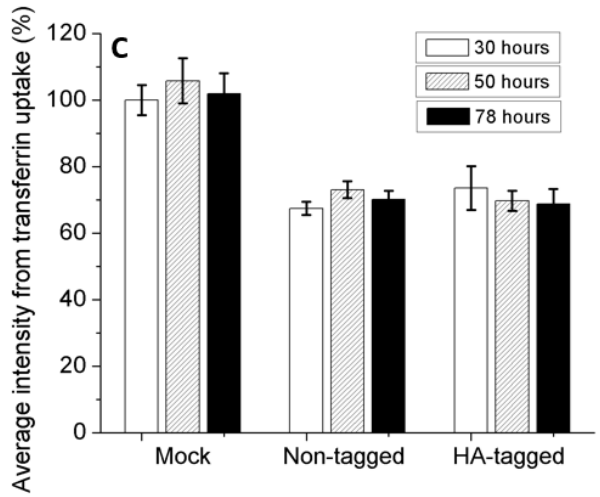
C
30 hours
50 hours
78 hours
Average intensity from transferrin uptake (%)
120
100
80
60
40
20
0
Mock
Non-tagged
HA-tagged

Figure 3.5. Specificity of inhibition on endocytosis in TZM-bl cells by measuring the uptake of Alexa 488-transferrin conjugate.

(A) Quantification of transferrin uptake in TZM-bl cells with different concentrations of dynasore treatment. The uptake was normalized based on a control without dynasore treatment. White bar (transferrin uptake at 37°C). Black bar (Negligible transferrin uptake at 4°C). (B) Measurement of transferrin uptake in TZM-bl cells transfected with different amounts of dyn I K44A plasmids. Open bar (pcDNA 3.1(-)). Filled squares (HA-tagged dyn I K44A from human). Open circles (Non-tagged dyn I K44A from rat). (C) Quantification of transferrin uptake in TZM-bl cells transfected with 2 µg of each plasmid using different time points. The effect of transfection persisted up to 78 hours post transfection. Open bars (30 hours post transfection). Gray bars (54 hours post transfection). Black bars (78 hours post transfection). Error bars were from the duplicate of same experiments.

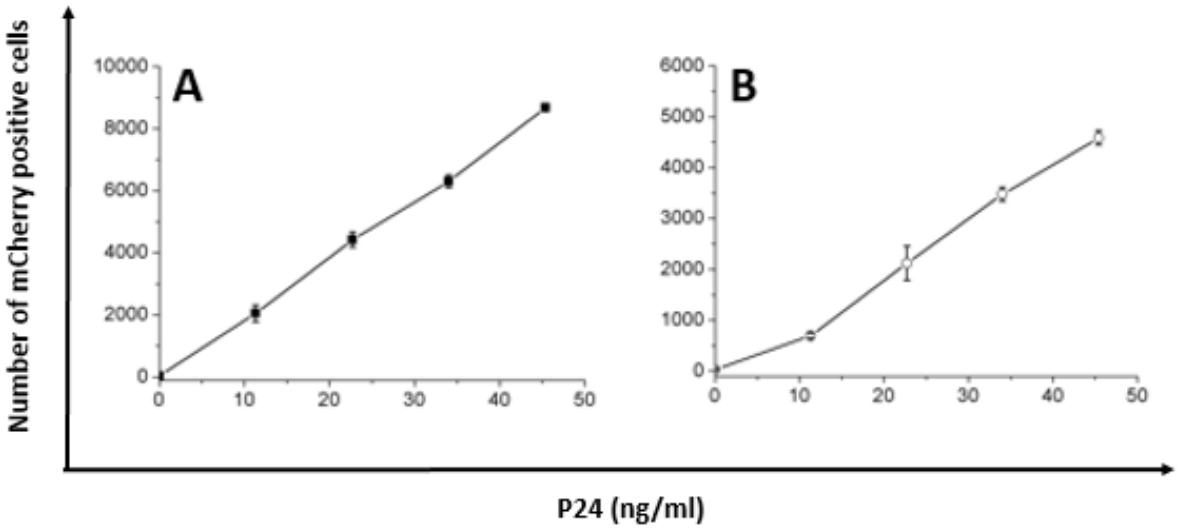

Figure 3.6. Correlation between productive infection and virus concentration based on mCherry signals.

The number of mCherry positive cells were quantitated with a flow cytometer using a 561 nm laser with various virus input. (A) Linear relationship between the number of mCherry positive cells and virus concentration in Rev-CEM cells. (B) Linear relationship between the number of mCherry positive cells and virus concentration in SupT1 cells. HIV-1 carrying free mCherrys in 100 µl was used. Error bars were from triplicates in the same experiment.

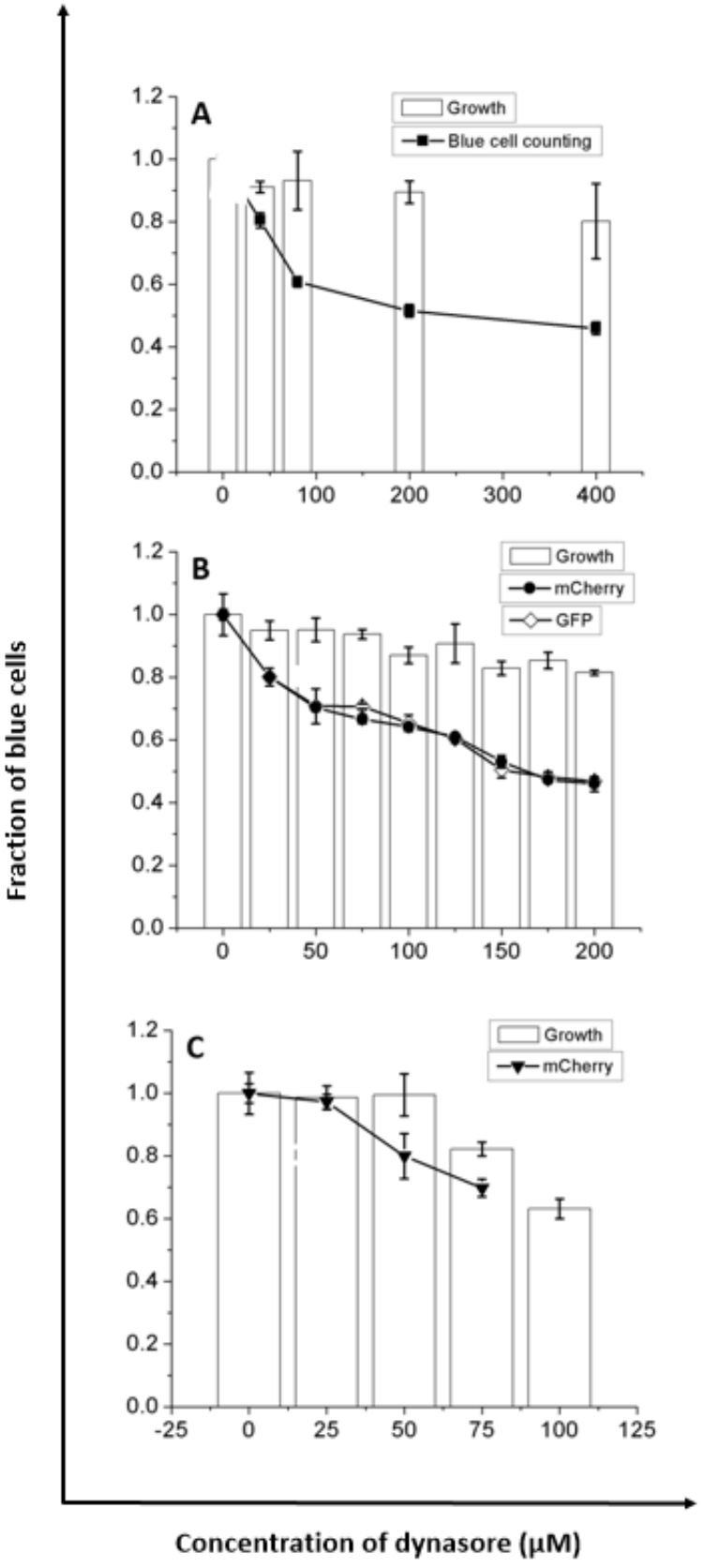
A
Growth
Blue cell counting
B
Growth
mCherry
GFP
C
Growth
mCherry
Fraction of blue cells
Concentration of dynasore (μM)

Figure 3.7. Measurement of inhibition on productive infections using dynasore in TZM-bl, Rev-CEM, and SupT1 cell lines.

Inhibition on productive infections by dynasore pretreatment in different cell lines. (A) Normalized productive infections by blue cell counting in TZM-bl with dynasore treatment. (B) Normalized infections in Rev-CEM based on the number of GFP or mCherry positive cells with dynasore treatment. Black circles (mCherry signasl). Open diamonds (EGFP signals). (C) Normalized infections in SupT1 based on the number of mCherry positive cells with dynasore treatment. All experiments used HIV-1 carrying free mCherrys. All white bars represent the growth normalized based on controls without dynasore pretreatment. Error bars were from triplicates. Within the range of concentrations, cellular permeability was above 95% by trypan blue assay (data not shown).

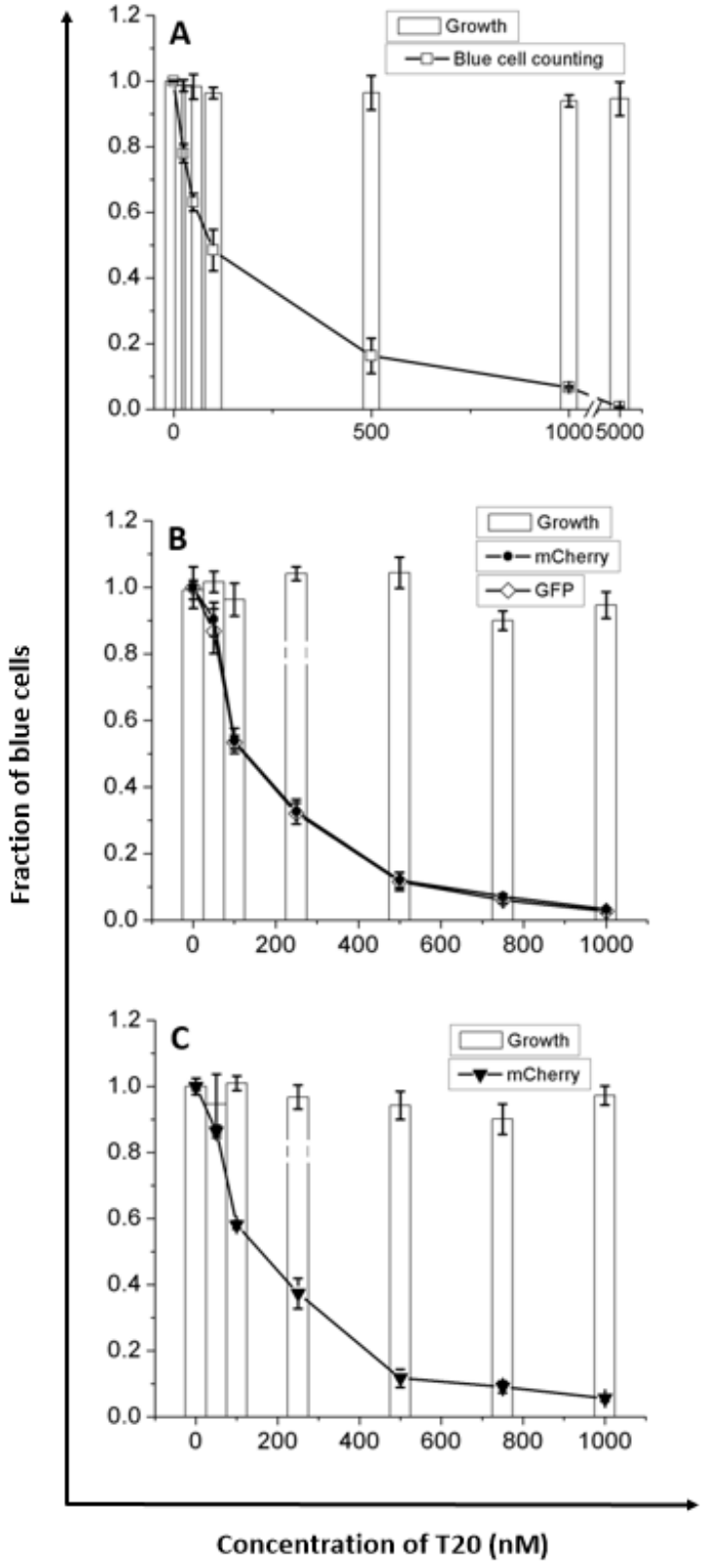
A
Growth
Blue cell counting
B
Growth
mCherry
GFP
C
Growth
mCherry
Fraction of blue cells
Concentration of T20 (nM)

Figure 3.8. Measurement of inhibition on productive infections using T20 in TZM-bl, Rev-CEM, and SupT1 cell lines.

Inhibition on productive infections by T20 in different cell lines. (A) Normalized productive infections by blue cell counting in TZM-bl with T20 treatment. (B) Normalized infections in Rev-CEM based on the number of GFP or mCherry positive cells with T20 treatment. Black circles (mCherry signasl). Open diamonds (EGFP signals). (C) Normalized infections in SupT1 based on the number of mCherry positive cells with T20 treatment. All experiments used HIV-1 carrying free mCherrys. All white bars represent the growth normalized based on controls without T20 pretreatment. No apparent T20 toxicity in terms of cellular growth on three different cell lines within the range of concentrations used. Error bars were from triplicates. Within the range of concentrations, cellular permeability was above 95% by trypan blue assay (data not shown).

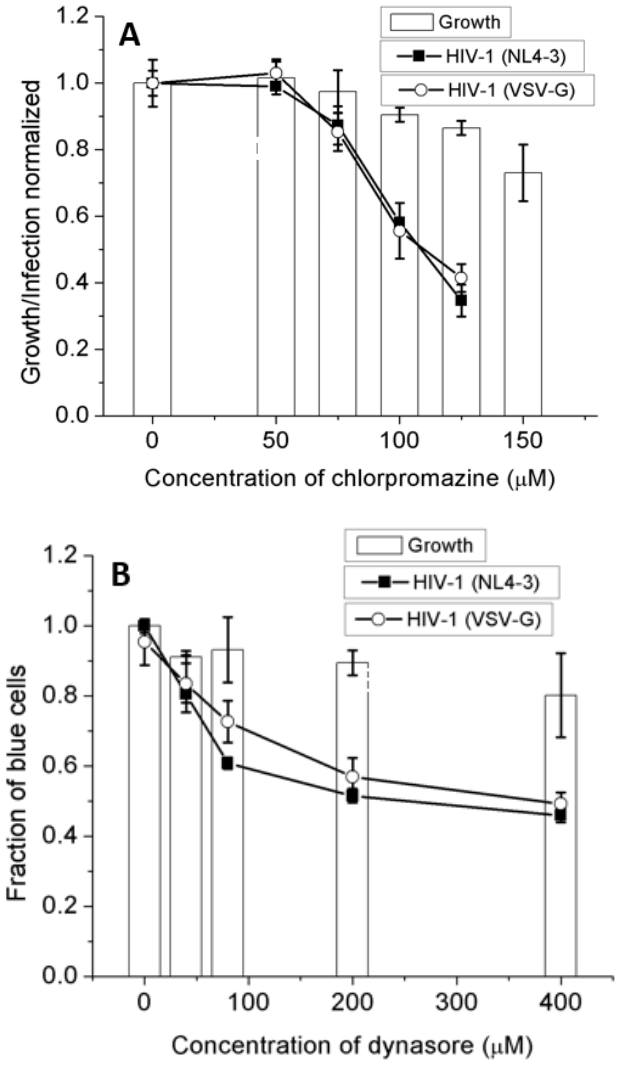

Figure 3.9. Measurement of inhibition on productive infections in TZM-bl by chlorpromazine or dynasore with HIV-1 or VSV-G pseudotyped virions.

Productive infections were measured by blue cell counting in TZM-bl cell line. (A) Measurement of productive infection in TZM-bl cells using chlorpromazine. (B) Measurement of productive infection in TZM-bl cells using dynasore. Filled squares (HIV-1 carrying free EGFPs with 1 μg of NL4-3 ENV). Open circles (VSV-G pseudotyped virions carrying free EGFPs with 1 μg of VSV-G ENV). Error bars were from duplicates of blue cell counting and growth cell counting. All white bars represent the growth normalized based on controls without each inhibitor. Within the range of concentrations, cellular permeability was above 95% by trypan blue assay.

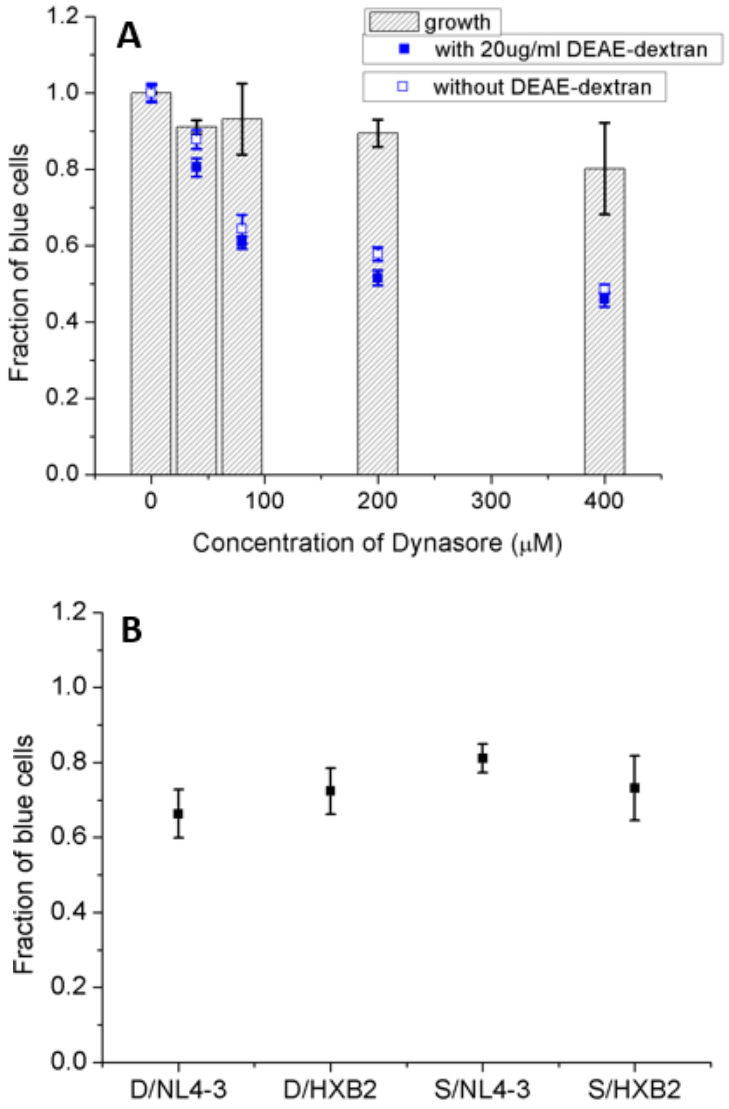

Figure 3.10. Inhibitory effect of dynasore on viral infection in TZM-bl cells regardless of different facilitating methods for virus binding to cell surface and viral envelopes from different strains

(A) Inhibition on productive infections by dynasore pretreatment in TZM-bl cell line in the absence or presence of DEAE-dextran. All white bars represent the growth normalized based on controls without dynasore pretreatment. Within the range of concentrations, cellular permeability was above 95% by trypan blue assay (data not shown). (B) Either 20 μg/ml DEAE-dextran (D) or spinoculation (S) was used for facilitating virus binding to host cells. HIV-1 was produced with 1 μg pNL4-3R^{-}E^{-}, 0.3 μg EGFP-Vpr, and 0.1 μg pcDNA3.1REC/NL4-3 or pcDNA3.1REC/HXB2. Error bars were from duplicates.

3.8 References

1. Miyauchi, K., Kim, Y., Latinovic, O., Morozov, V., and Melikyan, G. B. (2009) HIV enters cells via endocytosis and dynamin-dependent fusion with endosomes. Cell **137**, 433-444
2. Sloan, R. D., Kuhl, B. D., Mesplede, T., Munch, J., Donahue, D. A., and Wainberg, M. A. (2013) Productive entry of HIV-1 during cell-to-cell transmission via dynamin-dependent endocytosis. Journal of virology **87**, 8110-8123
3. Marsh, M., and Helenius, A. (2006) Virus entry: open sesame. Cell **124**, 729-740
4. McClure, M. O., Marsh, M., and Weiss, R. A. (1988) Human immunodeficiency virus infection of CD4-bearing cells occurs by a pH-independent mechanism. The EMBO journal **7**, 513-518
5. Eckert, D. M., and Kim, P. S. (2001) Mechanisms of viral membrane fusion and its inhibition. Annual review of biochemistry **70**, 777-810
6. Chan, D. C., and Kim, P. S. (1998) HIV entry and its inhibition. Cell **93**, 681-684
7. Charneau, P., Mirambeau, G., Roux, P., Paulous, S., Buc, H., and Clavel, F. (1994) HIV-1 reverse transcription. A termination step at the center of the genome. Journal of molecular biology **241**, 651-662
8. Laurent-Crawford, A. G., Krust, B., Riviere, Y., Desgranges, C., Muller, S., Kieny, M. P., Dauguet, C., and Hovanessian, A. G. (1993) Membrane expression of HIV envelope glycoproteins triggers apoptosis in CD4 cells. AIDS research and human retroviruses **9**, 761-773
9. Gandhi, R. T., Chen, B. K., Straus, S. E., Dale, J. K., Lenardo, M. J., and Baltimore, D. (1998) HIV-1 directly kills $CD4^+$ T cells by a Fas-independent mechanism. The Journal of experimental medicine **187**, 1113-1122
10. Wyatt, R., and Sodroski, J. (1998) The HIV-1 envelope glycoproteins: fusogens, antigens, and immunogens. Science **280**, 1884-1888
11. Gallo, S. A., Finnegan, C. M., Viard, M., Raviv, Y., Dimitrov, A., Rawat, S. S., Puri, A., Durell, S., and Blumenthal, R. (2003) The HIV Env-mediated fusion reaction. Biochimica et biophysica acta **1614**, 36-50
12. Bieniasz, P. D., Fridell, R. A., Aramori, I., Ferguson, S. S., Caron, M. G., and Cullen, B. R. (1997) HIV-1-induced cell fusion is mediated by multiple regions within both the viral envelope and the CCR-5 co-receptor. The EMBO journal **16**, 2599-2609
13. Brandt, S. M., Mariani, R., Holland, A. U., Hope, T. J., and Landau, N. R. (2002) Association of chemokine-mediated block to HIV entry with coreceptor internalization. The Journal of biological chemistry **277**, 17291-17299
14. Maddon, P. J., McDougal, J. S., Clapham, P. R., Dalgleish, A. G., Jamal, S., Weiss, R. A., and Axel, R. (1988) HIV infection does not require endocytosis of its receptor, CD4. Cell **54**, 865-874
15. Stein, B. S., Gowda, S. D., Lifson, J. D., Penhallow, R. C., Bensch, K. G., and Engleman, E. G. (1987) pH-independent HIV entry into CD4-positive T cells via virus envelope fusion to the plasma membrane. Cell **49**, 659-668
16. Hladik, F., Sakchalathorn, P., Ballweber, L., Lentz, G., Fialkow, M., Eschenbach, D., and McElrath, M. J. (2007) Initial events in establishing vaginal entry and infection by human immunodeficiency virus type-1. Immunity **26**, 257-270

17. Sougrat, R., Bartesaghi, A., Lifson, J. D., Bennett, A. E., Bess, J. W., Zabransky, D. J., and Subramaniam, S. (2007) Electron tomography of the contact between T cells and SIV/HIV-1: implications for viral entry. PLoS pathogens **3**, e63
18. Marechal, V., Prevost, M. C., Petit, C., Perret, E., Heard, J. M., and Schwartz, O. (2001) Human immunodeficiency virus type 1 entry into macrophages mediated by macropinocytosis. Journal of virology **75**, 11166-11177
19. Pauza, C. D., and Price, T. M. (1988) Human immunodeficiency virus infection of T cells and monocytes proceeds via receptor-mediated endocytosis. The Journal of cell biology **107**, 959-968
20. Fredericksen, B. L., Wei, B. L., Yao, J., Luo, T., and Garcia, J. V. (2002) Inhibition of endosomal/lysosomal degradation increases the infectivity of human immunodeficiency virus. Journal of virology **76**, 11440-11446
21. Schaeffer, E., Soros, V. B., and Greene, W. C. (2004) Compensatory link between fusion and endocytosis of human immunodeficiency virus type 1 in human CD4 T lymphocytes. Journal of virology **78**, 1375-1383
22. Wei, B. L., Denton, P. W., O'Neill, E., Luo, T., Foster, J. L., and Garcia, J. V. (2005) Inhibition of lysosome and proteasome function enhances human immunodeficiency virus type 1 infection. Journal of virology **79**, 5705-5712
23. Aiken, C. (1997) Pseudotyping human immunodeficiency virus type 1 (HIV-1) by the glycoprotein of vesicular stomatitis virus targets HIV-1 entry to an endocytic pathway and suppresses both the requirement for Nef and the sensitivity to cyclosporin A. Journal of virology **71**, 5871-5877
24. Daecke, J., Fackler, O. T., Dittmar, M. T., and Krausslich, H. G. (2005) Involvement of clathrin-mediated endocytosis in human immunodeficiency virus type 1 entry. Journal of virology **79**, 1581-1594
25. Sever, S., Damke, H., and Schmid, S. L. (2000) Garrotes, springs, ratchets, and whips: putting dynamin models to the test. Traffic **1**, 385-392
26. Song, B. D., and Schmid, S. L. (2003) A molecular motor or a regulator? Dynamin's in a class of its own. Biochemistry **42**, 1369-1376
27. Urrutia, R., Henley, J. R., Cook, T., and McNiven, M. A. (1997) The dynamins: Redundant or distinct functions for an expanding family of related GTPases? Proceedings of the National Academy of Sciences **94**, 377-384
28. Niemann, H. H., Knetsch, M. L., Scherer, A., Manstein, D. J., and Kull, F. J. (2001) Crystal structure of a dynamin GTPase domain in both nucleotide-free and GDP-bound forms. The EMBO journal **20**, 5813-5821
29. Herskovits, J. S., Burgess, C. C., Obar, R. A., and Vallee, R. B. (1993) Effects of mutant rat dynamin on endocytosis. The Journal of cell biology **122**, 565-578
30. Marks, B., Stowell, M. H., Vallis, Y., Mills, I. G., Gibson, A., Hopkins, C. R., and McMahon, H. T. (2001) GTPase activity of dynamin and resulting conformation change are essential for endocytosis. Nature **410**, 231-235
31. McClure, S. J., and Robinson, P. J. (1996) Dynamin, endocytosis and intracellular signalling (review). Molecular membrane biology **13**, 189-215
32. Pucadyil, T. J., and Schmid, S. L. (2008) Real-time visualization of dynamin-catalyzed membrane fission and vesicle release. Cell **135**, 1263-1275
33. Zhang, P., and Hinshaw, J. E. (2001) Three-dimensional reconstruction of dynamin in the constricted state. Nature cell biology **3**, 922-926

34. Roux, A., Uyhazi, K., Frost, A., and De Camilli, P. (2006) GTP-dependent twisting of dynamin implicates constriction and tension in membrane fission. Nature **441**, 528-531
35. Sun, X. J., Yau, V. K., Briggs, B. J., and Whittaker, G. R. (2005) Role of clathrin-mediated endocytosis during vesicular stomatitis virus entry into host cells. Virology **338**, 53-60
36. Moore, J. P., and Stevenson, M. (2000) New targets for inhibitors of HIV-1 replication. Nat Rev Mol Cell Bio **1**, 40-49
37. Kilby, J. M., Hopkins, S., Venetta, T. M., DiMassimo, B., Cloud, G. A., Lee, J. Y., Alldredge, L., Hunter, E., Lambert, D., Bolognesi, D., Matthews, T., Johnson, M. R., Nowak, M. A., Shaw, G. M., and Saag, M. S. (1998) Potent suppression of HIV-1 replication in humans by T-20, a peptide inhibitor of gp41-mediated virus entry. Nature medicine **4**, 1302-1307
38. Liu, S., Lu, H., Niu, J., Xu, Y., Wu, S., and Jiang, S. (2005) Different from the HIV fusion inhibitor C34, the anti-HIV drug Fuzeon (T-20) inhibits HIV-1 entry by targeting multiple sites in gp41 and gp120. The Journal of biological chemistry **280**, 11259-11273
39. Kim, J. H., Song, H., Austin, J. L., and Cheng, W. (2013) Optimized Infectivity of the Cell-Free Single-Cycle Human Immunodeficiency Viruses Type 1 (HIV-1) and Its Restriction by Host Cells. PloS one **8**, e67170
40. Adachi, A., Gendelman, H. E., Koenig, S., Folks, T., Willey, R., Rabson, A., and Martin, M. A. (1986) Production of acquired immunodeficiency syndrome-associated retrovirus in human and nonhuman cells transfected with an infectious molecular clone. Journal of virology **59**, 284-291
41. Connor, R. I., Chen, B. K., Choe, S., and Landau, N. R. (1995) Vpr is required for efficient replication of human immunodeficiency virus type-1 in mononuclear phagocytes. Virology **206**, 935-944
42. Cavrois, M., Neidleman, J., Bigos, M., and Greene, W. C. (2004) Fluorescence resonance energy transfer-based HIV-1 virion fusion assay. Methods in molecular biology **263**, 333-344
43. Sodroski, J., Goh, W. C., Rosen, C., Campbell, K., and Haseltine, W. A. (1986) Role of the HTLV-III/LAV envelope in syncytium formation and cytopathicity. Nature **322**, 470-474
44. Strober, W. (2001) Trypan blue exclusion test of cell viability. Current protocols in immunology / edited by John E. Coligan ... [et al.] **Appendix 3**, Appendix 3B
45. Phelan, M. C. (2007) Basic techniques in mammalian cell tissue culture. Current protocols in cell biology / editorial board, Juan S. Bonifacino ... [et al.] **Chapter 1**, Unit 1 1
46. McGraw, T. E., and Subtil, A. (2001) Endocytosis: biochemical analyses. Current protocols in cell biology / editorial board, Juan S. Bonifacino ... [et al.] **Chapter 15**, Unit 15 13
47. Macia, E., Ehrlich, M., Massol, R., Boucrot, E., Brunner, C., and Kirchhausen, T. (2006) Dynasore, a cell-permeable inhibitor of dynamin. Dev Cell **10**, 839-850
48. Mu, F. T., Callaghan, J. M., Steelemortimer, O., Stenmark, H., Parton, R. G., Campbell, P. L., Mccluskey, J., Yeo, J. P., Tock, E. P. C., and Toh, B. H. (1995) Eea1, an Early Endosome-Associated Protein - Eea1 Is a Conserved Alpha-Helical

Peripheral Membrane-Protein Flanked by Cysteine Fingers and Contains a Calmodulin-Binding Iq Motif. Journal of Biological Chemistry **270**, 13503-13511
49. Wilson, J. M., de Hoop, M., Zorzi, N., Toh, B. H., Dotti, C. G., and Parton, R. G. (2000) EEA1, a tethering protein of the early sorting endosome, shows a polarized distribution in hippocampal neurons, epithelial cells, and fibroblasts. Mol Biol Cell **11**, 2657-2671
50. Rubino, M., Miaczynska, M., Lippe, R., and Zerial, M. (2000) Selective membrane recruitment of EEA1 suggests a role in directional transport of clathrin-coated vesicles to early endosomes. Journal of Biological Chemistry **275**, 3745-3748
51. Kimpton, J., and Emerman, M. (1992) Detection of Replication-Competent and Pseudotyped Human-Immunodeficiency-Virus with a Sensitive Cell-Line on the Basis of Activation of an Integrated Beta-Galactosidase Gene. Journal of virology **66**, 2232-2239
52. Platt, E. J., Wehrly, K., Kuhmann, S. E., Chesebro, B., and Kabat, D. (1998) Effects of CCR5 and CD4 cell surface concentrations on infections by macrophagetropic isolates of human immunodeficiency virus type 1. Journal of virology **72**, 2855-2864
53. Derdeyn, C. A., Decker, J. M., Sfakianos, J. N., Wu, X., O'Brien, W. A., Ratner, L., Kappes, J. C., Shaw, G. M., and Hunter, E. (2000) Sensitivity of human immunodeficiency virus type 1 to the fusion inhibitor T-20 is modulated by coreceptor specificity defined by the V3 loop of gp120. Journal of virology **74**, 8358-8367
54. Wei, X., Decker, J. M., Liu, H., Zhang, Z., Arani, R. B., Kilby, J. M., Saag, M. S., Wu, X., Shaw, G. M., and Kappes, J. C. (2002) Emergence of resistant human immunodeficiency virus type 1 in patients receiving fusion inhibitor (T-20) monotherapy. Antimicrobial agents and chemotherapy **46**, 1896-1905
55. Takeuchi, Y., McClure, M. O., and Pizzato, M. (2008) Identification of gammaretroviruses constitutively released from cell lines used for human immunodeficiency virus research. Journal of virology **82**, 12585-12588
56. Platt, E. J., Bilska, M., Kozak, S. L., Kabat, D., and Montefiori, D. C. (2009) Evidence that ecotropic murine leukemia virus contamination in TZM-bl cells does not affect the outcome of neutralizing antibody assays with human immunodeficiency virus type 1. Journal of virology **83**, 8289-8292
57. Klausner, R. D., Van Renswoude, J., Ashwell, G., Kempf, C., Schechter, A. N., Dean, A., and Bridges, K. R. (1983) Receptor-mediated endocytosis of transferrin in K562 cells. The Journal of biological chemistry **258**, 4715-4724
58. Dautry-Varsat, A., Ciechanover, A., and Lodish, H. F. (1983) pH and the recycling of transferrin during receptor-mediated endocytosis. Proceedings of the National Academy of Sciences of the United States of America **80**, 2258-2262
59. Osborne, A., Flett, A., and Smythe, E. (2005) Endocytosis assays in intact and permeabilized cells. Current protocols in cell biology / editorial board, Juan S. Bonifacino ... [et al.] **Chapter 11**, Unit 11 18
60. Ahn, S., Kim, J., Lucaveche, C. L., Reedy, M. C., Luttrell, L. M., Lefkowitz, R. J., and Daaka, Y. (2002) Src-dependent tyrosine phosphorylation regulates dynamin self-assembly and ligand-induced endocytosis of the epidermal growth factor receptor. The Journal of biological chemistry **277**, 26642-26651

61. Wang, L. H., Rothberg, K. G., and Anderson, R. G. W. (1993) Mis-Assembly of Clathrin Lattices on Endosomes Reveals a Regulatory Switch for Coated Pit Formation. Journal of Cell Biology **123**, 1107-1117
62. Wu, Y., Beddall, M. H., and Marsh, J. W. (2007) Rev-dependent indicator T cell line. Current HIV research **5**, 394-402
63. Miyauchi, K., Kozlov, M. M., and Melikyan, G. B. (2009) Early steps of HIV-1 fusion define the sensitivity to inhibitory peptides that block 6-helix bundle formation. PLoS pathogens **5**, e1000585
64. Park, R. J., Shen, H., Liu, L., Liu, X., Ferguson, S. M., and De Camilli, P. (2013) Dynamin triple knockout cells reveal off target effects of commonly used dynamin inhibitors. Journal of cell science **126**, 5305-5312
65. Accola, M. A., Ohagen, A., and Gottlinger, H. G. (2000) Isolation of human immunodeficiency virus type 1 cores: retention of Vpr in the absence of p6(gag). Journal of virology **74**, 6198-6202
66. Layne, S. P., Merges, M. J., Dembo, M., Spouge, J. L., Conley, S. R., Moore, J. P., Raina, J. L., Renz, H., Gelderblom, H. R., and Nara, P. L. (1992) Factors underlying spontaneous inactivation and susceptibility to neutralization of human immunodeficiency virus. Virology **189**, 695-714
67. Bourinbaiar, A. S. (1994) The ratio of defective HIV-1 particles to replication-competent infectious virions. Acta virologica **38**, 59-61
68. Kwon, Y. J., Hung, G., Anderson, W. F., Peng, C. A., and Yu, H. (2003) Determination of infectious retrovirus concentration from colony-forming assay with quantitative analysis. Journal of virology **77**, 5712-5720
69. Rusert, P., Fischer, M., Joos, B., Leemann, C., Kuster, H., Flepp, M., Bonhoeffer, S., Gunthard, H. F., and Trkola, A. (2004) Quantification of infectious HIV-1 plasma viral load using a boosted in vitro infection protocol. Virology **326**, 113-129
70. Thomas, J. A., Ott, D. E., and Gorelick, R. J. (2007) Efficiency of human immunodeficiency virus type 1 postentry infection processes: evidence against disproportionate numbers of defective virions. Journal of virology **81**, 4367-4370
71. Platt, E. J., Kozak, S. L., Durnin, J. P., Hope, T. J., and Kabat, D. (2010) Rapid dissociation of HIV-1 from cultured cells severely limits infectivity assays, causes the inactivation ascribed to entry inhibitors, and masks the inherently high level of infectivity of virions. Journal of virology **84**, 3106-3110
72. O'Doherty, U., Swiggard, W. J., and Malim, M. H. (2000) Human immunodeficiency virus type 1 spinoculation enhances infection through virus binding. Journal of virology **74**, 10074-10080
73. Marechal, V., Clavel, F., Heard, J. M., and Schwartz, O. (1998) Cytosolic Gag p24 as an index of productive entry of human immunodeficiency virus type 1. Journal of virology **72**, 2208-2212
74. Vidricaire, G., Tardif, M. R., and Tremblay, M. J. (2003) The low viral production in trophoblastic cells is due to a high endocytic internalization of the human immunodeficiency virus type 1 and can be overcome by the pro-inflammatory cytokines tumor necrosis factor-alpha and interleukin-1. The Journal of biological chemistry **278**, 15832-15841

Chapter 4.

Impact of Virion Endocytosis on Membrane-impermeable HIV-1 Drugs

4.1. Abstract

To determine if virion endocytosis can lead to productive infection, we used various inhibitors that are known to block various steps of endocytosis. The results from three different cell lines suggest that endocytosis can indeed lead to productive infection, as revealed by the specific inhibition of HIV-1 infectivity by the dynamin I K44A mutant (discussed in chapter 3). However, endocytosis may not be the only productive pathway for HIV-1 infection because all these inhibitions that we have observed appear to be partial, which is in sharp contrast to inhibition by fusion inhibitor, T20. These results also suggest that endocytosed virion needs to fuse with endosomal membrane for productive infection. In comparison to direct fusion at the plasma membrane, endocytosis may allow virus to escape from membrane impermeable drugs (1, 2). The conclusion that endocytosis can

cause productive infection of HIV-1 virions in chapter 3 led us to investigate whether endocytosis affects membrane-impermeable drugs of HIV-1.

To address this question, we have tested both neutralizing antibodies and T20, and further focused on T20 to dissect the mechanisms of inhibition. There was no effect of T20 on HIV internalization by observing and analyzing confocal images. To further investigate the impact of endocytosis on the efficacy of T20, we did titration of T20 and also varied the time of addition for T20 with regard to virion infection by TZM-bl cells, whose endocytic activity had been inhibited. These experiments showed that endocytosis has no apparent effect on T20 efficacy, suggesting that endocytosis does not offer any measurable advantage for virus to escape. As a matter of fact, for both antibodies and T20, HIV-1 infection can be blocked close to 100%, indicating that these drugs are efficacious enough *in vitro* even though HIV can establish productive infection through endocytosis. Future experiments for the mechanism of T20 will be the colocalization studies between virions and anti-CD4 or fluorescently-labeled T20 inside endosomes in order to investigate the hypothesis that membrane-impermeable drugs exert its inhibitory effect on viral fusion within the endosome as virus bound to CXCR4 coreceptor followed by the engagement between CD4 receptor and gp120.

4.2. Introduction

HIV-1 has rapidly evolved due to the size of the viral population in individual patients (3, 4), extensive recombination (5, 6), and the high rate of viral replication, which

contributes to genetic variation (7, 8). This can cause a considerable challenge for anti HIV-1 drugs development (9). During HIV-1 infection, almost all individuals produce antibodies to viral envelope glyocoproteins, but only a small fraction can neutralize the virus (10, 11). Recently, several studies have shown that the sera of 10 to 25% of infected patients contain broadly reactive neutralizing antibodies (NAbs) for various primary strains of HIV-1 (12-16). Initially, the mechanism of this serum neutralization was poorly understood; however, it was revealed that viral neutralization epitopes came from the isolation of neutralizing human monoclonal antibodies (mAbs). These mAbs targeted three distinct regions of the viral envelope: the CD4 binding site of gp120 (b12), surface glycans on the outer domain of gp120 (2G12), and the membrane proximal external region of gp41, just prior to the transmembrane spanning sequence (2F5, 4E10, and Z13e). However, none of the above broadly neutralizing antibodies was able to neutralize the majority of diverse HIV-1 strains even with additional HIV-1 isolates from geographically various regions (17).

The envelope glycoprotein complex is indispensable to HIV-1 entry into cells by mediating the viral attachment to target cells and subsequent membrane fusion. Several steps of the entry process can be targets of antiviral drug development. Receptor antagonists prevent attachment of gp120 to the receptor or coreceptor, and conformational changes within gp41 required for membrane fusion can be blocked by fusion inhibitors. The first fusion inhibitor developed was peptide mimics of the HR2 (heptad repeat domain 2) sequence of gp41 that act by competitively binding to HR1 (heptad repeat domain 1). T20 (Enfuvirtide/Fuzeon, Roche/Trimeris) is a 36 amino acid peptide corresponding to the gp41 amino acid sequence of the HXB2 isolate, shifted several residues along the HR2

sequence with respect to each other (18-24). This peptide inhibits virus entry by binding to the HR1 core that is formed after binding of gp120 to CD4 and the coreceptor, thereby blocking the subsequent formation of the six-helix bundle (18, 24-26). It is active in the nanomolar range against various HIV strains and blocks virus infection of cells and viral spread via cell-cell contact, which may be the more physiological route (18-24, 27). T20 has been used as a salvage therapy for patients who have developed a resistance issue with highly active antiretroviral therapy (HARRT), which is a combination of several drugs that aims to control the amount of virus in patients' body (28, 29). It was approved for clinical use in March 2003 by the US Food and Drug Administration (FDA) and the European Medicines Agency (EMEA). T20, however, needs to be subcutaneously injected to reach a sufficiently high blood level for inhibiting viral infection and also causes common symptoms on the injection site (30-34). Thus, there are ongoing studies to develop the new generations of T20-like peptides with improved potency, stability, and formulation (35, 36). Besides T20 and derivatives, other fusion inhibitors have been developed that target different domains of gp41 (36, 37).

Although there have been promising data in the early phase I and II clinical trials, the company, Roche/Trimeris decided to stop developing further clinical trials for the next generation of fusion inhibitors. This decision was "due to challenges with achieving the technical profile required of the current investigational formulation of T1249". The company emphasized that the "current formulation of T1249 would not be suitable for large scale clinical use" (38). However, T20 was the first new class of HIV inhibitors targeting the viral entry step. T20 was therefore a promising ingredient of a therapeutic salvage regimen (39) since T20 action is not affected by the presence of resistance

mutations against protease and reverse transcriptase inhibitors. Thus, research on the next generation of fusion inhibitors, which optimally have enhanced efficacy, a higher genetic barrier to resistance issue, less frequent subcutaneous administration, and combined with the use of new formulation methods will help prevent both chronic and acute viral infections.

In this study, we hypothesized that virion endocytosis offer an advantage for virus to escape from membrane-impermeable antiviral drugs, such as broadly neutralizing antibodies, or specifically T20. Otherwise, it may exert its inhibitory effect on viral infections as endocytosed together with virions in endosomes. The results from three different cell lines suggest that endocytosis can indeed lead to productive infection, as revealed by the specific inhibition of HIV-1 infectivity by the dynamin K44A mutant (discussed in chapter 3). However, endocytosis may not be the only productive pathway for HIV-1 infection because all these inhibitions that we have observed appear to be partial, which is in sharp contrast to inhibition by T20. These results also suggest that endocytosed virion needs to fuse with endosomal membrane for productive infection. In comparison to direct fusion, endocytosis may allow virus to escape from membrane impermeable drugs (1, 2). To test this hypothesis, we observed the effect of T20 on the internalization of HIV-1 by analyzing confocal images. To further investigate the impact of endocytosis on the efficacy of T20, we did titration of T20 and also varied the time of addition for T20 with regard to virion infection by TZM-bl cells, whose endocytic activity had been inhibited. Investigating the behavior and mechanism of T20 is fundamentally important for molecular understanding of HIV-1 entry as well as developing the new generations of T20-like antiviral HIV-1 drugs.

4.3. Materials and Methods

Virus production

HEK 293T/17 cells (AYCC, Manassas, VA) were cultured at 37°C with 5% of CO_2 in media including 90% of DMEM and 10% of FBS (HyClone, Laboratories, Logan, UT). All cells for virus production were less than five times passaged. To produce single-cycle HIV-1 virions, 10^6 293T cells in 2-ml were seeded, settled overnight in 6-well plate and transfected with necessary plasmids using TransIT LT-1 transfection reagent (Mirus Bio, Madison, WI). For each well, 1 µg of proviral DNA as pNL4-3R$^-$E$^-$ was used together with various amount of envelope expression plasmid, pcDNA3.1REC and 0.3 µg of pEGFP-Vpr. HIV-1 virions carrying 50% free EGFPs were produced with 0.5 µg of pNL4-3E$^-$ and 0.5 µg of pNL4-3E$^-$MA-EGFP-CA plasmids with various amount of pcDNA3.1REC. The amount of plasmids for EGFP tags was determined based on the highest concentration of infectious virus particles (Ci.p.) (discussed in chapter 2) (40). The entire culture media including virus was replaced at 6 hours post transfection, collected and filtered using a 0.45-µm syringe filter (Millex-HV PVDF, Millipore) at 24 post transfection for EGFP-Vpr HIV-1. For free EGFP tagged virions, 18 hours was used as a harvesting time. All virus samples were flash frozen and stored -80°C. All detailed transfection and virus preparation procedures followed the protocol described earlier in our work (40).

To produce T cell-derived virions, $2X10^6$ Jurkat cells in 1-ml were transfected with 0.5 µg of pNL4-3E$^-$ and 0.5 µg of pNL4-3E$^-$MA-EGFP-CA plasmids with 1 µg pcDNA3.1REC. 2 µl of TransIT-Jurkat transfection reagent (Mirus Bio, Madison, WI) with 1 µg of DNA was used for the highest transfection efficiency. They were harvested

for 72 hours, centrifuged down in 300 g for 5 minutes, and filtered using a 0.45-μm syringe filter. Virus samples were then flash frozen and stored -80°C.

Measuring the inhibition on virus infection by membrane-impermeable drugs

$8X10^4$ TZM-bl cells were seeded in 12-well plate and cultured overnight at 37°C with 5% of CO_2 in media including 90% of DMEM and 10% of FBS. VRC03 (cat#12032, NIH AIDS Research and Reference Reagent Program), VRC01 (cat#12033), and b12 (cat#2640) were used as neutralizing antibodies (NAb). Virions carrying EGFP-Vpr in 40 μl was incubated with each concentration of antibodies in 10 μl for 1 hour at room temperature. The concentration of NAbs in Figure 4.1A and B was based on the concentration during preincubation step. The virion-NAb complex was then diluted with complete media including 20 μg/ml DEAE-dextran without vortexing, and inoculated with TZM-bl cells for 2 hours with every 30 min gentle rocking. In the case of T20, which acts on virus, cells were inoculated with a mixture of virus and certain concentration of T20 instead of pretreatment. Inoculation was done at 37°C for 2 hours with every 30 minutes rocking in the presence of 20 μg/ml DEAE-dextran. After 2 hours inoculation, inoculum was removed and cells were washed with using complete media once. Cells were further incubated for 2 days at 37°C by adding 1-ml of complete media. Cells were then fixed with 2% gluteraldehyde for 5 minutes at room temperature, and stained using β-galactosidase staining kit (Mirus Bio, Madison, WI) for 50 minutes at 37°C. The inhibition data was calculated by normalizing the number of blue cells in each well compared to TZM-bl inoculated with virions which had not been pretreated or premixed with neutralizing antibodies or T20.

Confocal imaging to classifying and quantitating the location of virions

SupT1 cells (cat#100, NIH AIDS Research and Reference Reagent Program) were cultured at 37°C with 5% of CO_2 in medium including 90% of RPMI and 10% of FBS. $2X10^5$ SupT1 cells in 200 µl were inoculated with virions carrying free EGFPs derived from 293T or Jurkat for 30 minutes, 2 or 4 hours with automatic rocking. 10 µg/ml DEAE-dextran was used with virus inoculation in SupT1 cell line, which was optimized previously (Figure 3.1). The virion in 100 µl was prepared as mixture with 1 µM T20, which is the saturating concentration in SupT1 cell line (Figure 3.8C). Free virions after inoculation were removed by washing with 300 µl of complete media using 300 g for 5 minutes. Cells were resuspended with l-ml of complete media and deposited on PLL-coated coverslip with 1,000 g for 5 minutes. Supernatant was removed and the coverslip was fixed with 4% paraformaldehyde for 10 minutes at room temperature. Cells were stained with 1,000 fold diluted Cholera Toxin Subunit B with alexa fluorophore 555 conjugate (Invitrogen), which was dissolved in phosphate buffered saline (PBS) as 1 µg/µl, and stored at -80°C freezer. The coverslip was then washed with PBS and mounted onto a glass cover slide with 3 µl mounting media, sealed with nail polish, and imaged using an Olympus FluoView 500 Laser Scanning Confocal Microscope.

The virions and cellular membrane in a fluorescence image were identified and the location of virions can be categorized as inside, outside, or on the cell surface using a custom-written MATLAB script. Since the many virions can be imaged on several near slices of confocal images, we need to determine the exact location of actual fluorescent virus particles. In order to correlate between virion regions and slices, we found all overlapping virions regions by globally finding the shortest centroid-to-centroid distances

and relabeled virion regions, which has the highest intensity. Also, a cell whose membranes stained by Cholera Toxin B-Alexa 555 conjugate can usually be detected using edge detection method and basic morphology given sufficient contrast. Detected cellular boundaries can be further dilated or eroded by a certain pixel size. Based on our several trials using different pixel sizes to see whether there is a significant difference in the fraction of virions inside cells, there was no apparent differences. We decided to use 5 pixels for dilation and 1 pixel for erosion based on the nearest boundaries between stained and detected membranes (data not shown). All confocal images were collected with 100X objective and 250 nm step size. From five to seven different areas on the same coverslip were collected for each data point.

Measuring the impact of endocytosis on T20 efficacy

$8X10^4$ TZM-bl cells in 1-ml were seeded in 12-well plate and cultured overnight at 37°C. Complete media was removed and 100 µl of complete media containing 80 µM dynasore was pretreated with TZM-bl cells for 30 minutes at 37°C. Dynasore was removed and cells were washed once. Then cells were inoculated with a mixture of virus and certain concentration of T20 instead of pretreatment. Inoculation was done at 37°C for 2 hours with every 15 minutes rocking in the presence of 20 µg/ml DEAE-dextran. Cells were further incubated for 2 days at 37°C by adding 1-ml of complete media. Cells were then fixed with 2% gluteraldehyde for 5 minutes at room temperature, and stained using β-galactosidase staining kit 50 minutes at 37°C. The number of blue cells were counted with a microscope. The inhibition data was normalized with two different ways. One is singly normalized to no dynasore control. The other is normalized to no dynasore without T20.

For measuring the effect of endocytosis inhibition by dyn I K44A on T20 efficacy, we transfected TZM-bl cells for 24 hours with 2 μg of each plasmid, pcDNA3.1(-), non-tagged dyn I K44A from rat, or HA-tagged dyn I K44A from human. We used TransIT LT-1 as a transfection reagent (Mirus Bio, Madison, WI). Then, cells were trypsinized and $8X10^4$ cells in 1-ml were seeded in 12-well plate and settled at 37°C. After 6 hours, complete media was removed and cells were inoculated with 100 μl of diluted HIV-1. Inoculation was done at 37°C for 2 hours with every 15 minutes rocking in the presence of 20 μg/ml DEAE-dextran. Cells were further incubated for 2 days at 37°C by adding 1-ml of complete media. Further assay was the same as previous experiments. The number of blue cells were counted with a microscope. The inhibition data was normalized with two different ways. One is singly normalized to pcDNA3.1(-) transfection control. The other is normalized to pcDNA3.1(-) transfected cells without T20.

T20 efficacy with different time points T20 added

$8X10^4$ TZM-bl cells in 1-ml were seeded in 12-well plate and cultured overnight at 37°C. Complete media was removed and 100 μl of complete media containing 80 μM dynasore was pretreated with TZM-bl cells for 30 minutes at 37°C. Dynasore was removed and inoculation was done at 37°C for 2 hours with every 15 minutes rocking in the presence of 20 μg/ml DEAE-dextran. 100 nM T20 in 10 μl added and mixed well to cells (with virus) at different time points from 0 minutes to 2 hours during 2 hours inoculation time. Cells were further incubated for 2 days at 37°C by adding 1-ml of complete media. Cells were then fixed with 2% gluteraldehyde for 5 minutes at room temperature, and stained using β-galactosidase staining kit 50 minutes at 37°C. The number of blue cells were counted with

a microscope. The inhibition data was normalized with two different ways as the same discussed above.

For measuring the effect of endocytosis inhibition by dyn I K44A on T20 efficacy with different time points T20 added, we transfected TZM-bl cells for 24 hours with 2 µg of each plasmid, pcDNA3.1(-), non-tagged dyn I K44A from rat, or HA-tagged dyn I K44A from human. We used TransIT LT-1 as a transfection reagent. Then, cells were trypsinized and $8X10^4$ cells in 1-ml were seeded in 12-well plate and settled at 37°C. After 6 hours, complete media was removed and cells were inoculated with 100 µl of diluted HIV-1. Inoculation was done at 37°C for 2 hours with every 15 minutes rocking in the presence of 20 µg/ml DEAE-dextran. Cells were further incubated for 2 days at 37°C by adding 1-ml of complete media. Further assay was the same as previous experiments. The number of blue cells can be singly normalized to pcDNA3.1(-) transfection control or respectively normalized to pcDNA3.1(-) transfected cells without T20.

4.4. Results

4.4.1. Potency of membrane-impermeable HIV-1 entry inhibitors

Broadly neutralizing antibodies have known to efficiently block viral envelope, either gp120 or gp41, to interact with its corresponding receptor. T20 is also one of the potent antiviral drugs and it is a 36 amino acid synthetic peptide homologous to gp41 and first fusion inhibitor clinically approved by FDA (29, 41). Although both neutralizing antibodies and fusion inhibitors are membrane-impermeable, they are a potent drugs *in vitro* (9, 42). Based on our observation that endocytosis lead to productive viral entry, we

hypothesized that membrane-impermeable drugs exert its inhibitory effect on viral fusion within the endosome as virus bound to CXCR4 coreceptor followed by the engagement between CD4 receptor and gp120. As shown in Figure 4.1A and B, VRC03 and b12 inhibited viral infections close to 100% regardless of their fluorescence tags although fluorescent-tagged antibodies needed higher concentrations for neutralization. T20 also showed a good efficacy on viral infection (Figure 4.1C), which was also confirmed with Rev-CEM and SupT1 cell lines in chapter 3. With our results, 1 μM T20 is enough to block almost all viral infections in TZM-bl, Rev-CEM, and SupT1 cell lines (Figure 3.7 and Figure 4.1).

4.4.2. Quantitation of virion internalization with T20 treatment

Based on our observation that endocytosis lead to productive viral entry, we hypothesized that membrane-impermeable drugs may be able to enter cells and inhibit viral fusion within the endosome as virus bound to CXCR4 coreceptor followed by the interaction between CD4 receptor and gp120. With further imaging experiments, even with saturated condition for all productive infections by T20, there were still many endocytosed virions inside cells (Figure 4.2B), which also led to our hypothesis that T20 might be able to block a fusion event between viral and endosomal membranes. If there is a direct fusion event of free EGFP-tagged virus at the plasma membrane, the signals from it will quickly disappear and not be detected due to infinite dilution with the plasma membrane and cytosol (43). Thus, we expected to see the higher fraction of virion internalization inside cells with T20 allowing no fusion events. The fraction of internalized virions was measured

as the number of internalized one divided by the total number of virus particles in a field of view (FOV). We are able to exclude the possibility that all productive infections are via a direct fusion at the plasma membrane, then all endocytosed virus particles are towards a nonproductive pathway, based on our previous data (discussed in chapter 3). With a custom-written MATLAB manuscript, we can classify the location of fluorescent virus particles based on the cellular plasma membrane. They can be located inside a cell, outside a cell, or as bound to cellular membrane.

First of all, the fraction of internalized gag particles, which don't have viral envelope on virion surface required for receptor-mediated endocytosis, was above 10% in different inoculation time points (Figure 4.3A). It is not significantly different from the fraction of virion internalization (Figure 4.3B and C). Therefore, more than half fraction of virion internalization can be nonspecifically endocytosed through receptor-independent endocytosis.

However, this phenomena might be due to host proteins of 293T cell line, which is used for virion production and is not a natural target/producer cell for HIV-1. The mechanisms of endocytic entries are uncertain. Whether they are mediated by gp120 or other host proteins on viral surface remains to be determined. In order to confirm whether the receptor-independent endocytosis we observed is host proteins-specific or not, we produced virions from Jurkat T cell line and conducted the same experiment as the above. The result from T cell-derived virions also showed that gag particles enter cells via receptor-independent pathway based on the similar fraction of virion internalization compared to virions carrying viral envelope regardless of the presence of T20 (Figure 4.4A and B).

Also, since we've not seen an apparent difference in the fraction of virus inside cells with 2 hours as inoculation time point, we decided to try 30 minutes and 4 hours as shorter and longer time points. Endocytosis is quite fast event, so we might not be able to capture the earlier fusion events. However, it turned out that there were statistically comparable fractions of internalized virions regardless of inoculation time points and T20 treatment (Figure 4.3B and C), suggesting that endocytosed virions are long-lived, which was also observed in TZM-bl cells (data not shown). One possible reason we couldn't see the difference is that the fusion events might be very low probability due to low infectivity. Based on these data, we concluded that endocytosed virus particles all progressed towards non-productive infection pathways in the presence of T20 and those inside endosomes have relatively long lifetime.

The above results generated several hypotheses that can be further tested. One of the possible experiments is to observe the colocalization of FITC-T20 and mCherry-labeled virus together with endosome markers using a microscope, which has resolution to resolve single fluorophores in mammalian cells. This will permit imaging of FITC-T20 since FITC-labeled virions cannot be observed in a confocal microscope without a resolution for single fluorophores.

4.4.3. Effect of T20 on virion endocytosis

The conclusion that endocytosis can cause productive infection of HIV-1 virions in chapter 3 led us to investigate whether endocytosis affects membrane-impermeable drugs of HIV-1.

To test this hypothesis, we have tested the effect of T20 on the internalization of HIV-1 by analyzing confocal images. As shown in Figure 4.3, there was no measurable effect of T20 on virion endocytosis regardless of the presence of viral envelope, the input of viral envelope, and different inoculation time points. Although we concluded we were not able to see the difference in the fraction of virion internalization between the absence and presence of 1 μM T20, the effect of T20 on virion internalization was not apparent. This phenomena was also confirmed with T cell-derived HIV-1 virions (Figure 4.4).

4.4.4. Impact of virion endocytosis on membrane impermeable HIV-1 drugs

It has been suggested in literature that endocytosis may allow virions to escape from the action of membrane-impermeable drugs (1, 2). To test whether endocytosis affects membrane-impermeable drugs of HIV-1, we did titration of T20 with dynasore-pretreated or dyn I K44A transfected TZM-bl cells.

TZM-bl cells were pretreated with 80 μM dynasore for 30 mintutes and dynasore was then removed. Cells were inoculated with virions in the presence of different concentrations of T20. Figure 4.5A showed the fraction of blue cells singly normalized to TZM-bl cells which had not been pretreated with dynasore. Consistently, there were ~30% inhibition on viral infection with 80 μM dynasore in the absence of T20 (Figure 3.7A). If we normalized the fraction of blue cells respect to each without T20, there was no difference in the efficacy of T20 between TZM-bl cells without dynasore pretreatment and cells whose endocytosis had been inhibited by dynasore (Figure 4.5B). For more specific manner, TZM-bl cells were transfected with two different dyn I K44A for 24 hours,

trypsinized, and settled for further infection assay. As shown in Figure 4.6A, the fraction of blue cells, which was singly normalized to TZM-bl cells which had been transfected with pcDNA3.1(-) also showed ~30% inhibition in the absence of T20 (consistent with Figure 3.3). If we respectively normalized the fraction of blue cells based on the absence of T20, T20 efficacy was similar regaredless of the inhibition on cell endocytosis by dyn I K44A (Figure 4.6B). Thus, endocytosis doesn't offer measurable advantages for virus to escape from T20.

4.4.5. T20 efficacy with different time points added

Since we observed that there was no apparent difference in T20 efficacy with inhibition on endocytosis by either dynasore or dyn I K44A, we hypothesized that T20 efficacy might be more related to T20 addition time.

We varied the time of 100nM T20 addition during virion inoculation. Consistently, if we varied the addition time of the mixture of virus and 100 nM of T20, which was shown at zero in the x-axis, there was ~50% inhibition on viral infection (Figure 4.1C and Figure 4.7). However, T20 efficacy dropped when we added T20 later during 2 hours inoculation window, suggesting T20 efficacy was different with T20 addition time (Figure 4.7 and 4.8). We have tested T20 efficacy in TZM-bl cells, whose endocytosis inhibited by dynasore or dyn I K44A, by varying the time of T20 addition.

The fraction of blue cells decreased by 30% in TZM-bl cells, which had been pretreated with dynasore (Figure 4.7A). When we normalized the number of blue cells with respect to each without T20, the fraction of blue cells was comparable in TZM-bl cells regardless of endocytosis inhibition (Figure 4.7B). This phenomena were also confirmed

when using TZM-bl cells transfected with each dyn I K44A. These experiments also showed that endocytosis has no apparent effect on T20 efficacy, suggesting that endocytosis does not offer an apparent advantage for virus to escape from membrane impermeable T20. There could be two mechanisms of T20. One possibility is that T20 blocks viral fusion at the site of action which is outside of the plasma membrane. The other mechanism is that T20 can be co-internalize with virus and exhibit inhibitory action within an endosome. For T20, we found that HIV-1 still undergoes endocytosis in the presence of saturating T20, suggesting the latter mechanism. However, there is one possibility for the former mechanism. The endocytosis in the presence of T20 are all receptor-independent and nonspecific. In order to exclude this, future experiment would be the colocalization studies of virions with anti-CD4 in an endosome.

4.5. Discussion

Some studies have suggested that endocytosis may allow virions to escape from the action of membrane-impermeable drugs (1, 2). The conclusion that endocytosis can contribute to productive infection of HIV-1 virions (discussed in chapter 3) leads to our investigation in this chapter: what is the impact of endocytosis on membrane impermeable drugs of HIV-1? To address this question, we have tested both neutralizing antibodies and one of the fusion inhibitors, T20, and further focused on T20 to dissect the mechanisms of inhibition.

First of all, both antibodies and T20 can block viral infections close to 100%, indicating that these drugs are efficacious enough *in vitro* even though HIV-1 can establish

productive infection through endocytosis, which was the conclusion from chapter 3. To test the hypothesis that endocytosis may allow virus to escape from membrane-impermeable drugs, we have tested the effect of T20 on the internalization of HIV-1 by analyzing confocal images. To further investigate the impact of endocytosis on the efficacy of T20, we did titration of T20 and also varied the time of addition for T20 with regard to virion infection by TZM-bl cells, whose endocytic activity had been inhibited. These experiments showed that T20 doesn't affect virion endocytosis and endocytosis has no apparent impact on T20 efficacy. It suggests that endocytosis does not offer measurable advantages for virus to escape from membrane-impermeable T20.

Since T20 is membrane-impermeable, there are two possible explanations for the above phenomena. T20 can block HIV-1 infection at the site of action outside of the plasma membrane. Otherwise, it might be co-internalize with virus and exhibit inhibitory action within an endosome. For T20, we observed many endocytosed HIV-1 in the presence of saturating T20, suggesting the latter mechanism. However, one possibility for the first mechanism is that the events of virion endocytosis in the presence of T20 are all receptor-independent and nonspecific. The possible experiment will be the colocalization of virions with anti-CD4 in an endosome.

The mechanism of T20 has been proposed that it binds to a region of gp41 that mediates the conformational change from pre-hairpin intermediate to the fusion-active structure based on its sequences homologous to C-terminal heptad repeat (CHR) region. Contrary to this belief, there are several studies suggesting other mechanisms of T20: T20 cannot inhibit the formation of stable six-helix bundles with N-peptides coming from N-

terminal heptad repeat (NHR) region, which is supposed to make stable six-helix bundle with CHR region; second, it is not able to block six-helix bundle formation of the fusogenic core; third, T20 efficacy can be significantly abrogated by peptides derived from the membrane-spanning domain in gp41 and coreceptor binding site in gp120 (28, 37). These data suggest that T20 inhibits HIV-1 entry by targeting multiple sites in gp41 and gp120. Investigating the behavior and mechanism of T20 is fundamentally important for molecular understanding of HIV-1 entry as well as developing the new generations of T20-like antiviral HIV-1 drugs with improved potency and stability.

4.6. Acknowledgements

This work was supported by NIH grant 1DP2OD008693-01 to Dr. Wei Cheng and also in part by Research Grant No. 5-FY10-490 to W.C. from the March of Dimes Foundation. The following reagents were obtained through the AIDS Research and Reference Reagent Program, Division of AIDS, National Institute of Allergy and Infectious Diseases (NIAID), National Institutes of Health (NIH): pNL4-3 from Dr. Malcolm Martin; pNL4-3.Luc.R^- E^- from Dr. Nathaniel Landau; pEGFP-Vpr from Warner C. Greene; TZM-bl cells from Dr. John C. Kappes, Dr. Xiaoyun Wu and Tranzyme Inc; SupT1 cells from Dr. Dharam Ablashi; Jurkat cells from Dr. Arthur Weiss. Authors thank Dr. Michael C. DeSantis for custom-written MATLAB, Microscopy and Image Analysis Laboratory for Olympus FluoView 500 Laser Scanning Confocal Microscope, and flow cytometry core in the University of Michigan.

4.7. Figures

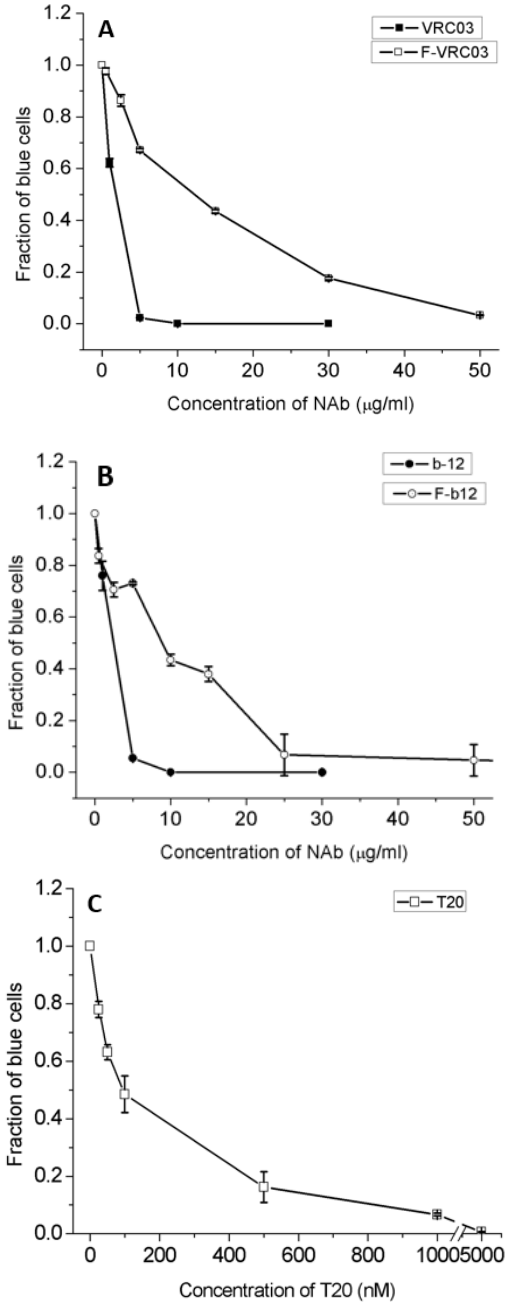

Figure 4.1. Potency of membrane-impermeable inhibitors in TZM-bl cell line.

(A) Neutralization of infectious HIV-1 particles by VRC03 antibody and Alexa-594-VRC03. (B) Neutralization of infectious HIV-1 particles by b12 antibody and Alexa-594-b12. (C) Inhibition on viral infection by T20. HIV-1 carrying EGFP-Vpr was used. Error bars are standard deviations from three independent replicates of the same experiments.

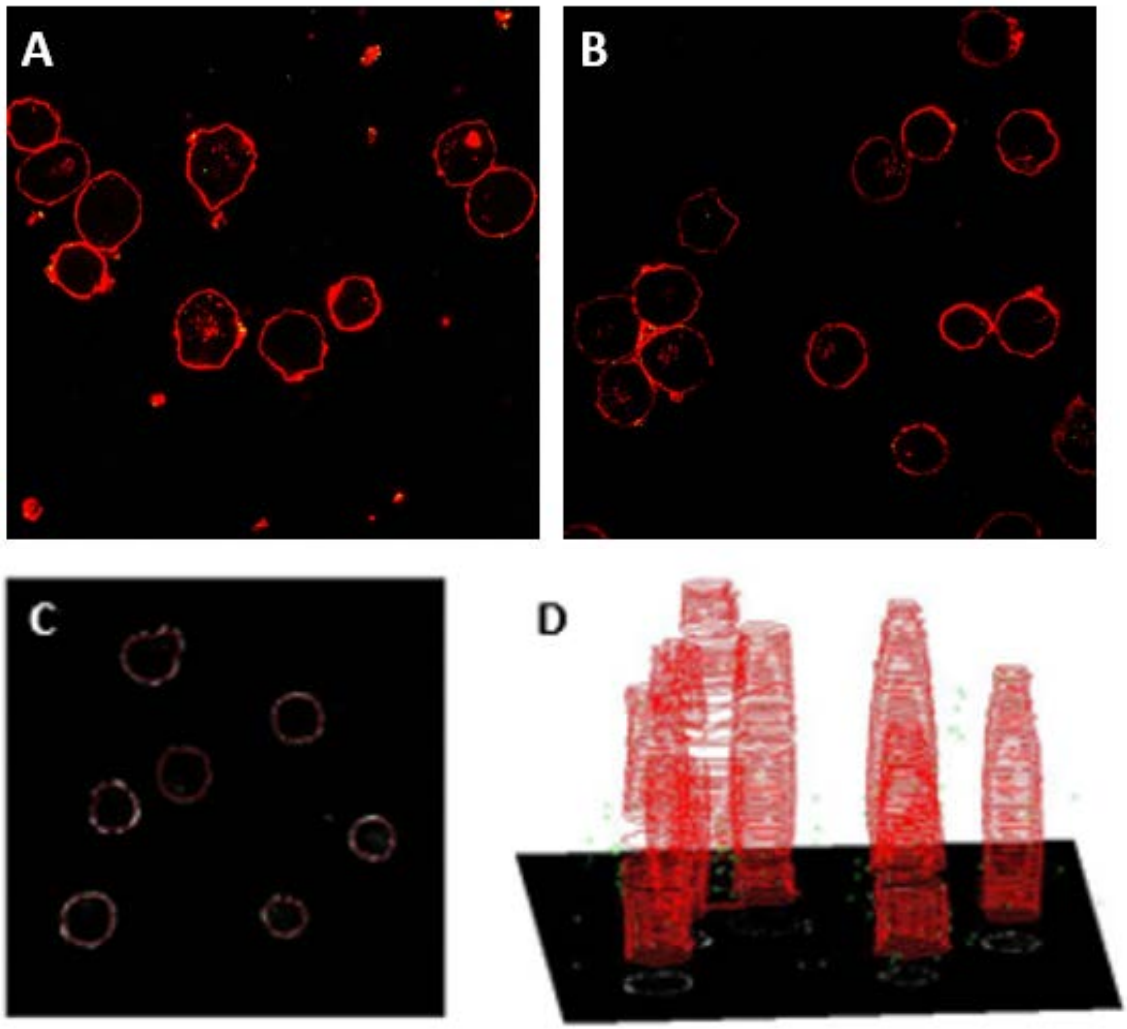

Figure 4.2. Classifying the location of virions inside, outside, or on cellular surface.

(A) A representative confocal image of SupT1 cells inoculated for 2 hours with HIV-1 carrying free EGFPs in the absence of T20. (B) A representative confocal image of SupT1 cells inoculated for 2 hours with HIV-1 carrying free EGFPs in the presence of 1 μM T20. (C) Cellular membranes identified (red circles) by custom-written MATLAB. (D) Whole stacks of confocal images in a FOV with identifying cellular membrane and classifying the location of virions. A cell can be detected using edge detection method and basic morphology given sufficient contrast. Identified cellular membrane was further dilated by 5 pixels and eroded by 1 pixel. Since fluorescent viral particles can be imaged more than 2 stacks of confocal image, we identified all virions and relabeled them as unique virions. All overlapping virion regions were globally found based on the shortest centroid-to-centroid distances and a virion on the slice having the strongest intensity were relabeld as a unique virion.

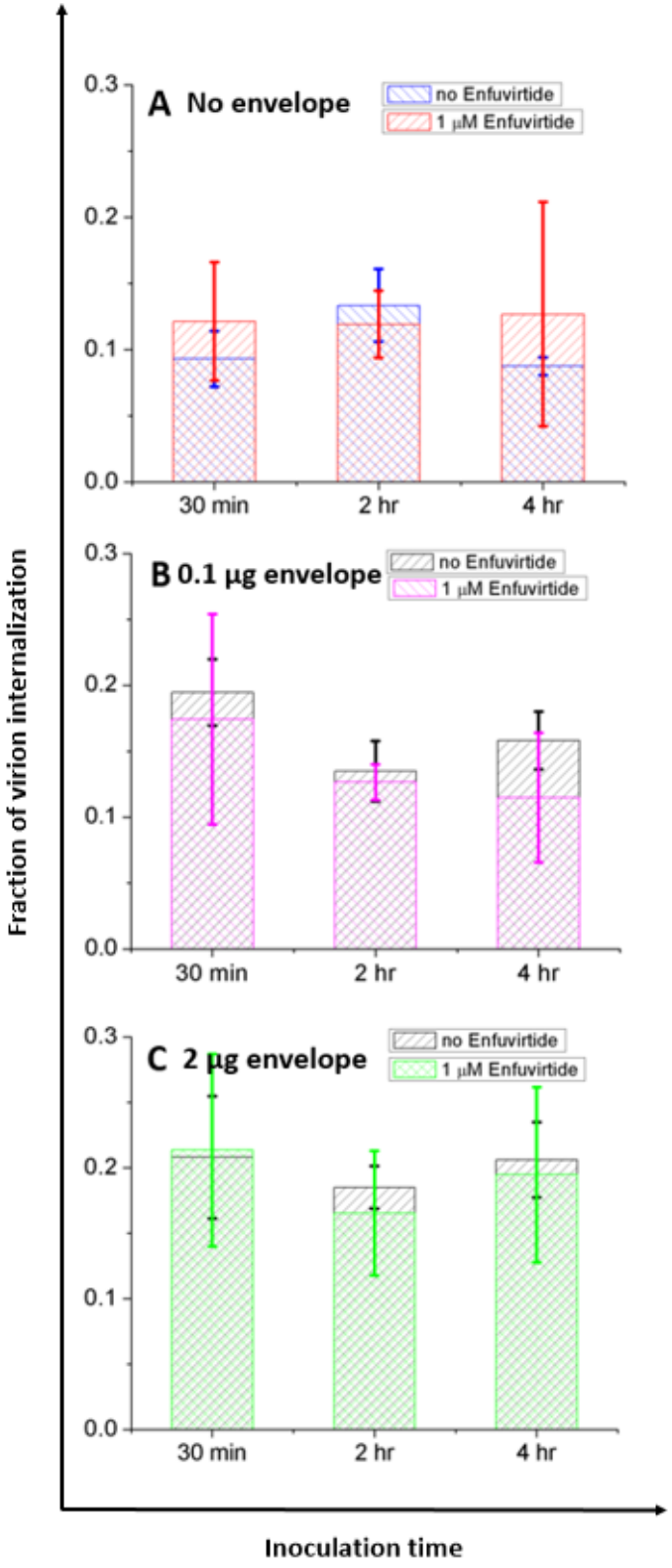
A No envelope
no Enfuvirtide
1 μM Enfuvirtide
B 0.1 μg envelope
no Enfuvirtide
1 μM Enfuvirtide
C 2 μg envelope
no Enfuvirtide
1 μM Enfuvirtide
0.3
0.2
0.1
0.0
30 min
2 hr
4 hr
Fraction of virion internalization
Inoculation time

Figure 4.3. Quantitation of endocytosed virions in SupT1 cell line in the absence or presence of saturating concentration of T20.

(A) Fraction of virion internalization with gag particles, which have no HIV-1 envelope on virion surface with different inoculation time points. Blue (no T20). Red (1 μM T20). (B) Fraction of virion internalization with HIV-1 having 0.1 μg NL4-3 envelope with different inoculation time points. Black (no T20). Purple (1 μM T20). (C) Fraction of virion internalization with HIV-1 carrying 1 μg NL4-3 envelope with different inoculation time points. Black (no T20). Green (1 μM T20). The location of virions can be analyzed as outside cells, inside cells, or on the cellular membrane. The fraction of virion internalization was calculated as a ratio of the number of virions inside cells to the total number of virions in a FOV. All virions were produced from 293T cells. MOP value was 200 for all samples. Error bars are from 35 cells in the average from five different areas were collected for each data point.

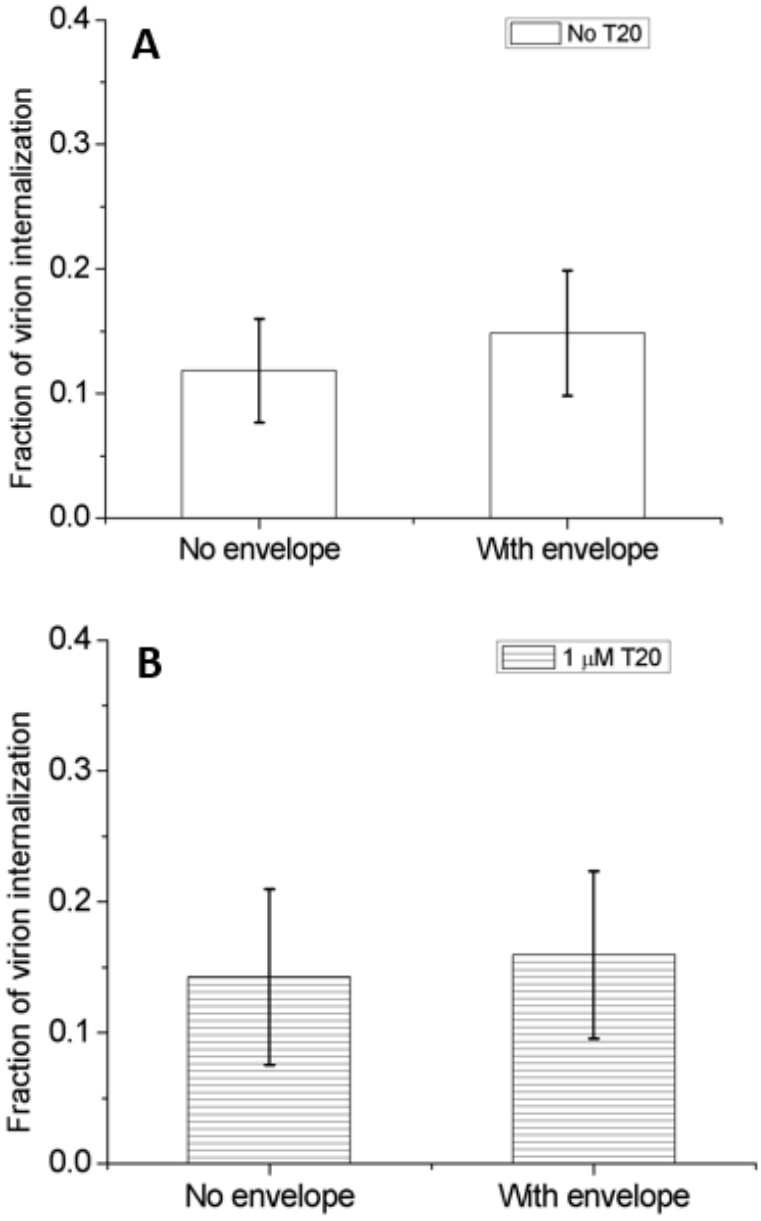

Figure 4.4. Receptor-independent endocytosis with T-cell derived virions in SupT1 cell line.

Quantitation of endocytosed virions derived from Jurkat T cells in the absence or presence of saturating concentration of T20. (A) Fraction of virion internalization with gag particles, which have no HIV-1 envelope or HIV-1 carrying 1 μg NL4-3 envelope with 2 hours inoculation time points in the absence of T20. (B) Fraction of virion internalization with gag particles, which have no HIV-1 envelope or HIV-1 carrying 1 μg NL4-3 envelope with 2 hours inoculation time points in the presence of 1 μM T20. MOP value was 200 for all samples. Error bars are from 30 cells in the average from five different areas were collected for each data point.

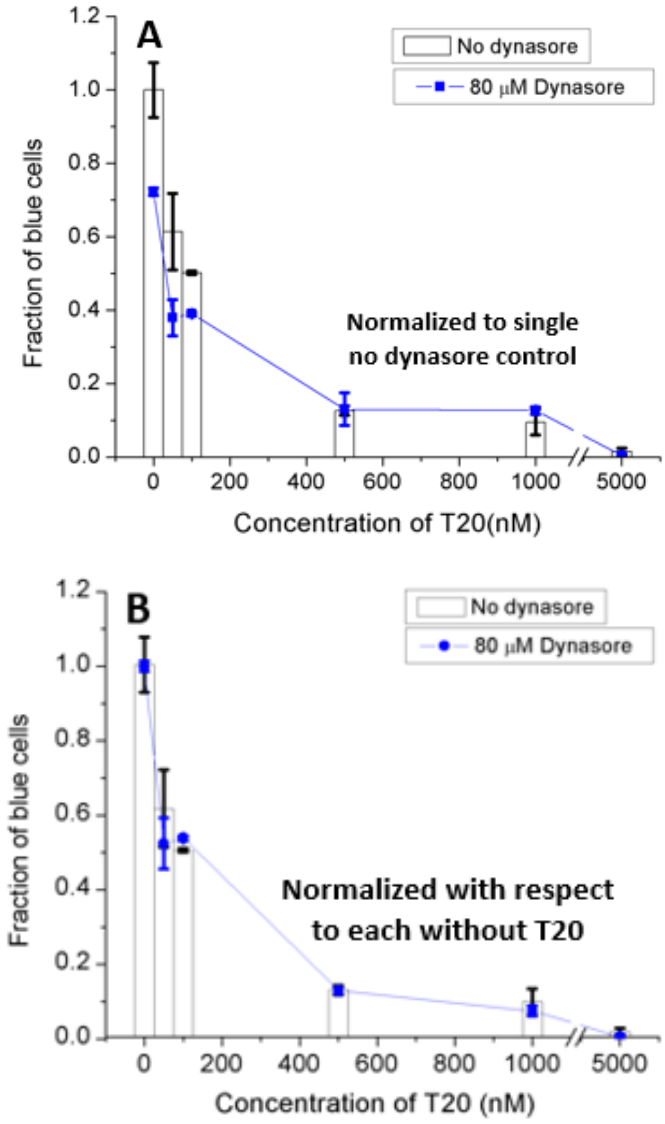

Figure 4.5. Effect of endocytosis inhibition by dynasore on T20 efficacy.

(A) Measurement of productive infections with different concentrations of T20 in TZM-bl cells pretreated with 80 μM of dynasore. The mixture of HIV-1 with different concentrations of T20 was inoculated for 2 hours. Fraction of blue cells were singly normalized to no dynasore control. (B) Same experimental data as (A) was analyzed with a different way. Fraction of blue cells were respectively normalized to no dynasore without T20. Black (no dynasore, the concentration of DMSO was the same as 80 μM dynasore). Blue (80 μM dynasore). Error bars are standard deviations from three independent replicates of the same experiments.

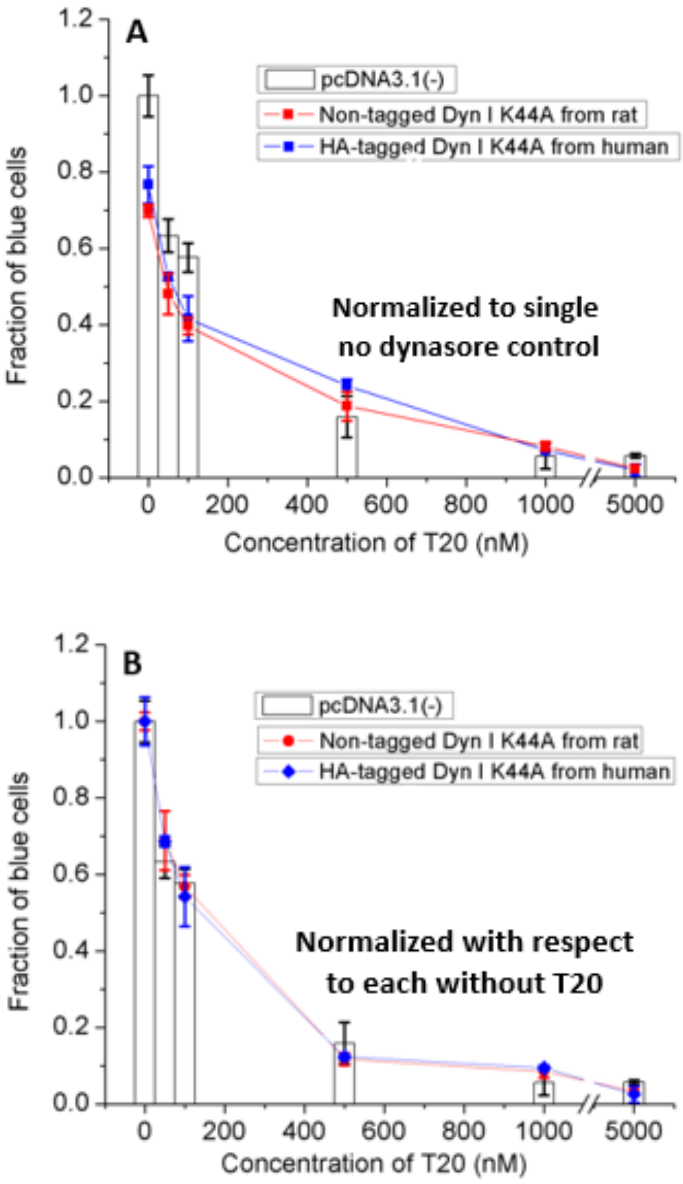

Figure 4.6. Effect of endocytosis inhibition by dyn I K44A on T20 efficacy.

(A) Measurement of productive infections with different concentrations of T20 in TZM-bl cells pretreated with 80 μM of dynasore. The mixture of HIV-1 with different concentrations of T20 was inoculated for 2 hours. Fraction of blue cells were singly normalized to pcDNA3.1(-) control. (B) Same experimental data as (A) was analyzed with a different way. Fraction of blue cells were respectively normalized to pcDNA3.1(-) without T20. Black (pcDNA3.1(-)). Red (non-tagged dyn I K44A from rat). Blue (HA-tagged dyn I K44A from human). Error bars are standard deviations from three independent replicates of the same experiments.

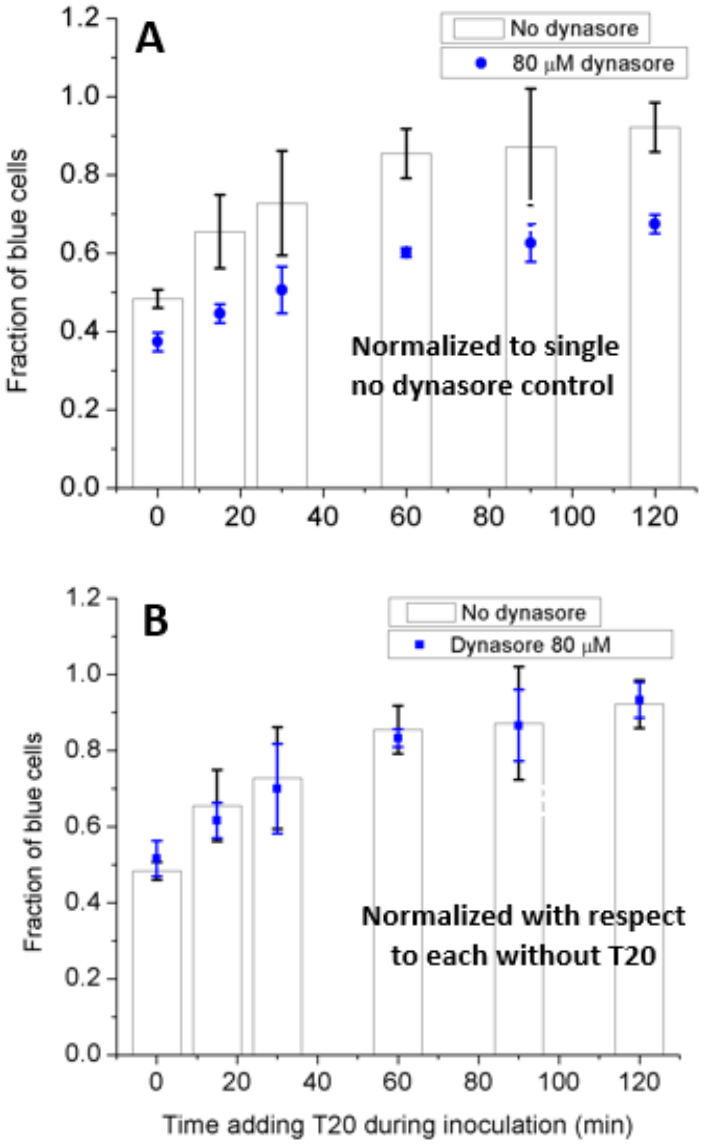

Figure 4.7. T20 efficacy in the presence of endocytosis inhibition by dynasore with different time points T20 added.

(A) Measurement of productive infections with different time points T20 added in TZM-bl cells pretreated with 80 μM of dynasore. Cells were inoculated with HIV-1 and 100 nM of T20 was added for each designated time within 2 hours inoculation. Fraction of blue cells were singly normalized to no dynasore control. (B) Same experimental data as (A) was analyzed with a different way. Fraction of blue cells were respectively normalized to no dynasore without T20. Black (no dynasore, the concentration of DMSO was the same as 80 μM dynasore). Blue (80 μM dynasore). Error bars are standard deviations from three independent replicates of the same experiments.

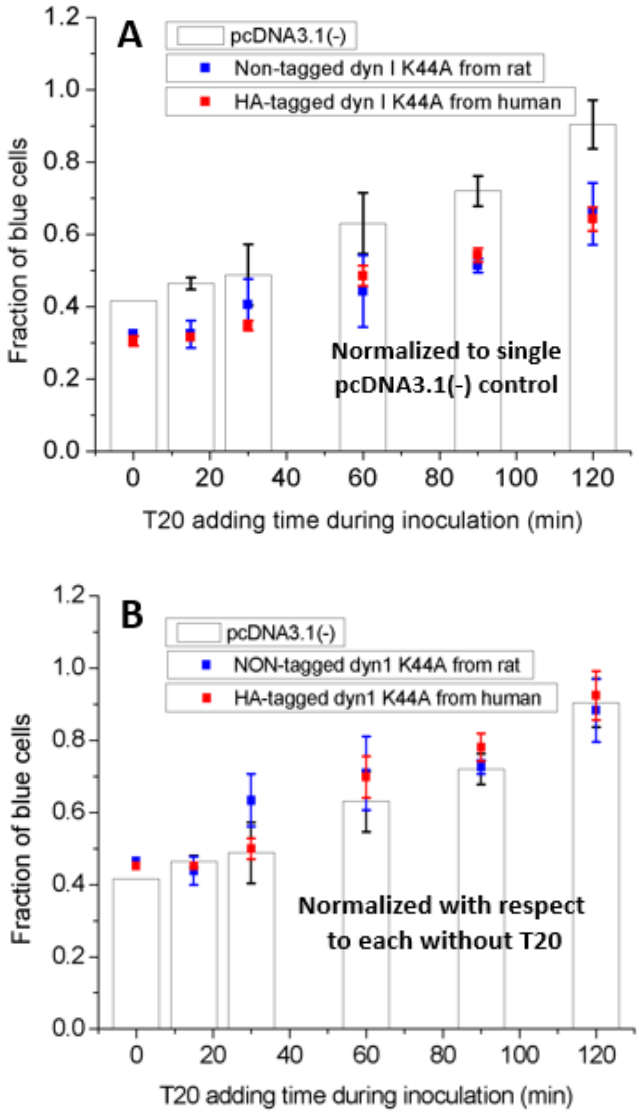

Figure 4.8. T20 efficacy in the presence of endocytosis inhibition by dyn I K44A with different time points T20 added.

(A) Measurement of productive infections with different time points T20 added in TZM-bl cells transfected with 2 µg of pcDNA3.1, non-tagged dyn I K44A (from rat), or HA-tagged dyn I K44A (from human). Cells were inoculated with HIV-1 and 100 nM of T20 was added for each designated time within 2 hours inoculation. Fraction of blue cells were singly normalized to pcDNA3.1(-) control. (B) Same experimental data as (A) was analyzed with a different way. Fraction of blue cells were respectively normalized to pcDNA3.1(-) without T20. Black (pcDNA3.1(-)). Blue (non-tagged dyn I K44A from rat). Red (HA-tagged dyn I K44A from human). Error bars are standard deviations from three independent replicates of the same experiments.

4.8 References

1. Roberts PC, Kipperman T, Compans RW. 1999. Vesicular stomatitis virus G protein acquires pH-independent fusion activity during transport in a polarized endometrial cell line. Journal of virology 73:10447-10457.
2. de la Vega M, Marin M, Kondo N, Miyauchi K, Kim Y, Epand RF, Epand RM, Melikyan GB. 2011. Inhibition of HIV-1 endocytosis allows lipid mixing at the plasma membrane, but not complete fusion. Retrovirology 8:99.
3. Ho DD, Neumann AU, Perelson AS, Chen W, Leonard JM, Markowitz M. 1995. Rapid turnover of plasma virions and CD4 lymphocytes in HIV-1 infection. Nature 373:123-126.
4. Campbell TB, Schneider K, Wrin T, Petropoulos CJ, Connick E. 2003. Relationship between in vitro human immunodeficiency virus type 1 replication rate and virus load in plasma. Journal of virology 77:12105-12112.
5. Jetzt AE, Yu H, Klarmann GJ, Ron Y, Preston BD, Dougherty JP. 2000. High rate of recombination throughout the human immunodeficiency virus type 1 genome. Journal of virology 74:1234-1240.
6. Zhuang J, Jetzt AE, Sun G, Yu H, Klarmann G, Ron Y, Preston BD, Dougherty JP. 2002. Human immunodeficiency virus type 1 recombination: rate, fidelity, and putative hot spots. Journal of virology 76:11273-11282.
7. Coffin JM. 1986. Genetic variation in AIDS viruses. Cell 46:1-4.
8. Coffin JM. 1995. HIV population dynamics in vivo: implications for genetic variation, pathogenesis, and therapy. Science 267:483-489.
9. Wu X, Yang ZY, Li Y, Hogerkorp CM, Schief WR, Seaman MS, Zhou T, Schmidt SD, Wu L, Xu L, Longo NS, McKee K, O'Dell S, Louder MK, Wycuff DL, Feng Y, Nason M, Doria-Rose N, Connors M, Kwong PD, Roederer M, Wyatt RT, Nabel GJ, Mascola JR. 2010. Rational design of envelope identifies broadly neutralizing human monoclonal antibodies to HIV-1. Science 329:856-861.
10. Pantophlet R, Burton DR. 2006. GP120: target for neutralizing HIV-1 antibodies. Annual review of immunology 24:739-769.
11. Montefiori DC, Morris L, Ferrari G, Mascola JR. 2007. Neutralizing and other antiviral antibodies in HIV-1 infection and vaccination. Current opinion in HIV and AIDS 2:169-176.
12. Doria-Rose NA. 2010. HIV neutralizing antibodies: clinical correlates and implications for vaccines. The Journal of infectious diseases 201:981-983.
13. Doria-Rose NA, Klein RM, Daniels MG, O'Dell S, Nason M, Lapedes A, Bhattacharya T, Migueles SA, Wyatt RT, Korber BT, Mascola JR, Connors M. 2010. Breadth of human immunodeficiency virus-specific neutralizing activity in sera: clustering analysis and association with clinical variables. Journal of virology 84:1631-1636.
14. Sather DN, Armann J, Ching LK, Mavrantoni A, Sellhorn G, Caldwell Z, Yu X, Wood B, Self S, Kalams S, Stamatatos L. 2009. Factors associated with the development of cross-reactive neutralizing antibodies during human immunodeficiency virus type 1 infection. Journal of virology 83:757-769.
15. Simek MD, Rida W, Priddy FH, Pung P, Carrow E, Laufer DS, Lehrman JK, Boaz M, Tarragona-Fiol T, Miiro G, Birungi J, Pozniak A, McPhee DA, Manigart O,

Karita E, Inwoley A, Jaoko W, Dehovitz J, Bekker LG, Pitisuttithum P, Paris R, Walker LM, Poignard P, Wrin T, Fast PE, Burton DR, Koff WC. 2009. Human immunodeficiency virus type 1 elite neutralizers: individuals with broad and potent neutralizing activity identified by using a high-throughput neutralization assay together with an analytical selection algorithm. Journal of virology 83:7337-7348.

16. Stamatatos L, Morris L, Burton DR, Mascola JR. 2009. Neutralizing antibodies generated during natural HIV-1 infection: good news for an HIV-1 vaccine? Nature medicine 15:866-870.
17. Mascola JR, Haynes BF. 2013. HIV-1 neutralizing antibodies: understanding nature's pathways. Immunological reviews 254:225-244.
18. Chan DC, Fass D, Berger JM, Kim PS. 1997. Core structure of gp41 from the HIV envelope glycoprotein. Cell 89:263-273.
19. Wild C, Oas T, McDanal C, Bolognesi D, Matthews T. 1992. A synthetic peptide inhibitor of human immunodeficiency virus replication: correlation between solution structure and viral inhibition. Proceedings of the National Academy of Sciences of the United States of America 89:10537-10541.
20. Wild CT, Shugars DC, Greenwell TK, McDanal CB, Matthews TJ. 1994. Peptides corresponding to a predictive alpha-helical domain of human immunodeficiency virus type 1 gp41 are potent inhibitors of virus infection. Proceedings of the National Academy of Sciences of the United States of America 91:9770-9774.
21. Kilby JM, Hopkins S, Venetta TM, DiMassimo B, Cloud GA, Lee JY, Alldredge L, Hunter E, Lambert D, Bolognesi D, Matthews T, Johnson MR, Nowak MA, Shaw GM, Saag MS. 1998. Potent suppression of HIV-1 replication in humans by T-20, a peptide inhibitor of gp41-mediated virus entry. Nature medicine 4:1302-1307.
22. Armand-Ugon M, Gutierrez A, Clotet B, Este JA. 2003. HIV-1 resistance to the gp41-dependent fusion inhibitor C-34. Antiviral research 59:137-142.
23. Jiang S, Lin K, Strick N, Neurath AR. 1993. HIV-1 inhibition by a peptide. Nature 365:113.
24. Lu M, Blacklow SC, Kim PS. 1995. A trimeric structural domain of the HIV-1 transmembrane glycoprotein. Nature structural biology 2:1075-1082.
25. Munoz-Barroso I, Durell S, Sakaguchi K, Appella E, Blumenthal R. 1998. Dilation of the human immunodeficiency virus-1 envelope glycoprotein fusion pore revealed by the inhibitory action of a synthetic peptide from gp41. The Journal of cell biology 140:315-323.
26. Gallo SA, Puri A, Blumenthal R. 2001. HIV-1 gp41 six-helix bundle formation occurs rapidly after the engagement of gp120 by CXCR4 in the HIV-1 Env-mediated fusion process. Biochemistry 40:12231-12236.
27. Martin N, Welsch S, Jolly C, Briggs JA, Vaux D, Sattentau QJ. 2010. Virological synapse-mediated spread of human immunodeficiency virus type 1 between T cells is sensitive to entry inhibition. Journal of virology 84:3516-3527.
28. Liu S, Lu H, Niu J, Xu Y, Wu S, Jiang S. 2005. Different from the HIV fusion inhibitor C34, the anti-HIV drug Fuzeon (T-20) inhibits HIV-1 entry by targeting multiple sites in gp41 and gp120. The Journal of biological chemistry 280:11259-11273.

29. LaBonte J, Lebbos J, Kirkpatrick P. 2003. Enfuvirtide. Nature reviews. Drug discovery 2:345-346.
30. Reynes J, Arasteh K, Clotet B, Cohen C, Cooper DA, Delfraissy JF, Eron JJ, Henry K, Katlama C, Kuritzkes DR, Lalezari JP, Lange J, Lazzarin A, Montaner JS, Nelson M, M OH, Stellbrink HJ, Trottier B, Walmsley SL, Buss NE, Demasi R, Chung J, Donatacci L, Guimaraes D, Rowell L, Valentine A, Wilkinson M, Salgo MP. 2007. TORO: ninety-six-week virologic and immunologic response and safety evaluation of enfuvirtide with an optimized background of antiretrovirals. AIDS patient care and STDs 21:533-543.
31. Trottier B, Walmsley S, Reynes J, Piliero P, O'Hearn M, Nelson M, Montaner J, Lazzarin A, Lalezari J, Katlama C, Henry K, Cooper D, Clotet B, Arasteh K, Delfraissy JF, Stellbrink HJ, Lange J, Kuritzkes D, Eron JJ, Jr., Cohen C, Kinchelow T, Bertasso A, Labriola-Tompkins E, Shikhman A, Atkins B, Bourdeau L, Natale C, Hughes F, Chung J, Guimaraes D, Drobnes C, Bader-Weder S, Demasi R, Smiley L, Salgo MP. 2005. Safety of enfuvirtide in combination with an optimized background of antiretrovirals in treatment-experienced HIV-1-infected adults over 48 weeks. Journal of acquired immune deficiency syndromes 40:413-421.
32. Lalezari JP, DeJesus E, Northfelt DW, Richmond G, Wolfe P, Haubrich R, Henry D, Powderly W, Becker S, Thompson M, Valentine F, Wright D, Carlson M, Riddler S, Haas FF, DeMasi R, Sista PR, Salgo M, Delehanty J. 2003. A controlled Phase II trial assessing three doses of enfuvirtide (T-20) in combination with abacavir, amprenavir, ritonavir and efavirenz in non-nucleoside reverse transcriptase inhibitor-naive HIV-infected adults. Antiviral therapy 8:279-287.
33. Lalezari JP, Eron JJ, Carlson M, Cohen C, DeJesus E, Arduino RC, Gallant JE, Volberding P, Murphy RL, Valentine F, Nelson EL, Sista PR, Dusek A, Kilby JM. 2003. A phase II clinical study of the long-term safety and antiviral activity of enfuvirtide-based antiretroviral therapy. Aids 17:691-698.
34. Kilby JM, Lalezari JP, Eron JJ, Carlson M, Cohen C, Arduino RC, Goodgame JC, Gallant JE, Volberding P, Murphy RL, Valentine F, Saag MS, Nelson EL, Sista PR, Dusek A. 2002. The safety, plasma pharmacokinetics, and antiviral activity of subcutaneous enfuvirtide (T-20), a peptide inhibitor of gp41-mediated virus fusion, in HIV-infected adults. AIDS research and human retroviruses 18:685-693.
35. Ni L, Gao GF, Tien P. 2005. Rational design of highly potent HIV-1 fusion inhibitory proteins: implication for developing antiviral therapeutics. Biochemical and biophysical research communications 332:831-836.
36. Qi Z, Shi W, Xue N, Pan C, Jing W, Liu K, Jiang S. 2008. Rationally designed anti-HIV peptides containing multifunctional domains as molecule probes for studying the mechanisms of action of the first and second generation HIV fusion inhibitors. The Journal of biological chemistry 283:30376-30384.
37. Liu S, Jing W, Cheung B, Lu H, Sun J, Yan X, Niu J, Farmar J, Wu S, Jiang S. 2007. HIV gp41 C-terminal heptad repeat contains multifunctional domains. Relation to mechanisms of action of anti-HIV peptides. The Journal of biological chemistry 282:9612-9620.
38. Martin-Carbonero L. 2004. Discontinuation of the clinical development of fusion inhibitor T-1249. AIDS reviews 6:61.

39. Eggink D, Berkhout B, Sanders RW. 2010. Inhibition of HIV-1 by fusion inhibitors. Current pharmaceutical design 16:3716-3728.
40. Kim JH, Song H, Austin JL, Cheng W. 2013. Optimized Infectivity of the Cell-Free Single-Cycle Human Immunodeficiency Viruses Type 1 (HIV-1) and Its Restriction by Host Cells. PloS one 8:e67170.
41. Jenny-Avital ER. 2003. Enfuvirtide, an HIV-1 fusion inhibitor. The New England journal of medicine 349:1770-1771; author reply 1770-1771.
42. Burton DR, Pyati J, Koduri R, Sharp SJ, Thornton GB, Parren PW, Sawyer LS, Hendry RM, Dunlop N, Nara PL, et al. 1994. Efficient neutralization of primary isolates of HIV-1 by a recombinant human monoclonal antibody. Science 266:1024-1027.
43. Miyauchi K, Kim Y, Latinovic O, Morozov V, Melikyan GB. 2009. HIV enters cells via endocytosis and dynamin-dependent fusion with endosomes. Cell 137:433-444.

Chapter 5.

Discussion of Results and Future Directions

5.1. Overview of Results

Cellular pathways for productive HIV-1 entry and molecular mechanisms of its inhibition have not been fully understood yet. Also, the characteristics of individual virion have not been extensively studied, but it recently turned out that virions in culture fluids show heterogeneous features in the number of envelope glycoproteins (1). In order to investigate the behaviors of virus including how it enters its target cell and where membrane fusion process for releasing virus genome occurs, it is necessary to fluorescently label virions. Furthermore, molecularly cloned HIV-1 that is capable of only a single round of infection (2, 3), called single-cycle replicative virion, offers a unique tool to address important questions related to the early event of viral infection, such as viral entry. Thus, we characterized single-cycle replicative, fluorescently-labeled HIV-1 in chapter 2. First of all, we established how to measure the concentration of infectious particles (Ci.p.) for measuring infectivity by taking an advantage of viral protein, Vpr, suppressing G2 cell

cycle (4). The infectivity was then optimized by varying several virus culture conditions. Among these culture variables, EGFP-Vpr plasmid input, virion harvest time, media replacement after transfection, and envelope plasmid input can all improve HIV-1 infectivity by reducing the number of defective virions. We then visualized virions by tagging Vpr, a viral accessory protein physically associated with the virus core, with EGFP (5-7). Fluorescent-tagged virion using EGFP-Vpr fusion protein, which showed ~50% labeling efficiency, allows direct visualization of HIV-1. Although the imaging method cannot provide a direct conversion between the number of virion particles and the concentration of physical particles (Cp.p.) due to the potential presence of virions without EGFP, they were strongly correlated supporting p24 values as a measurement of viral Cp.p. in our imaging method. Furthermore, we characterized HIV-1 tagged with EGFP-Vpr in terms of size, mean intensity, and sum intensity distributions. Even though there was a trade-off effect between fluorescent intensity and infectivity, we were able to pick 0.15 μg/ml of EGFP-Vpr plasmid input which results in the highest infectivity and reasonable intensity profiles amid the broad distribution of intensities. These studies help further investigate the mechanism of viral entry as well as develop deep understanding of individual HIV-1 virions.

In chapter 3, first of all, we can clearly visualize HIV-1 virions colocalized with early endosomes. Also, the fraction of colocalization was comparable when using VSV-G pseudotyped virions. This suggests the localized HIV-1 inside early endosomes may go to further productive infections based on the fact that VSV-G is able to cause infections via receptor-dependent endocytosis (8). To examine the extent to which endocytosis leads to productive infection of HIV-1, we have used several inhibitors of dynamin to investigate

whether there is a correlation between the inhibition of HIV-1 infection and the inhibition of cell endocytosis. Transfection of TZM-bl indicator cells by dyn1 K44A, the dominant-negative mutant of dynamin I, decreased HIV-1 infection by ~30%, which correlated with the decrease of endocytosis as monitored via transferrin uptake, suggesting that dynamin-dependent endocytosis contributes to the productive infection of HIV-1. Furthermore, dynasore, a noncompetitive inhibitor of dynamin (9), inhibited HIV-1 infection in various cell lines, suggesting that endocytosis can indeed lead to productive infection, as revealed by the specific inhibition of HIV-1 infectivity by the dyn I K44A mutant. The specificity of inhibitors is critical for the interpretation of these data, and through this study we uncovered the off-target effect of dynasore. Our all inhibition data showed the partial inhibition on viral infection by blocking endocytosis due to cellular cytotoxicity with high concentrations of dynasore and chlorpromazine. However, there was no apparent difference in the extent of inhibition on viral infection between HIV-1 and VSV-G pseudotyped virion. This also suggests that endocytosis can indeed contribute to productive infection.

Either direct fusion or endocytosis, there should be membrane fusion process between viral membrane and plasma or endosome membrane for viral productive infection (10, 11). Interestingly, endocytosed HIV-1 can be clearly observed in SupT1 cells even in the presence of saturating T20, suggesting that T20 may be endocytosed together with HIV-1 and exerts its inhibitory effect inside an endosome. However, endocytosis may not be the only productive pathway for HIV-1 infection because all these inhibitions that we have observed appear to be partial, which is in sharp contrast to inhibition by T20. T20, the membrane-impermeable inhibitor of HIV-1 fusion, potently inhibited HIV-1 infection in

all cell lines investigated in our studies. These results also suggest that endocytosed virions need to fuse with endosomal membrane for productive infection. Therefore, we concluded receptor-dependent endocytosis contributes to the productive entry of HIV-1.

Furthermore, some studies have suggested that endocytosis may allow virions to escape from the action of membrane-impermeable drugs (12, 13). The conclusion that endocytosis can lead to productive infection of HIV-1 virions leads to our investigation in chapter 4: what is the impact of endocytosis on membrane impermeable drugs of HIV-1? To address this question, we have tested both neutralizing antibodies and one of the fusion inhibitors, T20, and further focused on T20 to dissect the mechanisms of inhibition. First of all, both antibodies and T20 can block viral infections close to 100%, indicating that these drugs are potent enough *in vitro* even though HIV-1 can establish productive infection through endocytosis, which was the conclusion from chapter 3. To test the hypothesis that endocytosis may allow virus to escape from membrane-impermeable drugs, we have tested the effect of T20 on the internalization of HIV-1 by analyzing confocal images. To further investigate the impact of endocytosis on the efficacy of T20, we did titration of T20 and also varied the time of addition for T20 with regard to virion infection by TZM-bl cells, whose endocytic activity had been inhibited. These experiments showed that T20 doesn't affect virion endocytosis and endocytosis has no apparent impact on T20 efficacy. It suggests that endocytosis does not offer a measurable advantage for virus to escape. Investigating the behavior and mechanism of T20 is fundamentally important for molecular understanding of HIV-1 entry as well as developing new generations of T20-like anti HIV-1 drugs having improved potency and stability.

5.2. Future Directions

5.2.1. Correlation between only transfected cells with dyn I K44A and viral fusion

Although we observed the correlation between the inhibition on endocytosis and the inhibition on viral productive infections by using dyn I K44A mutant and several inhibitors related to endocytosis, we are taking an approach as an ongoing experiment, which can improve our previous studies with several aspects: first of all, we observed partial inhibition on viral infection when seeking the correlation between the inhibition on dynamin-dependent endocytosis and viral infections in chapter 3; second, this specific correlation was observed in TZM-bl cells, which is an engineered HeLa cell line, not T cells, the natural target of HIV-1; finally, there is a possibility that the partial inhibition in sharp contrast to the complete inhibition by T20, might be due to the partial transfection efficiency. Thus, the approach we have taken is transfecting Jurkat cells with dyn I K44A-mCherry, conducting beta-lactamase (BlaM) assay, which can quantitate the viral fusion events (14), and then analyze viral fusion events using only transfected cells by gating mCherry positive cells.

5.2.2. Physiologically relevant primary CD4 T^+ cells

Productive viral entry might be different among cell lines or primary human cells. Our results showing that endocytosis contributes to viral infection would be more conclusive if the inhibition on endocytosis and inhibition on viral infection shows a strong correlation using primary human $CD4^+$ T cells. Also, we were not able to block all functional dynamin molecules due to toxicity of dynasore and partial transfection

efficiency. In order to definitively assess the effect of dynamin-dependent endocytosis on viral infection, it would be required to knock down all three dynamin isoforms (15).

5.2.3. Controversial conclusion regarding productive HIV-1 entry recently studied

Although there have been extensive studies for productive HIV-1 entry, the conclusion from different research groups are still controversial. Also, it may be distinct with different virus spread modes, such as cell-to-cell transmission although there is a paper claiming that dynamin-dependent endocytosis is a main entry pathway in viral spread mode of cell-to-cell transmission (16). Recently, a research group claimed that productive HIV-1 entry occurs predominantly at the plasma membrane in SupT1-R5, CEM-ss, and primary $CD4^+$ T cells, with little, if any, contribution coming from endocytosed virions (17, 18). This is following up on their own published work, which had shown that endocytosis contributes to productive HIV-1 entry in HeLa cell-derived cell lines (19). This study mainly used the technique called temperature-arrested state (TAS) at 22°C, which can block membrane fusion, not endocytosis. Even though it has systematically used well-controlled temperature system and different cell lines including primary cells, there is a possibility that productive viral entry is affected by TAS based on the fact that endocytosis is a dynamic process (20) and fusion events among endosomes containing virus or T20. Contrary to this observation, another research group has claimed that the visualization of single viral lipid/content transfer events under physiological conditions can reveal the HIV-1 entry sites in lymphocytes and macrophages. Their approach is to distinguish between virus fusion with the PM and endosomes based on the extent of dilution of the viral lipid marker with single virus tracking (21). Therefore, in order to fully understand HIV-1 entry

mechanism, this areas of research needs more accumulation of other critical evidences, such as capturing diffusive signals from virion membrane fusion with more advance imaging techniques without interfering the normal functions of cells.

5.2.4. The mechanism and location of T20 action

Since T20 is membrane-impermeable, there are two possible explanations for the phenomena showing T20 potently inhibits viral infection. T20 can block HIV-1 infection at the site of action outside of the plasma membrane. Otherwise, it might be co-internalize with virus and exhibit its inhibitory action within an endosome. For T20, we found that HIV still undergoes endocytosis in the presence of saturating T20, suggesting the latter mechanism. However, one possibility for the first mechanism is that the events of virion endocytosis in the presence of T20 are all receptor-independent and nonspecific. The possible experiment will be the colocalization of virions with anti-CD4 in an endosome. Further colocalization studies using FITC-T20 and mCherry-labeled virus inside endosomes at single-molecule resolution will definitely test the hypothesis that T20 might be able to act its inhibitory effect inside endosomes.

5.3. Concluding Remarks

On the basis of the findings presented in this thesis, characterizing the features of individual HIV-1 particles helps understand the events of virus infection as well as data interpretation. First of all, one of the mechanisms explaining the low infectivity of HIV-1 was revealed that there are many defective virus particles in virus pool (22, 23). Another potential mechanism is the low number of envelope spikes on virion surface, which may

suppress the immune response making a difficulty in developing HIV vaccines (24, 25). Second, there was a trade-off effect between fluorescent intensity and infectivity, however, the distribution of intensity was pretty broad, suggesting individual HIV-1 particles have heterogeneity in terms of protein compositions or other features (1). Lastly, the labeling efficiency was around 50%, meaning the rest of particles are not fluorescent. This issue should be taken care of when interpreting data for fluorescent imaging and inhibition assays. In order to overcome the partial labeling efficiency as well as make it more natural conditions, using label-free virus with optical biosensors might be a good strategy to study nanoparticles, such as HIV-1, or other viruses (26).

In chapter 3 and chapter 4, our results suggest that endocytosis contributes to HIV-1 productive entry. The phenomena were not coming from virus envelopes from different strains, or methods for facilitating virus binding to cell surface. Our conclusions may be different with other cell lines, or different infection environment, such as cell-to-cell transmission. However, a recent study also showed that HIV-1 virions enter cells via dynamin-dependent endocytosis during cell-to-cell transmission (16). The both conclusions that endocytosis contributes to HIV-1 productive entry and there is a negligible impact of endocytosis on T20 efficacy help understand viral pathogenesis and eventually improve the development of antiviral drugs.

5.4. References

1. Pang Y, Song H, Kim JH, Hou X, Cheng W. 2014. Optical trapping of individual human immunodeficiency viruses in culture fluid reveals heterogeneity with single-molecule resolution. Nature nanotechnology 9:624-630.
2. Munk C, Landau NR. 2003. Production and use of HIV-1 luciferase reporter viruses. Current protocols in pharmacology / editorial board, S.J. Enna Chapter 12:Unit12 15.
3. Richards KH, Clapham PR. 2006. Human immunodeficiency viruses: propagation, quantification, and storage. Current protocols in microbiology Chapter 15:Unit15J 11.
4. He J, Choe S, Walker R, Di Marzio P, Morgan DO, Landau NR. 1995. Human immunodeficiency virus type 1 viral protein R (Vpr) arrests cells in the G2 phase of the cell cycle by inhibiting p34cdc2 activity. Journal of virology 69:6705-6711.
5. Schaeffer E, Geleziunas R, Greene WC. 2001. Human immunodeficiency virus type 1 Nef functions at the level of virus entry by enhancing cytoplasmic delivery of virions. Journal of virology 75:2993-3000.
6. McDonald D, Vodicka MA, Lucero G, Svitkina TM, Borisy GG, Emerman M, Hope TJ. 2002. Visualization of the intracellular behavior of HIV in living cells. The Journal of cell biology 159:441-452.
7. Accola MA, Ohagen A, Gottlinger HG. 2000. Isolation of human immunodeficiency virus type 1 cores: retention of Vpr in the absence of p6(gag). Journal of virology 74:6198-6202.
8. Sun XJ, Yau VK, Briggs BJ, Whittaker GR. 2005. Role of clathrin-mediated endocytosis during vesicular stomatitis virus entry into host cells. Virology 338:53-60.
9. Macia E, Ehrlich M, Massol R, Boucrot E, Brunner C, Kirchhausen T. 2006. Dynasore, a cell-permeable inhibitor of dynamin. Dev Cell 10:839-850.
10. Chan DC, Kim PS. 1998. HIV entry and its inhibition. Cell 93:681-684.
11. Eckert DM, Kim PS. 2001. Mechanisms of viral membrane fusion and its inhibition. Annual review of biochemistry 70:777-810.
12. Roberts PC, Kipperman T, Compans RW. 1999. Vesicular stomatitis virus G protein acquires pH-independent fusion activity during transport in a polarized endometrial cell line. Journal of virology 73:10447-10457.
13. de la Vega M, Marin M, Kondo N, Miyauchi K, Kim Y, Epand RF, Epand RM, Melikyan GB. 2011. Inhibition of HIV-1 endocytosis allows lipid mixing at the plasma membrane, but not complete fusion. Retrovirology 8:99.
14. Cavrois M, De Noronha C, Greene WC. 2002. A sensitive and specific enzyme-based assay detecting HIV-1 virion fusion in primary T lymphocytes. Nat Biotechnol 20:1151-1154.
15. Park RJ, Shen H, Liu L, Liu X, Ferguson SM, De Camilli P. 2013. Dynamin triple knockout cells reveal off target effects of commonly used dynamin inhibitors. Journal of cell science 126:5305-5312.
16. Sloan RD, Kuhl BD, Mesplede T, Munch J, Donahue DA, Wainberg MA. 2013. Productive entry of HIV-1 during cell-to-cell transmission via dynamin-dependent

endocytosis. Journal of virology 87:8110-8123.
17. Herold N, Anders-Osswein M, Glass B, Eckhardt M, Muller B, Krausslich HG. 2014. HIV-1 entry in SupT1-R5, CEM-ss, and primary CD4+ T cells occurs at the plasma membrane and does not require endocytosis. Journal of virology 88:13956-13970.
18. Herold N, Muller B, Krausslich HG. 2015. Reply to "Can HIV-1 entry sites be deduced by comparing bulk endocytosis to functional readouts for viral fusion?". Journal of virology 89:2986-2987.
19. Daecke J, Fackler OT, Dittmar MT, Krausslich HG. 2005. Involvement of clathrin-mediated endocytosis in human immunodeficiency virus type 1 entry. Journal of virology 79:1581-1594.
20. Marin M, Melikyan GB. 2015. Can HIV-1 entry sites be deduced by comparing bulk endocytosis to functional readouts for viral fusion? Journal of virology 89:2985.
21. Miyauchi K, Kim Y, Latinovic O, Morozov V, Melikyan GB. 2009. HIV enters cells via endocytosis and dynamin-dependent fusion with endosomes. Cell 137:433-444.
22. Platt EJ, Kozak SL, Durnin JP, Hope TJ, Kabat D. 2010. Rapid dissociation of HIV-1 from cultured cells severely limits infectivity assays, causes the inactivation ascribed to entry inhibitors, and masks the inherently high level of infectivity of virions. Journal of virology 84:3106-3110.
23. Kim JH, Song H, Austin JL, Cheng W. 2013. Optimized Infectivity of the Cell-Free Single-Cycle Human Immunodeficiency Viruses Type 1 (HIV-1) and Its Restriction by Host Cells. PloS one 8:e67170.
24. Schiller J, Chackerian B. 2014. Why HIV virions have low numbers of envelope spikes: implications for vaccine development. PLoS pathogens 10:e1004254.
25. Klein JS, Bjorkman PJ. 2010. Few and far between: how HIV may be evading antibody avidity. PLoS pathogens 6:e1000908.
26. Block O, Mitra A, Novotny L, Dykes C. 2012. A rapid label-free method for quantitation of human immunodeficiency virus type-1 particles by nanospectroscopy. Journal of virological methods 182:70-75.